July 1973

On Digital Simulation of Multicorrelated Random Processes and Its Applications

A. K. Sinha
Department of Engineering Science and Mechanics

This research was supported by the National Aeronautics and Space Administration, Washington, D. C.
Under Grant No. NGL 47-004-067

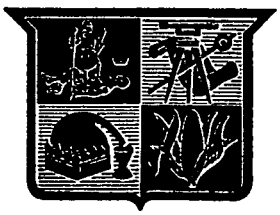

Virginia Polytechnic Institute and State University

ON DIGITAL SIMULATION OF MULTICORRELATED RANDOM PROCESSES AND ITS APPLICATIONS

by

Ajit Kumar Sinha

(ABSTRACT)

Two methods of simulation of multicorrelated random processes from the given matrix of spectral density function have been presented. It has been noted that FFT method works as efficiently as the Trigonometric method and is much faster. It has been found that there are certain cases in which Trigonometric approach has advantages over the FFT method. Some example problems are solved to show the usefulness of this approach in solving the problems of linear and nonlinear random vibrations. It has been observed that this technique and particularly the FFT method offers a very fast and convenient alternative for performing random nonlinear response analysis. Various possible areas in which this approach can be extended have been also discussed.

TABLE OF CONTENTS

Chapter

ACKNOWLEDGEMENTS iv

LIST OF FIGURES v

LIST OF TABLES vii

LIST OF SYMBOLS viii

I. INTRODUCTION 1

II. LITERATURE SURVEY 4

1. Review of Existing Simulation Methods 4

2. Review of Stationary Random Response of Multidegree of Freedom Nonlinear System 10

III. DISCUSSION OF SIMULATION METHODS 22

1. Trigonometric Model 22

2. Fast Fourier Transform Method 33

3. Simulation of Strong Wind Turbulence 38

IV. APPLICATIONS OF SIMULATION TECHNIQUE 57

1. Forced Oscillation of Free Standing Latticed Tower . . 57

2. Nonlinear Random Vibration of String 71

3. Nonlinear Panel Response Due to Turbulent Boundary Layer 80

V. CONCLUSIONS AND FUTURE EXTENSIONS 99

REFERENCES 102

APPENDICES 106

A. Random Variable and Probability 106

B. Fast Fourier Transform 112

C. Matrix Method for Singular Cases 116

D. Computer Program 119

VITA 166

ACKNOWLEDGEMENTS

The author greatly appreciates the wise counseling, helpful suggestions, and encouragement of Professor Larry E. Wittig, his committee chairman. Special thanks must go to Professor M. Hoshiya, who is now in Japan and under whom the foundation for this work was laid to start with.

He further thanks each committee member for the aid and assistance they have provided throughout his tenure at Virginia Polytechnic Institute and State University.

The author acknowledges the sponsorship of this research by the National Aeronautics and Space Administration under Grant No. NGL 47-004-067.

Final thanks must go to Mrs. Peggy Epperly for typing this dissertation.

LIST OF FIGURES

Figure		Page
1.	Schematic Sketch of a Continuous Power Spectrum Used to Generate Time Series	28
2.	Schematic Sketch of a Discrete Power Spectrum from a Simulated Time Series	29
3a.	Simulated Wind Velocities by Tirgonometric Model	42
3b.	Simulated Wind Velocities by FFT Method	43
4a.	Comparison Between the Original Spectrum of Horizontal Turbulent Wind Velocity at 100 Ft. and the Simulated One by Trigonometric Method	44
4b.	Comparison Between the Original Spectrum of Horizontal Turbulent Wind Velocity at 100 Ft. and the Simulated One by FFT Method	45
5a.	Comparison Between the Original Spectrum of Lateral Turbulent Wind Velocity at 100 Ft. and the Simulated One by Trigonometric Method	46
5b.	Comparison Between the Original Spectrum of Lateral Turbulent Wind Velocity at 100 Ft. and the Simulated One by FFT Method	47
6a.	Comparison Between the Original Spectrum of Vertical Turbulent Wind Velocity at 100 Ft. and the Simulated One by Trigonometric Method	48
6b.	Comparison Between the Original Spectrum of Vertical Turbulent Wind Velocity at 100 Ft. and the Simulated One by FFT Method	49
7a.	Comparison Between the Original Spectrum of Horizontal Turbulent Wind Velocity at 50 Ft. and the Simulated One by Trigonometric Method	50
7b.	Comparison Between the Original Spectrum of Horizontal Turbulent Wind Velocity at 50 Ft. and the Simulated One by FFT Method	51

8a. Comparison Between Original Co-spectrum of Horizontal Turbulent Wind Velocities at 100' and 50' and the Simulated One by Trigonometric Method 52

8b. Comparison Between Original Co-spectrum of Horizontal Turbulent Wind Velocities at 100' and 50' and the Simulated One by FFT Method 53

9a. Comparison Between Original Quadrature Spectrum of Horizontal Turbulent Wind Velocities at 100' and 50' and the Simulated One by Trigonometric Method 54

9b. Comparison Between the Original Quadrature Spectrum of Horizontal Turbulent Wind Velocities at 100' and 50' and the Simulated One by FFT Method 55

10. Latticed Tower Subjected to Turbulent Wind Load 66

11. Simulated Generalized Forces and Displacement for Tower Problem 70

12. Simulated Generalized Forces for Nonlinear String Problem 77

13. Simulated Displacement Time Histories for Nonlinear String 78

14. Comparison Between Linear and Nonlinear Response of a String by FFT Method 79

15. Problem Geometry for Nonlinear Plate Vibration Due to Turbulent Boundary Layer Pressure 81

16. Simulated Generalized Forces and Displacement for the Plate Vibration 96

17. Comparative Study of Plate Response Due to Subsonic Pressure Fluctuations by FFT Method 97

1-A. PDF of Continuous Random Variable 107

LIST OF TABLES

Table		Page
1.	Concentrated Masses and Projected Areas at Panel Points for Latticed Tower	67
2.	Flexibility Matrix of the Latticed Tower in Y-direction .	68
3.	Computed Normalized Mode Shapes with Respect to the Bottom Panel for Tower Problem	69

LIST OF SYMBOLS

$\overline{A}_n$	Displacement vector of the nth mode
a_∞	Velocity of sound for external flow
a_c	Velocity of sound for cavity flow
$a_{mp}(K)$, $b_{mp}(K)$	Time series amplitude coefficients
b_{ij}	Modal amplitude of plate vibration
$C_{ij}(w)$	Co-spectral density
D	Plate stiffness
$E[\cdot]$	Expectation operator
$F_{oj}(t)$	Dynamic wind load at the location j
F_{aj}	Static wind load at the location j
$\overline{F}_{mn}$	Random generalized force for plate vibration
$\overline{F}^e_{mn}$, $\overline{F}^c_{mn}$	Aerodynamic generalized forces for external and cavity flow respectively
$\overline{F}(t)$, $\overline{f}(t)$	Forcing function vector
$f(x,t)$	Force per unit length of the string
$\hat{f}(x,t)$	Nondimensional forcing function
$f_i(t)$	Simulated time series
$\tilde{G}(w)$	Spectral matrix
$G_{mn}(w)$	One-sided cross-spectral density
$H_{mp}(w)$	Element of lower triangular matrix derived from G(w)

K	Stiffness matrix
K_{mnp}	Covariance
k_1, k_2, k_3	Wave numbers in x_1, x_2, x_3 directions respectively
k, ℓ	Frequency index
M	Mass matrix
M_{ig}	Generalized mass in the tower problem
$p(\bar{x},\bar{y},\bar{t})$	Turbulent pressure
$p^e(\bar{x},\bar{y},\bar{t})$	Fluid pressure, external flow
$p^c(\bar{x},\bar{y},\bar{t})$	Fluid pressure due to cavity flow
$\bar{p}, \bar{p}^e, \bar{p}^c$	Nondimensional turbulent pressure, external flow pressure and cavity flow pressure respectively
$Q_{ij}(w)$	Quadrature spectrum
$Q_i(t)$	Generalized force in the tower problem
q_n	n-th generalized coordiante
q	$\rho_\infty U^2_\infty/2$, dynamic pressure
R_{mn}	Cross-correlation function
$S_{v_{oj}v_{ok}}$	Cross-spectrum of the fluctuating velocities at points j and k
$S_{QiQ\ell}$	Cross-spectrum of the generalized force
$S_{qiq\ell}(w)$	Cross-spectrum of the generalized coordiante
S_{yky}	Spectral density of the dynamic displacement
T_o	Initial tension in the spring
$\bar{t}$	$\frac{t}{ab}\frac{D}{\rho}$
U_∞	Mean external flow velocity
U_c	Convectional speed

$\hat{u}(\frac{L}{2},t)$	Nondimensional displacement of the center of the string
V_{aj}	Mean wind velocity at the location
$V_{oj}(t)$	Pulsating velocity component
w	Angular frequency
W_u	Upper frequency cut-off
w_L	Lower frequency cut-off
$\bar{w}$	Nondimensional plate thickness
X_{pk}	Elements of complex vector
$\bar{x}$, $\bar{y}$, $\bar{z}$	Nondimensional co-ordinate
y_k	Dynamic displacement
$\alpha_{mp}(k)$	Phase angle
α_{yi}	Modes of natural oscillation
β_1, β_2	Damping coefficients
δ	Logrithmic damping decrement of oscillation
Δw	Frequency increments
ζpk	Complex random number
ζ^*	Boundary layer thickness
ν	Poisson's ratio
ξ_p, η_p	Gaussian random variables
ρ	Mass per unit length of the string
ρ_∞	Free stream density
ρ_c	Cavity flow density
$\sigma_{\hat{u}}$	R.M.S. of nondimensional response at the center of the string

$\overline{\Phi}$	Airy stress function for membrane stress
$\Phi_i(w)$	Transfer function in the tower problem
Φ, Φ^c	Velocity potential, external and cavity flows

CHAPTER I

INTRODUCTION

In this dissertation, two methods are described to simulate on a digital computer a set of correlated, stationary and Gaussian time series with zero mean from the given matrix of power spectral densities and cross-spectral densities. Some example problems are investigated to show the power of this technique to solve the problems of linear and in particular nonlinear random vibrations. The development set forth is for any arbitrary number of correlated series; however, in practice, the number is limited by the storage capability of the computer.

The first method is based upon trigonometric series with random amplitudes and deterministic phase angles. The random amplitudes are generated by using a standard random number generator subroutine. An example is presented which corresponds to three components of wind velocities at two different spatial locations for a total of six correlated time series. Selected spectral densities computed from the simulated time series are compared to the original spectral densities from which the time series were generated.

In the second method, the whole process is carried out using the Fast Fourrier Transform approach in place of trigonometric series. It is found that this method gives more accurate results and works about twenty times faster for a set of six correlated time series.

To show one of the many areas of application of the present method of simulation, namely the class of random structural vibration analysis, the following problems have been investigated: (1) The linear vibration characteristics of a long tower under the action of correlated wind loads have been presented. Taking it to be a fourteen degrees of freedom system, the time history of the displacement of the top of the tower has been plotted considering up to three modes of vibration. The usefulness of this method in the case of linear analysis can be significant and very important, e.g., looking for the occurrence of maximum structural response rather than the r.m.s. value of response. This knowledge will be very useful for the reliability study of structures under random loads; (2) One of the most interesting and significant applications of the proposed method is the simulation of random generalized forces. The necessity of simulating random generalized forces arises when the dynamic response analysis is performed in time domain either for the purpose of obtaining information beyond the second order statistics (such as first passage time distribution) or when the structure is nonlinear and therefore an approximate random response is sought by simulating the excitation.

In order to assert the validity of the preceding discussion, the problem of the nonlinear vibration of a string has been solved in the time domain by simulating the random generalized forces.

Finally to show the application of this method to a more complex problem, the random nonlinear vibration of a flexible plate immersed in a fluid flow on one side and backed by a fluid filled cavity of

finite dimensions on the other side is considered. The nonlinear plate stiffness induced in the plate by out-of-plane bending and the mutual interaction between the external and the internal fluid flow is included.

The FFT simulation technique is utilized for the response analysis of the plate undergoing large deformation. The same problem has been done by Shinozuka [1] where he has taken a multidimensional trigonometric series model for the generalized forces. The analysis is performed in the time domain rather than in the frequency or wave number domain as is usually done in linear response analysis. The numerical example has been presented for subsonic flow over the plate.

CHAPTER II

LITERATURE SURVEY

Part A: Review of Existing Simulation Methods

Numerous papers dealing with simulation of random process have been published in recent years. Although many authors dealt with the simulation of single random processes utilizing trigonometric series [2], filtered white noise [2], filtered shot noise [3] and correlated random pulse trains [4] etc, only Hoshiya and Tideman [5], Shinozuka [6] and Borgman [7] studied the simulation of multicorrelated processes.

I. In the simulation of ocean surface elevation, Borgman used wave superposition by choosing the frequency in such a way that the amplitude of each wave function was an equal portion of the cumulative spectrum. Borgman also presented a method for simulating several simultaneous time series by passing a white noise vector through filters. He proposed the following model [7].

$$y_m(t) = \sum_{j=1}^{m} \int_{-\infty}^{\infty} k_{mj}(\tau) x_j(t-\tau) d\tau,$$

$$m = 1, 2, \ldots M \qquad (2\text{-}1)$$

where,

$y_m(t)$ = m th time series

$x_j(t)$ = independent random inputs

$k_{mj}(\tau)$ = kernals

Let $S_{mr}(f)$ represent the cross spectral density between $y_m(t)$ and $y_r(t)$. Kernals $k_{mj}(\tau)$ and its Fourier Transform $K_{mj}(f)$ are determined from the relation

$$S_{mr}(f) = \sum_{j=1}^{r} \overline{K_{mj}(f)} K_{rj}(f) S_{xj}(f),$$

$$r = 1, 2, \ldots, m \text{ and} \qquad (2\text{-}2)$$

$$m = 1, 2, \ldots, M$$

where the bar denotes the complex conjugate.

This system of equation can be solved sequentially (taking K_{jj} to have zero gain for j = 1, 2, 3 ...) as

$$K_{11}(f) = \sqrt{S_{11}(f)}$$

$$K_{21}(f) = \frac{\overline{\sqrt{S_{21}(f)}}}{\sqrt{S_{11}(f)}} \qquad (2\text{-}3)$$

$$K_{22}(f) = [S_{22}(f) - |K_{21}(f)|^2]^{\frac{1}{2}} \text{etc.}$$

This, in turn, determines the digital filter co-efficients, a_{nmj}, needed to approximate the kernel associated with the system function $k_{mj}(f)$. Then the final simulation equation reduces to

$$y_m(k\Delta t) = \sum_{j=1}^{N} \sum_{n=-N}^{N} a_{nmj} x_j,\ k-n,$$

$$m = 1, 2, \ldots M \qquad (2\text{-}4)$$

in which x_j, n for n = 1, 2, 3, ... is the j th generated sequence of independent, zero mean, unit variance, normal random variables.

II. Later Hoshiya and Tieleman [5] considered the following trigonometric model for simulating two correlated random processes:

$$x(t) = \sum_{j=1}^{n} (a_j \cos w_j t + b_j \sin w_j t)$$

$$y(t) = \sum_{j=1}^{n} \{c_j \cos (w_j t + \alpha_j) + d_j \sin (w_j t + \alpha_j) \qquad (2\text{-}5)$$

where a_j, b_j, c_j and d_j are random variables and α_j is deterministic. The two stationary normal processes are correlated if there exists a non-zero correlation between a_j and c_j and/or b_j and d_j. The covariance C_{xyj} between the two random variables a_j and c_j is defined as

$$C_{xyj} = E[a_j c_j] = E[b_j d_j]$$

and the standard deviation at frequency w_j, σ_{xj} and σ_{yj} are given as

$$\sigma_{xj} = \sqrt{2 S_x^c(w_j) \Delta w} \qquad (2\text{-}6)$$

$$\sigma_{yj} = \sqrt{2 S_y^c(w_j) \Delta w} \qquad (2\text{-}7)$$

where $S_x^c(w_j)$ and $S_y^c(w_j)$ are the discrete form of the power spectra for processes x and y respectively.

Expressions for the co-spectrum and the quadrature spectrum are given as

$$2C_{xy}^c(w_j)\Delta w = \sigma_{xj}\sigma_{yj}\rho_{xyj}\cos \alpha_j \qquad (2\text{-}8)$$

$$2Q_{xy}^c(w_j)\Delta w = -\sigma_{xj}\sigma_{yj}\rho_{xyj}\sin \alpha_j \qquad (2\text{-}9)$$

whence,

$$\alpha_j = \tan^{-1}\left[-\frac{Q_{xy}^c(w_j)}{C_{xy}^c(w_j)}\right] \qquad (2\text{-}10)$$

and

$$\rho_{xyj}^2 = \frac{\{C_{xy}^c(w_j)\}^2 + \{Q_{xy}^c(w)\}^2}{S_x^c(w_j) S_y^c(w_j)} \qquad (2\text{-}11)$$

The random variables a_j and b_j are generated independently from a normal distribution with zero mean and a standard deviation $\sigma_{xy} = \sqrt{2S_x^c(w)\Delta w}$ and $\sigma_{yj} = \sqrt{2S_y^c(w_j)\Delta w}$ respectively. Then c_j and d_j are generated as follows. Since a_j and c_j are both normally distributed, the joint probability density function of a_j and c_j is

$$P(a_j,c_j) = \frac{1}{2\pi\sigma_{xj}\sigma_{yj}} \exp\left\{-\frac{1}{2(1-\rho_{xyj}^2}\left[\frac{a_j^2}{\sigma_{xj}^2} - \frac{2\rho_{xyj}a_jc_j}{\sigma_{xj}\sigma_{yj}} + \frac{c_j^2}{\sigma_{yj}^2}\right]\right\} \tag{2-11a}$$

and the probability density function of a_j is

$$P(a_j) = \frac{1}{\sqrt{2\pi}\sigma_{xj}} \exp\left\{-\frac{a_j^2}{2\sigma_{xj}^2}\right\}. \tag{2-11b}$$

The conditional probability density function of c_j for given a_j is

$$P(c_j/a_j) = \frac{P(a_j,c_j)}{P(a_j)} = \frac{1}{\sqrt{2\pi}\sigma_{yj}\sqrt{1-\rho_{xyj}^2}} \times \exp\left\{-\frac{1}{2\sigma_{yj}^2(1-\rho_{xyj}^2}\left(c_j-\rho_{xyj}\frac{\sigma_{yj}}{\sigma_{xj}}a_j\right)^2\right\}. \tag{2-11c}$$

Consequently, the conditional probability density function of c_j for given a_j is also Gaussian with mean $\rho_{xyj}\frac{\sigma_{yj}}{\sigma_{xj}}a_j$ and a standard deviation $\sigma_{yj}\sqrt{1-\rho_{xyj}^2}$. Similarly, the conditional distribution of d_j for a given b_j is Gaussian with mean $\rho_{xyj}\frac{\sigma_{yj}}{\sigma_{xj}}b_j$ and standard deviation of $\sigma_{yj}\sqrt{1-\rho_{xyj}^2}$. Thus random variable c_j is generated from Gaussian distribution with mean $\rho_{xyj}\frac{\sigma_{yj}}{\sigma_{xj}}a_j$ and a standard deviation of $\sigma_{yj}\sqrt{1-\rho_{xyj}^2}$. Similarly, the random variable d_j is generated from a Gaussian distribution with mean $\rho_{xyj}\frac{\sigma_{yj}}{\sigma_{xj}}b_j$ and a standard deviation of $\sigma_{yj}\sqrt{1-\rho_{xyj}^2}$.

III. In his paper [8], Shinozuka proposed a different trigonometric model for the simulation of multivariate random processes. He used a series of cosine functions with weighted amplitudes, almost evenly spaced random frequencies and random phase angles with uniform distribution. He considered a set of n stationary random processes $fo_i(t)$ (i = 1, 2, ... n) with a specified cross-spectral density matrix $S^o_f(w) = [S^o{}_{f_i f_j}(w)]$, where $S^o{}_{f_i f_j}(w)$ are mean square spectral densities if i = j and cross spectral densities of $fo_i(t)$ and $fo_j(t)$ if $i \neq j$.

He proposed the following model

$$f_i(t) = \sum_{j=1}^{i} \sigma_j \left(\frac{2}{N}\right)^{\frac{1}{2}} \sum_{k=1}^{N} \gamma_{ij}(w_{jk}) \times \cos\left[w_{jk}t + Q_{jk} + \theta_{ij}(w_{jk})\right] \qquad (2\text{-}12)$$

where,

w_{jk} (k = 1, 2, ... N) are random variables identically and independently distributed with the density function

$$g_j(w) = |H_{jj}(w)|^2/\sigma_j{}^2 \qquad (2\text{-}13)$$

$$\text{with } \sigma_j{}^2 = \int_{-\infty}^{\infty} |H_{jj}(w)|^2 dw \qquad (2\text{-}14)$$

and Q_{jk} (k = 1, 2, ... N) are also identically and independently distributed with the uniform density $1/(2\pi)$ between 0 and 2π. $H_{ji}(w)$ are obtained from

$$S_{ij}(w) = \sum_{k=1}^{n} H_{ik}(w)\overline{H}_{jk}(w) \qquad (2\text{-}15)$$

and,

$$\gamma_{ij}(w) = \left|\frac{H_{ij}(w)}{H_{jj}(w)}\right| \tag{2-16}$$

$$\theta_{ij}(w) = t_{an}^{-1}\left[\frac{I_m H_{ij}(w)}{R_e H_{ij}(w)}\right] . \tag{2-17}$$

The series simulated by the above technique have the asymptotic ergodicity.

IV. Comparison of Various Approaches.

It appears that method of simulation proposed by Shinozuka [8] is the most efficient so far. This model [8] seems to be more general than that due to Hoshiya and is more efficient than that due to Borgman [7]. Since the measured cross spectral densities are usually given numerically in terms of the real and the imaginary parts or the modulii and the angles, the computation work associated with finding $|H_{ij}(w)|$, from which $\gamma_{ij}(w) = |H_{ij}(w)|/H_{jj}(w)$ and the angles $\theta_{ij}(w)$ can be directly evaluated in the case of Ref. [8]. Therefore, method of simulation presented here appears more practical than that proposed in Ref. [7], which requires (a) the inverse Fourier Transformation of $N(N+1)/2$ functions of w, $H_{ij}(w)$ and (b) the same number of integration in the time domain. Also, form of simulated functions consisting of sum of cosine functions can be proved extremely advantageous, when used as input, in evaluating the corresponding output of a linear system.

PART B.

The main usefulness of the simulation method is in the area of (a) a numerical analysis of dynamic response of non-linear structures, (b) time domain analysis of linear structures under random excitations performed for the purpose of obtaining the kind of information, such as first excursion probability and exact time history of a sample function, that is not obtainable from the standard frequency domain analysis, and (c) numerical solution of stress wave propagation through a random medium and eigen value problems of structures with randomly non-homogeneous material properties. The usefulness of this method has been demonstrated in the later chapter of this dissertation. In this connection, it looks appropriate to make a relative study of the prevalent methods of handling the non-linear random vibration problems.

Review of Stationary Random Response of Multidegree of Freedom Nonlinear Systems

Fokker-Planck Approach.

One exact method of studying the stationary random response of a nonlinear system is the Fokker-Planck approach. If the excitation is a Gaussian white noise, then the transitional probability density of the response process is governed by the Fokker-Planck equation. The equation governing the first probability density function for the stationary response has been solved under the following rather restrictive conditions:

(1) the damping force is proportional to the velocity

(2) the excitation is a Gaussian white noise

(3) the correlation function matrix of the excitation is proportional to the damping matrix of the system. Under the above conditions, the equation of motion may be written as follows:

$$M\ddot{\bar{x}} + C\dot{\bar{x}} + \frac{\partial u(\bar{x})}{\partial \bar{x}} = \bar{f}(t) \tag{2-18}$$

with

$$\bar{m}_f = 0$$

$$R_f(\tau) = 2\gamma C\delta(\tau) \tag{2-19a}$$

where γ is a constant, $u(\bar{x})$ is the potential energy of the system and

$$\frac{\partial u(\bar{x})}{\partial \bar{x}} = \begin{pmatrix} \frac{\partial u}{\partial x_1} \\ \vdots \\ \frac{\partial u}{\partial x_n} \end{pmatrix}. \tag{2-19b}$$

Suppose that there exists an orthogonal matrix A which can simultaneously diagonalize the mass matrix M and the damping matrix C:

$$\left.\begin{aligned} A^T A &= I \\ A^T M A &= V \\ A^T C A &= \Lambda \end{aligned}\right\} \tag{2-20}$$

where V and Λ are two diagonal matrices. Then, upon using the transformation $\bar{x} = A\bar{z}$ and noting that

$$A^T \frac{\partial u(\bar{x})}{\partial \bar{x}} = A^T \frac{\partial \bar{z}}{\partial \bar{x}} \frac{\partial u(\bar{z})}{\partial \bar{z}} = \sum_{j,k=1}^{n} a_{jm} a_{jk} \frac{\partial u(\bar{z})}{\partial z_k}$$

$$m = 1, \ldots n$$

$$= \frac{\partial u(\bar{z})}{\partial z_m}$$

$$= \frac{\partial u(\bar{z})}{\partial \bar{z}}. \tag{2-21}$$

Equation (2-18) becomes

$$V\ddot{\bar{z}} + \Lambda\dot{\bar{z}} + \frac{\partial u(\bar{z})}{\partial \bar{z}} = A^T\bar{f}(t) = \bar{b}(t) \tag{2-22a}$$

and the correlation function matrix of $\bar{b}(t)$ is given by

$$R_{\bar{b}}(\tau) = 2\gamma\Lambda\delta(\tau)\,. \tag{2-22b}$$

The stationary Fokker Planck equation associated with (2-22a) is given by

$$\sum_{j=1}^{n} \frac{\partial}{\partial z_j}(z_j p) - \sum_{j=1}^{n} \frac{1}{v_j} \frac{\partial}{\partial \dot{z}_j}\left\{\left[\lambda_j \dot{z}_j + \frac{\partial u(\bar{z})}{\partial z_j}\right] p\right\}$$

$$- \sum \frac{\gamma\lambda_j}{v_j^2} \frac{\partial^2 p}{\partial \dot{z}_j^2} = 0 \tag{2-23}$$

where λ_j and v_j denote the j th diagonal element of Λ and V, p is the abbreviation for the first probability density of the Markovian vector$\begin{pmatrix} z \\ \dot{z} \end{pmatrix}$. The solution to (2-23) may be written as follows:

$$p(z,\dot{z}) = \beta \exp\left\{ - \frac{1}{\gamma}\left[\frac{1}{2}\sum_{j=1}^{n} v_j \dot{z}_j^2 + u(\bar{z})\right]\right\}. \tag{2-24}$$

This solution was first obtained by Ariarathan [9] for a two-degree-of freedom system, and it was extended to the above form by Caughey [10]. The constant β in (2-24) is a normalizing factor such that

$$\int_{-\infty}^{\infty} \cdots \int_{-\infty}^{\infty} p(\bar{z},\dot{\bar{z}})\, dz_1 \ldots dz_n d\dot{z}_1 \ldots d\dot{z}_n = 1\,. \tag{2-25}$$

In the original co-ordinates, equation (2-24) becomes

$$p(\bar{x},\dot{\bar{x}}) = \beta \exp\left\{ - \frac{1}{\gamma}\left[\frac{1}{2}\dot{x}^T M \dot{x} + u(\bar{x})\right]\right\}. \tag{2-26}$$

It will be noted that the terms in the square brackets are respectively the kinetic energy and the potential energy of the system.

Equation (2-26) may also be written as

$$p(\bar{x},\dot{\bar{x}}) = \beta \exp\{-\frac{\partial}{\partial\gamma}\dot{\bar{x}}M^T\dot{\bar{x}}\} \exp\{-\frac{1}{\gamma}u(\bar{x})\} \qquad (2\text{-}27)$$

Hence $\bar{x}$ and $\dot{\bar{x}}$ are linearly independent.

Normal Mode Approach

Consider an n-degree-of-freedom system governed by the equation of motion

$$M\ddot{\bar{x}} + C^{(o)}\dot{\bar{x}} + K^{(o)}\bar{x} + \mu\bar{g}(\dot{\bar{x}},\bar{x}) = \bar{f}(t), \qquad (2\text{-}28)$$

μ = a small parameter

The matrices $C^{(o)}$ and $K^{(o)}$ are respectively the damping matrix and the stiffness matrix of the system due to the linear part of the damping forces and the spring forces, and $\mu\bar{g}(\bar{x},\dot{\bar{x}})$ represents the nonlinear forces of the system. Here, $\bar{f}(t)$ is a stationary Gaussian random vector. Without loss of generality, one can assume that the mean vector of $\bar{f}$ $\bar{m}_{\bar{f}} = 0$.

In using this approach, the following two conditions must be satisfied: (1) the linear system obtained by neglecting the nonlinear term $\bar{g}(\dot{\bar{x}},\bar{x})$ in (2-28) must possess normal modes; (2) the correlation function matrix $R_{\bar{f}}(\tau)$ must be diagonalized by the same matrix which diagonalizes the matrices M, $C^{(o)}$ and $K^{(o)}$.

The second condition is quite restrictive and is seldom realized in real systems.

Assume that the above restriction can be met, then there exists a matrix A such that

$$
\begin{aligned}
&A^T M A = I \\
&A^T K(o) A = \Omega(o),\ w_{kj}(o) = w_k(o)\delta_{kj} \\
&A^T C(o) A = \Lambda(o),\ \lambda_{kj}(o) = \lambda_k(o)\delta_{kj} \\
&A^T R_f(\tau) A = D(\tau),\ d_{kj} = d_k(\tau)\delta_{kj}\,.
\end{aligned}
\tag{2-29}
$$

By using the transformation $\bar{x} = A\bar{z}$, Eq. (2-28) reduces to

$$
\ddot{\bar{z}} + \Lambda(o)\dot{\bar{z}} + \Omega(o)\bar{z} + \mu A^T g(\dot{\bar{z}},\bar{z}) = A^T \bar{f}(\tau) = \bar{b}(t) \tag{2-30a}
$$

Where the correlation function matrix of $\bar{b}$ is

$$
R_{\bar{b}}(\tau) = D(\tau)\,. \tag{2-30b}
$$

In component form Eq. (2-30a) becomes

$$
\ddot{z}_j + \lambda_j(o) z_j + (w_j(o))^2 z_j + \sum_{k=1}^{n} a_{kj} g_k(\dot{\bar{z}},z) = b_j(t) \tag{2-31a}
$$

and Eq. (2-30b) becomes

$$
E[b_k(t) b_j(t+\tau)] = d_k(\tau)\delta_{kj},\ j,\ k = 1,\ \ldots\ n\,. \tag{2-31b}
$$

The differential equation in (2-31a) may be written as

$$
\begin{aligned}
&\ddot{z}_j + \lambda_j \dot{z}_j + w_j^2 z_j + e_j(\dot{\bar{z}},\bar{z}) = b_j(t) \\
&\qquad\qquad j = 1,\ \ldots\ n
\end{aligned}
\tag{2-32}
$$

where the deficiency term e_j is given by

$$
\begin{aligned}
e_j = {} & (\lambda_j(o) - \lambda_j)\dot{z}_j + [(w_j(o))^2 - w_j^2] z_j \\
& + \mu \sum_{k=1}^{n} a_{kj} g_k(\dot{\bar{z}},\bar{z}),\ j = 1,\ \ldots\ n
\end{aligned}
\tag{2-33}
$$

If the quantities λ_j and w_j^2 are chosen in such a way that some measure of the deficiency term is minimized, then it seems reasonable that the statistics of the response of the nonlinear system can be approximated by those of the linear system described by

$$
\ddot{z}_j + \lambda_j \dot{z}_j + w_j^2 z_j = b_j(t),\ j = 1,\ \ldots\ n \tag{2-34}
$$

At this stage, the differential equations are uncoupled and the excitation $\bar{b}(t)$ is an uncorrelated vector process. Hence each uncoupled differential equation can be solved separately.

In order to determine λ_j and w_j^2, Caughey [11] chose them so as to minimize the mean square value of the deficiency term $\bar{e}$. This can be achieved by requiring that

$$\left.\begin{aligned} &\frac{\partial}{\partial x_j} E[\bar{e}^T\bar{e}] = 0 \\ &\frac{\partial}{\partial (w_j^2)} E[\bar{e}^T\bar{e}] = 0 \end{aligned}\right\} j = 1, \ldots n. \tag{2-35}$$

Substituting (2-33) in (2-35) and interchanging the order of differentiation and expectation, we obtain

$$\begin{aligned} \lambda_j &= \lambda_j^{(o)} + \mu \sum_{k=1}^{n} a_{kj} E[z_j g_k(\dot{\bar{z}},\bar{z})]/E[\dot{z}_j^2] \\ w_j^2 &= (w_j^{(o)})^2 + \mu \sum_{k=1}^{n} a_{kj} E[z_j E[z_j g_k(\dot{\bar{z}},\bar{z})] \\ &\qquad /E[z_j^2] . \end{aligned} \tag{2-36}$$

Equations (2-34) and (2-36) can be used to find various mean square values of the response process.

In certain cases, the contribution from the first mode may be dominant. In these cases, we may let $x_j = a_{j1} z_1$ in the above derivation. Then

$$\begin{aligned} w_1^2 &= (w_1^{(o)})^2 + \mu \sum_{j=1}^{n} a_{j1} E[z_1 g_j(\dot{z}_1, z_1)]/E[z_1^2] \\ \lambda_1 &= \lambda_1^0 + \mu \sum_{j=1}^{n} a_{j1} E[\dot{z}_1 g_j(\dot{z}_1, z_1)]/E[\dot{z}_1^2] . \end{aligned} \tag{2-37}$$

This is rather a rough approximation, but it is very simple and in some cases, it does give reasonably approximate solutions.

Perturbation Approach

Consider the same problem as defined in the previous section, whose equations of motion are

$$M\ddot{\bar{x}} + C^{(o)}\dot{\bar{x}} + K^{(o)}\bar{x} + \mu\bar{g}(\dot{\bar{x}},x) = \bar{f}(t) \tag{2-38}$$

Assume that μ is so small that the solution of Eq. (2-38) can be approximately represented by [12]

$$\bar{x} = \bar{x}_0 + \mu\bar{x}_1 \tag{2-39}$$

Substituting (2-39) into (2-38), neglecting terms involving μ^2, μ^3, ... and equating corresponding coefficients of μ^0 and μ^1 yields the following sets of linear differential equations:

$$M\ddot{\bar{x}}_0 + C^{(o)}\dot{\bar{x}}_0 + K^{(o)}\bar{x}_0 = \bar{f}(t) \tag{2-40a}$$

$$M\ddot{\bar{x}}_1 + C^{(o)}\dot{\bar{x}}_1 + K^{(o)}\bar{x}_1 = -\bar{g}(\dot{\bar{x}}_0(t),\bar{x}_0(t)) \tag{2-40b}$$

Correct to the same order of accuracy, the instantaneous correlation matrix for displacement becomes

$$E[\bar{x}\bar{x}^T] = E[\bar{x}_0\bar{x}_0^T] + \mu\{E[\bar{x}_0\bar{x}_1^T] + E[\bar{x}_1\bar{x}_0^T]\}. \tag{2-41}$$

Note that

$$E[\bar{x}_0\bar{x}_1^T] = (E[\bar{x}_0\bar{x}_1^T])^T. \tag{2-42}$$

The matrix $E[\bar{x}_0\bar{x}_0^T]$ can be found from (2-40a) by the various approaches as in linear analysis, and $E[\bar{x}_0\bar{x}_1^T]$ may be evaluated as follows. Since (2-40a) and (2-40b) are linear, their stationary solutions are

$$\bar{x}_0 = \int_{-\infty}^{\infty} G(t-\tau)\bar{f}(\tau)d\tau \tag{2-43a}$$

$$\bar{x}_1 = \int_{-\infty}^{\infty} G(t-\tau)\bar{g}(\tau)d\tau \,, \tag{2-43b}$$

where $G(t)$ is the common impulse response function matrix of (2-40a) and (2-40b) and $g(\tau)$ is the abbreviation of $\bar{g}(\dot{x}_0(\tau),x_0(\tau))$. Thus,

$$E[\bar{x}_0\bar{x}_1^T] = -\int_{\infty}^{\infty}\int_{-\infty}^{\infty} G(t-\tau_1)E[\bar{f}(\tau_1)\bar{g}^T(\tau_2)]$$

$$\times\, G^T(t-\tau_2)d\tau_1 d\tau_2 \,. \tag{2-44}$$

The matrix $E[\bar{f}(\tau_1)\bar{g}^T(\tau_2)]$ can be evaluated with the help of properties of Gaussian processes. Therefore, we can find $E[\bar{x}_0\bar{x}_1^T]$ and hence $E[\bar{x}\bar{x}^T]$.

Usually, the evaluation of the integrals in (2-44) is not easy, so Tung [13] has developed a different approach to generate $E[\bar{x}\bar{x}^T]$ from (2-40a) and (2-40b). He applies Foss's method [14] to uncouple (2-40a) and (2-40b) into first order differential equations and then solves the resulting equations to find the various instantaneous correlation matrices.

This approach will fail if the damping matrix $C^{(o)}$ is a null matrix. In this case, Equation (2-40a) does not have a stationary solution since all its correlation functions will finally go to infinity. Another limitation of this approach is that not only must the nonlinearity of the system has to be small, but also the excitation has to be sufficiently low.

Generalized Equivalent Linearization

The normal mode approach is quite powerful if it applies. However, due to the conditions imposed on the excitation, its application

is rather limited.

In his thesis Yang [15] introduced a more general approach. Except that the excitation must be stationary, the only additional restriction to this approach is that the excitation be Gaussian. In this approach, we define an auxiliary set of linear differential equations for the original nonlinear system. The solution of the original nonlinear system is approximated by the solution of an auxiliary set and the unknown co-efficients are chosen in such a way that some measure of the difference between the two sets of equations is a minimum.

Consider the following linear equation

$$M\ddot{\bar{x}} + C\dot{\bar{x}} + K\bar{x} = \bar{f}(t) \tag{2-45}$$

and the nonlinear system given by

$$M\ddot{\bar{x}} + \bar{g}(\dot{\bar{x}},\bar{x}) = \bar{f}(t). \tag{2-46}$$

The difference between (2-46) and (2-45)

$$\bar{e} = g(\dot{\bar{x}},\bar{x}) - C\dot{\bar{x}} - K\bar{x} \tag{2-47}$$

The necessary conditions to minimize $E[\bar{e}^T\bar{e}]$ are given by

$$\begin{aligned} \frac{\partial E[\bar{e}^T\bar{e}]}{\partial c_{jk}} &= 2E\left[\bar{e}^T \frac{\partial \bar{e}}{\partial c_{jk}}\right] = 2E[e_j\dot{x}_k] = 0 \\ \frac{\partial E[\bar{e}^T\bar{e}]}{\partial k_{jk}} &= 2E\left[\bar{e}^T \frac{\bar{e}}{\partial k_{jk}}\right] = 2E[e_j x_k] = 0. \end{aligned} \tag{2-48}$$

Upon using Eq. (2-47), they become in the matrix form

$$\begin{aligned} E[\bar{e}\dot{\bar{x}}^T] &= E[\bar{g}(\dot{\bar{x}},\bar{x})\dot{\bar{x}}^T] - E[\ddot{\bar{x}}\dot{\bar{x}}^T] - KE[\bar{x}\dot{\bar{x}}^T] = 0 \\ E[\bar{e}\bar{x}^T] &= E[\bar{g}(\dot{\bar{x}},\bar{x})\bar{x}^T] - CE[\ddot{\bar{x}}\bar{x}^T] - KE[\dot{\bar{x}}\bar{x}^T] = 0 \end{aligned} \tag{2-49}$$

It has been shown that the conditions in Eq. (2-49) do define a minimum for $E[\bar{e}^T\bar{e}]$[15].

In order to solve Eq. (2-49) for K and C, it is first necessary to express $E[\bar{g}(\dot{\bar{x}},\bar{x})\bar{x}^T]$ and $E[\bar{g}(\dot{\bar{x}},\bar{x})\dot{\bar{x}}^T]$ in terms of $E[\bar{x}\bar{x}^T]$, $E[\bar{x}\dot{\bar{x}}^T]$ and $E[\dot{\bar{x}}\dot{\bar{x}}^T]$. Let y_{kr} denote the displacement of k th mass relative to the r th mass and let the approximate force acting on the k th mass by the nonlinear element connecting the k th mass and the r th mass be denoted by $S_{kr}(\dot{y}_{kr},y_{kr})$. Then

$$\begin{aligned} E[g_k(\dot{\bar{x}},\bar{x})x_j] &= \sum_{\substack{r \\ r\neq k}} E[S_{kr}(\dot{y}_{kr},y_{kr})x_j] \\ E[g_k(\dot{\bar{x}},\bar{x})\dot{x}_j] &= \sum_{\substack{r \\ r\neq k}} E[S_{kr}(\dot{y}_{kr},y_{kr})\dot{x}_j] , \end{aligned} \tag{2-50}$$

where the sum is taken over all nonlinear elements connected to the k th mass. Since $\bar{x}$ is a Gaussian vector, it follows that the quantities $\dot{y}_{kr}$, y_{kr}, x_j, and $\dot{x}_j$ will be Gaussian distributed. Hence

$$\begin{aligned} E[S_{kr}(\dot{y}_{kr},y_{kr})x_j] &= E[S_{kr}(\dot{y}_{kr},y_{kr})\dot{y}_{kr}] \\ &\quad \times E[\dot{y}_{kr}x_j]/E[\dot{y}_{kr}^2] \\ &\quad + E[S_{kr}(\dot{y}_{kr},y_{kr})y_{kr}]\cdot E[y_{kr}x_j]/E[y_{kr}^2] \\ E[S_{kr}(\dot{y}_{kr},y_{kr})\dot{x}_j] &= E[S_{kr}(\dot{y}_{kr},y_{kr})\dot{y}_{kr}] \\ &\quad \times E[\dot{y}_{kr}\dot{x}_j]/E[\dot{y}_{kr}^2] \\ &\quad + E[S_{kr}(\dot{y}_{kr},y_{kr})y_{kr}]\cdot E[y_{kr}\dot{x}_j]/E[y_{kr}^2] . \end{aligned} \tag{2-51}$$

Define

$$\begin{aligned} \gamma_{kr} &= E[S_{kr}(\dot{y}_{kr},y_{kr})\dot{y}_{kr}]/E[\dot{y}_{kr}^2] \\ X_{kr} &= E[S_{kr}(\dot{y}_{kr},y_{kr})y_{kr}]/E[y_{kr}^2] \end{aligned} \qquad k\neq r . \tag{2-52}$$

Then Eq. (2-51) reduces to

$$\begin{aligned} E[S_{kr}(\dot{y}_{kr},y_{kr})x_j] &= E[(\gamma_{kr}\dot{y}_{kr} + X_{kr}y_{kr})x_j] \\ E[S_{kr}(\dot{y}_{kr},y_{kr})\dot{x}_j] &= E[(\gamma_{kr}\dot{y}_{kr} + X_{kr}y_{kr})\dot{x}_j] \end{aligned} \tag{2-53}$$

Hence, there exists a linear system with spring constant X_{kr} and damping co-efficient γ_{kr} defined by Eq. (2-52) such that if the nonlinear system is replaced by this linear system, the expectation values $E[\bar{g}(\dot{\bar{x}},\bar{x})\bar{x}^T]$ and $E[\bar{g}(\dot{\bar{x}},\bar{x})\dot{\bar{x}}^T]$ will not be changed. Substituting Eq. (2-53) in Eq. (2-50) gives

$$\begin{aligned} E[\bar{g}_k(\dot{\bar{x}},\bar{x})x_j] &= E[\sum_{\substack{r \\ r\neq k}}(\gamma_{kr}y_{kr} + X_{kr}y_{kr})x_j] \\ E[\bar{g}_k(\dot{\bar{x}},\bar{x})\dot{x}_j] &= E[\sum_{\substack{r \\ r\neq k}}(\gamma_{kr}\dot{y}_{kr} + X_{kr}y_{kr})\dot{x}_j] \end{aligned} \tag{2-54}$$

Let the stiffness matrix and the damping matrix of the linear system defined by Eq. (2-52) be denoted by $K^{(e)}$ and $C^{(e)}$. Then Eq. (2-54) can also be written as

$$\begin{aligned} E[g_k(\dot{\bar{x}},\bar{x})x_j] &= E[\sum_{s=1}^{n}(C_{ks}^{(e)}x_s + K_{ks}^{(e)}x_s)x_j] \\ E[g_k(\dot{\bar{x}},\bar{x})\dot{x}_j] &= E[\sum_{s=1}^{n}(C_{ks}^{(e)}x_s + K_{ks}^{(e)}x_s)\dot{x}_j] \end{aligned} \tag{2-55}$$

since the right-hand side of (2-54) and (2-55) are just two different representations of the total force acting on the k th mass. In matrix form Eq. (2-55) becomes

$$\begin{aligned} E[\bar{g}(\dot{\bar{x}},\bar{x})\bar{x}^T] &= C^{(e)}E[\dot{\bar{x}}\bar{x}^T] + K^{(e)}E[\bar{x}\bar{x}^T] \\ E[\bar{g}(\dot{\bar{x}},\bar{x})\dot{\bar{x}}^T] &= C^{(e)}E[\dot{\bar{x}}\dot{\bar{x}}^T] + K^{(e)}E[\bar{x}\dot{\bar{x}}^T] \end{aligned} \tag{2-56}$$

Substituting Eq. (2-56) in Eq. (2-49) and solving for K and C which minimizes $E[\bar{e}^T\bar{e}]$, yields

$$\begin{aligned} (K - K^{(e)})E[\bar{x}\bar{x}^T] + (C - C^{(e)})E[\dot{\bar{x}}\bar{x}^T] &= 0 \\ (K - K^{(e)})E[\bar{x}\dot{\bar{x}}^T] + (C - C^{(e)})E[\dot{\bar{x}}\dot{\bar{x}}^T] &= 0 \end{aligned} \tag{2-57}$$

which can also be written as

$$\begin{bmatrix} E[\bar{x}\bar{x}^T] & E[\bar{x}\dot{\bar{x}}^T] \\ E[\dot{\bar{x}}\bar{x}^T] & E[\dot{\bar{x}}\dot{\bar{x}}^T] \end{bmatrix} \begin{bmatrix} (K - K^{(e)})^T \\ (C - C^{(e)})^T \end{bmatrix} = 0. \tag{2-58}$$

If the square matrix is non-singular, the only solution to Eq. (2-58) is

$$\begin{aligned} K &= K^{(e)} \\ C &= C^{(e)}. \end{aligned} \tag{2-59}$$

If the square matrix is singular, (2-59) is not the only solution. But in this case any solution to Eq. (2-58) will lead to the same minimum for $E[\bar{e}\bar{e}^T]$. So we still can use Eq. (2-59).

Thus, it has been shown that the linear system formed by replacing each nonlinear element by a linear spring and a linear damper defined by Eq. (2-52) will minimize $E[\bar{e}\bar{e}^T]$ provided that the excitation is Gaussian.

It should be pointed out that the smallness of the nonlinear term in the original equation was not a presupposition in the development of the above method. In general, the accuracy of this method depends on the smallness of the nonlinearity. When the nonlinear terms are not small, this method is often an iterative procedure.

This concludes the relevant literature survey. In the light of the review study in this chapter, we will be better able to appreciate, in the next chapters, the power and usefulness of the simulation approach in the analysis of random linear and nonlinear problems.

CHAPTER III

DISCUSSION OF SIMULATION METHODS

In this chapter we will present two methods to simulate a set of Gaussian processes $\{f_1(t), f_2(t), \ldots f_m(t), \ldots f_M(t)\}$ when the power spectral density function of each process and cross spectral density functions between any two processes are known. These spectral densities are usually arranged in the form of a matrix commonly known as spectral matrix. This matrix is given by

$$\tilde{G}(w) = \begin{bmatrix} G_{11}(w) & G_{12}(w) & \ldots & G_{1M}(w) \\ G_{21}(w) & G_{22}(w) & \ldots & G_{2M}(w) \\ \ldots\ldots & \ldots\ldots & & \ldots\ldots \\ G_{M1}(w) & G_{M2}(w) & \ldots & G_{MM}(w) \end{bmatrix} \tag{3-1}$$

where $G_{mn}(w)$ is the one-sided cross spectral density between the process $f_m(t)$ and $f_n(t)$. When $m \neq n$, $G_{mn}(w)$ is complex with real part $C_{mn}(w)$ called the co-spectrum and imaginary part - $Q_{mn}(w)$ called the quad-spectrum. When $m = n$, the quad-spectrum is zero and then $G_{mn}(w)$ stands for power spectrum for that particular process.

I. Trigonometric Model

Here we will show that a set of random processes can be simulated by a trigonometric series of the form

$$f_1(t) = \sum_{k=1}^{N} \{a_{11}(k)\cos [w_k t + \alpha_{11}(k)] + b_{11}(k)\sin [w_k t + \alpha_{11}(k)]\} \tag{3-2a}$$

$$f_2(t) = \sum_{k=1}^{N} \{a_{21}(k)\cos\,[w_k t + \alpha_{21}(k)] + b_{21}(k)\sin\,[w_k t + \alpha_{21}(k)]$$

$$+ \{a_{22}(k)\cos\,[w_k t + \alpha_{22}(k)] + b_{22}(k)\sin\,[w_k t + \alpha_{22}(k)]\} \tag{3-2b}$$

.

.

.

$$f_m(t) = \sum_{k=1}^{N} \{a_{m1}(k)\cos\,[w_k t + \alpha_{m1}(k)] + b_{m1}(k)\sin\,[w_k t + \alpha_{m1}(k)]$$

$$+ a_{m2}(k)\cos\,[w_k t + \alpha_{m2}(k)] + b_{m2}(k)\sin\,[w_k t + \alpha_{m2}(k)]$$

$$+ \quad . \quad . \quad .$$

$$+ a_{mm}(k)\cos\,[w_k t + \alpha_{mm}(k)] + b_{mm}(k)\sin\,[w_k t + \alpha_{mm}(k)]. \tag{3-2c}$$

More generally, the above set of processes can be represented as

$$f_m(t) = \sum_{p=1}^{m} \sum_{k=1}^{N} \{a_{mp}(k)\cos\,[w_k t + \alpha_{mp}(k)]$$

$$+ b_{mp}(k)\sin\,[w_k t + \alpha_{mp}(k)]. \tag{3-3}$$

The coefficients $a_{mp}(k)$ and $b_{mp}(k)$ are Gaussian random variables with zero mean that have the following additional properties: (i) $a_{mp}(k)$ and $b_{nq}(\ell)$ are always independent and for the case when $m = n$, $p = q$ and $k = \ell$ they are identically distributed, (ii) $a_{mp}(k)$ and $a_{nq}(\ell)$ (or $b_{mp}(k)$ and $b_{nq}(\ell)$) are statistically correlated if $p = q$ and $k = \ell$, otherwise they are independent.

The phase angles $\alpha_{mp}(k)$ are deterministic. Since the coefficients $a_{mp}(k)$ and $b_{nq}(k)$ are Gaussian distributed it follows from

the Central Limit Theorem that the time series $f_m(t)$ will also be Gaussian distributed.

The form of the simulated time series given by Eq. (3-3) lends itself to a very simple physical interpretation. For the first time series (m = 1) the index of summation p takes the value of unity. For the second time series (m = 2) the index p takes the values unity and two. The value of p = 2 adds to the second series two terms that are independent of the first series. Physically it adds some energy to the second process independent of the first process. Likewise for each new process two additional terms are tacked on which allow that process to have some energy that is independent of all the previous processes.

In order to see how the co-efficients $a_{mp}(k)$ and $b_{nq}(\ell)$, and the phase angles $\alpha_{mp}(k)$ should be determined it is necessary to consider the cross correlation between the time series $f_m(t)$ and $f_n(t)$. Here for convenience we will assume $m \leq n$. The cross correlation between these time series is given by

$$R_{mn}(\tau) = E[f_m(t)f_n(t+\tau)]$$

$$= E\Big[\sum_{p=1}^{m}\sum_{q=1}^{n}\sum_{k=1}^{N}\sum_{\ell=1}^{N}$$

$$\{a_{mp}(k)a_{nq}(\ell)\cos[w_k t + \alpha_{mp}(k)]\cos[w_\ell(t+\tau) + \alpha_{nq}(\ell)]$$

$$+ a_{mp}(k)b_{nq}(\ell)\cos[w_k t + \alpha_{mp}(k)]\sin[w_\ell(t+\tau) + \alpha_{nq}(\ell)]$$

$$+ b_{mp}(k)a_{nq}(\ell)\sin[w_k t + \alpha_{mp}(k)]\cos[w_\ell(t+\tau) + \alpha_{nq}(\ell)]$$

$$+ b_{mp}(k)b_{nq}(\ell)\sin[w_k t + \alpha_{mp}(k)]\sin[w_\ell(t+\tau) + \alpha_{nq}(\ell)]\}] \quad (3\text{-}4)$$

The expectation operator can be brought inside the summations, and since the expectation of a sum is the sum of the expectations, we get

$$R_{mn}(\tau) = \sum_{p=1}^{m} \sum_{q=1}^{n} \sum_{k=1}^{N} \sum_{\ell=1}^{N}$$

$$\{E[a_{mp}(k)a_{nq}(\ell)]\cos\,[w_k t + \alpha_{mp}(k)]\cos\,[w_k(t+\tau) + \alpha_{nq}(\ell)]$$

$$+ E[a_{mp}(k)b_{nq}(\ell)]\cos\,[w_k t + \alpha_{mp}(k)]\sin\,[w_\ell(t+\tau) + \alpha_{nq}(\ell)]$$

$$+ E[b_{mp}(k)a_{nq}(\ell)]\sin\,[w_k t + \alpha_{mp}(k)]\cos\,[w_\ell(t+\tau) + \alpha_{nq}(\ell)]$$

$$+ E[b_{mp}(k)b_{nq}(\ell)]\sin\,[w_k t + \alpha_{mp}(k)]\sin\,[w_\ell(t+\tau) + \alpha_{nq}(\ell)]\} \qquad (3\text{-}5)$$

Because $a_{mp}(k)$ and $b_{nq}(\ell)$ are always independent the middle terms in the above expression are both zero. Furthermore, since $a_{mp}(k)$ and $a_{nq}(\ell)$ (or $b_{mp}(k)$ and $b_{nq}(\ell)$) are independent unless $p = q$ and $k = \ell$, Eq. (3-5) reduces to $R_{mn}(\tau)$

$$R_{mn}(\tau) = \sum_{p=1}^{m} \sum_{k=1}^{N}$$

$$\{E[a_{mp}(k)a_{np}(k)]\cos\,[w_k t + \alpha_{mp}(k)]\cos\,[w_k(t+\tau) + \alpha_{np}(k)]$$

$$+ E[b_{mp}(k)b_{np}(k)]\sin\,[w_k t + \alpha_{mp}(k)]\sin\,[w_k(t+\tau) + \alpha_{np}(k)]\} \qquad (3\text{-}6)$$

Let $K_{mnp}(k) = E[a_{mp}(k)a_{np}(k)]$. That is $K_{mnp}(k)$ is the covariance between $a_{mp}(k)$ and $a_{np}(k)$. Because $b_{mp}(k)$ has the same distribution as $a_{mp}(k)$, we also have $K_{mnp}(k) = E[b_{mp}(k)b_{np}(k)]$. Using these relationships and a trigonometric identity Eq. (3-6) becomes

$$R_{mn}(\tau) = \sum_{p=1}^{m} \sum_{k=1}^{N} K_{mnp}(k)\cos\,[w_k\tau - \alpha_{mp}(k) + \alpha_{np}(k)] \qquad (3\text{-}7)$$

The right hand side of Eq. (3-7) is independent of the time t; therefore, the assumed trigonometric form for the time series yields stationary random processes.

Noting the fact that the spectral density is the Fourier Transform of the correlation function, the one-sided cross-spectral density for processes $f_m(t)$ and $f_n(t)$ is given by

$$G_{mn}(w) = \begin{cases} 2\int_{-\infty}^{\infty} R_{mn}(\tau)e^{-jw\tau}d\tau, & w \geq 0 \\ 0, & w < 0 \end{cases} \tag{3-8}$$

The next step is to substitute Eq. (3-7) into Eq. (3-8) and perform the integration. However, it should be recalled that $K_{mnp}(k)$ in Eq. (3-7) is the expected value of $a_{mp}(k)$ times $a_{np}(k)$ (or $b_{mp}(k)$ times $b_{np}(k)$). Therefore, by substituting Eq. (3-7) into Eq. (3-8) what we obtain is an expected value for the cross-spectral density. Thus we have

$$E[G_{mn}(w)] = \begin{cases} 2\sum_{p=1}^{m}\sum_{k=1}^{N}\{K_{mnp}(k) \\ \quad x\int_{-\infty}^{\infty}\cos[w_k\tau - \alpha_{mp}(k) + \alpha_{np}(k)]e^{-jw\tau}d\tau\} \\ \qquad\qquad w \geq 0 \\ 0, \quad w < 0 \end{cases} \tag{3-9}$$

Carrying out the integration gives

$$E[G_{mn}(w)] = \begin{cases} 2\pi\sum_{p=1}^{m}\sum_{k=1}^{N}K_{mnp}(k)\delta(w - w_k) \\ \quad x\{\cos[\alpha_{mp}(k) - \alpha_{np}(k)] - j\sin[\alpha_{mp}(k) - \alpha_{np}(k)]\}, \quad w \geq 0 \\ 0, \quad w < 0 \end{cases} \tag{3-10}$$

where $\delta(w - w_k)$ is the Dirac delta function.

We thus see that for the assumed trigonometric time series given by Eq. (3-3) G_{mn} is composed of both real and imaginary terms. When $m = n$, G_{mn} corresponds to a power spectral density and the imaginary portion is zero. A schematic plot of Eq. (3-10) is shown in Figure 1. The frequencies w_k are chosen such that

$$w_k = w_\ell + (k - \frac{1}{2})\Delta w, \quad k = 1, 2, \ldots N$$

$$\Delta w = \frac{w_u - w_\ell}{N} \tag{3-11}$$

where w_u and w_ℓ are respectively the upper and lower cut off frequencies of the spectra that is used to generate the time series. Suppose an actual power spectrum $G(w)$ for which we want to obtain a simulated time series is shown in Figure 2. We can slice this spectrum up into N intervals of width Δw as shown. The amount of energy contained in the slice centered at $w = w_k$ is $G(w_k)\Delta w$. We want the expected value of the spectrum corresponding to our simulated time series to have the same amount of energy at $w = w_k$. This means that the expected amplitude of the delta function at $w = w_k$ should be $G(w)\Delta w$. Similar criteria must be applied for the cross-spectra of the simulated time series.

We assume that at any frequency $w = w_k$ the cross-spectral matrix can be factored into an upper and lower triangular matrix, where the upper triangular matrix is the complex transpose of the lower triangular matrix, as indicated below:

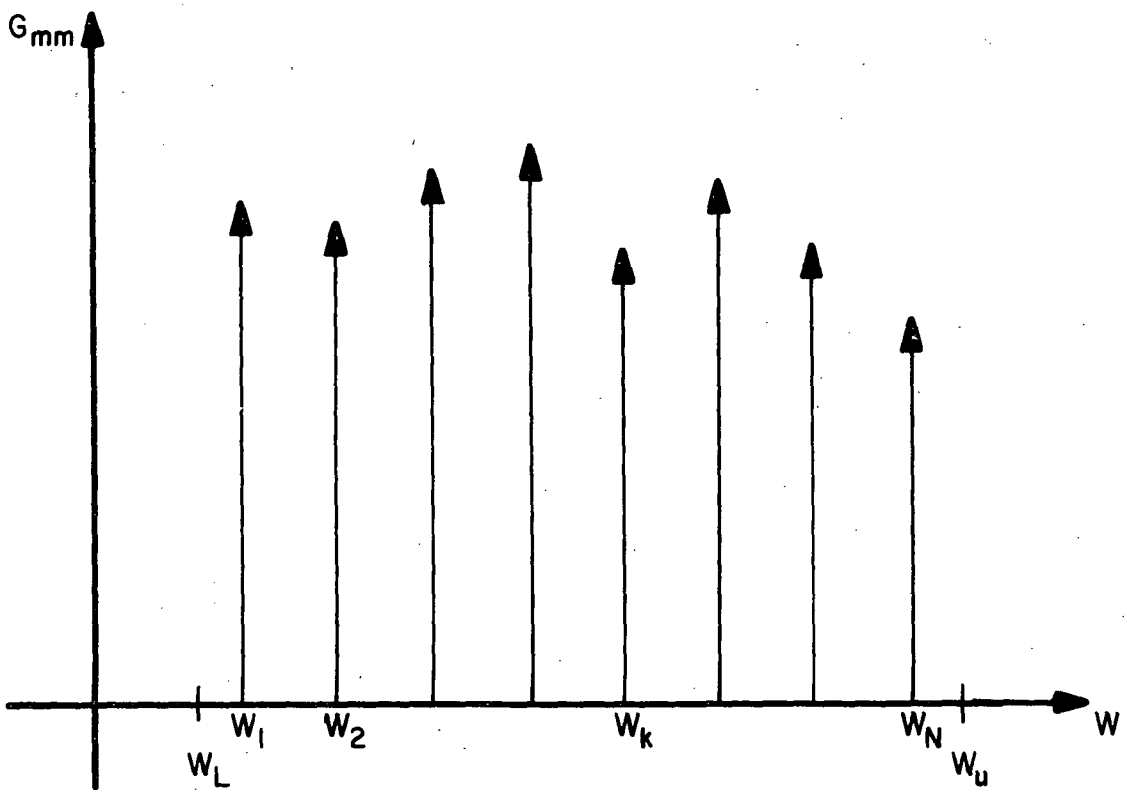

Fig. 1. Schematic sketch of a discrete power spectrum from a simulated time series.

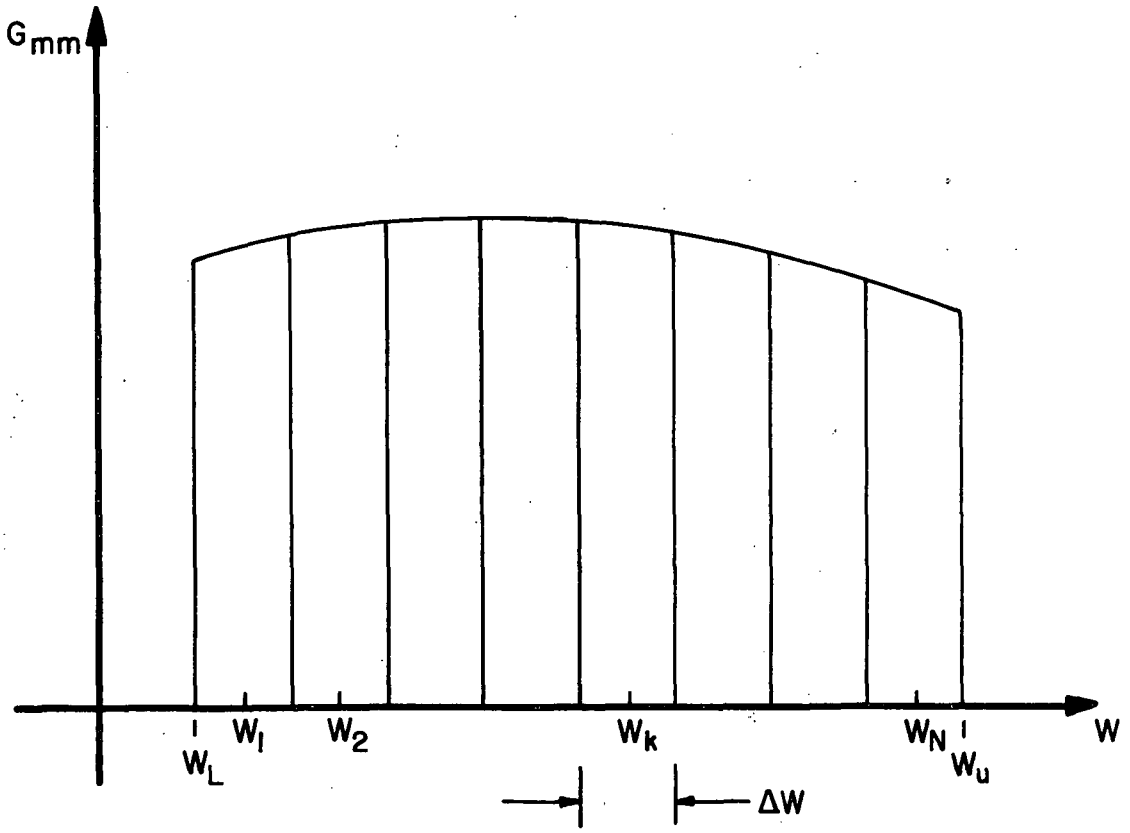

Fig. 2. Schematic sketch of a continuous power spectrum used to generate a time series

$$\begin{bmatrix} G_{11}(w_k) & G_{12}(w_k) & \cdots & G_{1M}(w_k) \\ G_{21}(w_k) & G_{22}(w_k) & \cdots & G_{2M}(w_k) \\ \cdots & \cdots & \cdots & \cdots \\ G_{M1}(w_k) & G_{M2}(w_k) & \cdots & G_{MM}(w_k) \end{bmatrix} =$$

$$\begin{bmatrix} H_{11}(w_k) & 0 & \cdots & 0 \\ H_{21}(w_k) & H_{22}(w_k) & \cdots & 0 \\ \cdots & \cdots & \cdots & \cdots \\ H_{M1}(w_k) & H_{M2}(w_k) & \cdots & H_{MM}(w_k) \end{bmatrix} \begin{bmatrix} \overline{H}_{11}(w_k) & \overline{H}_{21}(w_k) & \cdots & \overline{H}_{M1}(w_k) \\ 0 & \overline{H}_{22}(w_k) & \cdots & \overline{H}_{M2}(w_k) \\ \cdots & \cdots & \cdots & \cdots \\ 0 & 0 & & \overline{H}_{MM}(w_k) \end{bmatrix} \tag{3-12}$$

The bar is used to denote the complex conjugate.

If Eq. (3-12) holds then

$$G_{mn}(w) = \sum_{p=1}^{n} H_{mp}(w)\overline{H}_{np}(w) \tag{3-13}$$

for $n \leq m$. Eq. (3-13) can be rewritten with the limit of summation taken as m instead of n since $H_{mn}(w) = 0$ for $m > n$. Thus Eq. (3-13) becomes

$$G_{mn}(w) = \sum_{p=1}^{m} H_{mp}(w)\overline{H}_{np}(w) \tag{3-14}$$

Using the above relation, solutions are obtained as

$$H_{mm}(w_k) = \left[\frac{D_m(w_k)}{D_{m-1}(w_k)}\right]^{\frac{1}{2}}, \quad m = 1, 2, \ldots M \tag{3-15}$$

where $D_m(w_k)$ is the m th principal minor of $\tilde{G}(w_k)$ with D_0 being defined as unity, and

$$H_{mp}(w_k) = H_{pp}(w_k) \frac{G_{\substack{1, 2, \ldots, p-1, m \\ 1, 2, \ldots, p-1, p}}}{D_k(w)}, \qquad (3\text{-}16)$$

$$p = 1, 2, \ldots M, \; m = p + 1, \ldots M$$

where,

$$G_{\substack{1, 2, \ldots, p-1, m \\ 1, 2, \ldots, p-1, p}} = \begin{vmatrix} G_{11} & G_{12} \cdots G_{1,p-1} & G_{1p} \\ G_{21} & G_{22} \cdots G_{2,p-1} & \\ \cdots & \cdots & \\ G_{p-1,1} & G_{p-1,2} \cdots G_{p-1,p-1} & G_{p-1,p} \\ G_{m1} & G_{m2} \cdots G_{m,p-1} & G_{mp} \end{vmatrix}$$

is the determinant of a submatrix obtained by deleting all elements except (1, 2, ... p-1, m) th rows and (1, 2, ... p-1, p) th columns of $\tilde{G}(w_k)$.

It is noted that the above solutions are valid only when the matrix $G(w)$ is Hermitian and positive definite, as can be seen from Eq. (3-15).

Because the cross-spectral density matrix $\tilde{G}(w)$ is known to be only non-negative definite, special consideration is needed in those cases where $\tilde{G}(w)$ has a zero principal minor. This is discussed in Appendix C.

For the band of frequency $[w_k - \frac{1}{2}\Delta w, w_k + \frac{1}{2}\Delta w]$ we want the expected value of the energy in the spectrum of the simulated time series to be equal to the energy $G_{mn}(w)\Delta w$ of the original spectrum. Thus equating the energy in the band centered at $w = w_k$ as given by Eqs. (3-10) and (3-14) we get

$$2\pi K_{mnp}(k)\{\cos [\alpha_{mp}(k) - \alpha_{np}(k)] - j \sin [\alpha_{mp}(k) - \alpha_{np}(k)]\}$$
$$= H_{mp}(w_k)\bar{H}_{np}(w_k)\Delta w \qquad (3\text{-}17)$$

If we write

$$H_{mp}(w_k) = |H_{mp}(w_k)|\, e^{-j\alpha_{mp}(k)} \tag{3-18a}$$

$$= |H_{mp}(w_k)|[\cos \alpha_{mp}(k) - j \sin \alpha_{mp}(k)] \tag{3-18b}$$

$$= RE[H_{mp}(w_k)] + j\ IM[H_{mp}(w_k)] \tag{3-18c}$$

then by substituting Eq. (3-18a) into Eq. (3-17) we can see that

$$K_{mnp}(k) = \frac{\Delta w}{2\pi}|H_{mp}(w_k)||\overline{H}_{np}(w_k)| \tag{3-19}$$

From Eqs. (3-18b) and (3-18c) we find

$$\alpha_{mp}(k) = - \tan^{-1}\left\{\frac{IM[H_{mp}(w_k)]}{RE[H_{mp}(w_k)]}\right\} \tag{3-20}$$

Thus it follows, as stated earlier, that the phase angles are deterministic.

We recall that

$$K_{mnp}(k) = \begin{cases} E[a_{mp}(k)a_{np}(k)] & (3\text{-}21a) \\ \text{or} & \\ E[b_{mp}(k)b_{np}(k)] & (3\text{-}21b) \end{cases}$$

That is we want $a_{mp}(k)$ and $b_{mp}(k)$ to be independent random variables with their covariances given by the right hand side of Eq. (3-19). This can be done in the following manner, if we let

$$a_{mp}(k) = \frac{\Delta w}{2\pi}|H_{mp}(w_k)|\xi_p \tag{3-22a}$$

and

$$b_{mp}(k) = \frac{\Delta w}{2\pi}|H_{mp}(w_k)|\eta_p \tag{3-22b}$$

where $m = 1, 2, \ldots M$; $p = m, m + 1, \ldots M$ and ξ_p and η_p are independent Gaussian random variables generated on a digital computer. Because the ξ's and η's are Gaussian distributed, the a's and b's will also be Gaussian distributed.

Substituting Eq. (3-22a) in Eq. (3-21a) or Eq. (3-22b) in Eq. (3-21b) and taking the expectation of both sides we see that in order to make the left-hand-side equal to right-hand-side, the mean of ξ or η should be zero and their variances should be unity.

From Eq. (3-21a) we have

$$E[a_{mp}(k)] = \frac{\Delta w}{2\pi}|H_{mp}(w_k)|E[\xi_p] = 0 \tag{3-23a}$$

and

$$\begin{aligned} E[a_{mp}(k)a_{np}(k)] &= \frac{\Delta w}{2\pi}|H_{mp}(w_k)||H_{np}(w_k)|E[\xi_p{}^2] \\ &= \frac{\Delta w}{2\pi}|H_{mp}(w_k)|\overline{H}_{np}(w_k)|\cdot \end{aligned} \tag{3-23b}$$

Thus the terms $a_{mp}(k)$ (or $b_{mp}(k)$) satisfy the properties stated earlier and they also satisfy Eq. (3-17).

This concludes our explanation of how to simulate several multi-correlated time series.

After discussing the Fast Fourier Transform in the next section, we will give an example problem to check and compare the two methods.

II. Fast Fourier Transform (FFT) Method

Assume that a set of discrete time series can be represented by the following expression:

$$f_{pn} = \frac{1}{N}\sum_{k=0}^{N-1} X_{pk}\,EXP\left[j\,\frac{2\pi kn}{N}\right] \tag{3-24}$$

where,

p = number of time series
n = time index
k = frequency index

The terms X_{pk} are elements of a complex vector generated in the following way

$$\{X_{pk}\} = \left[\frac{N}{2h}\right]^{\frac{1}{2}} [H_k]\{\zeta_{pk}\} \tag{3-25}$$

where,

$h = \Delta t$, discrete time increment

$[H_k]$ is a lower triangular matrix obtained from the given spectrum matrix as discussed in the preceding section, that is, it satisfies the relation

$$[H_k][\bar{H}_k]^T = [G_k] \tag{3-26}$$

and, $\zeta_{pk} = \xi_{pk} + j\,\eta_{pk}$ (3-27)

where ξ_{pk} and η_{pk} are independent Gaussian random numbers such that

$$E[\xi_{pk}] = E[\eta_{pk}] = 0 \tag{3-28a}$$

$$E[\xi_{pk}^2] = E[\eta_{pk}^2] = 0.5 \tag{3-28b}$$

Writing Eq. (3-25) in expanded form

$$\begin{bmatrix} X_{1k} \\ X_{2k} \\ \vdots \\ X_{Mk} \end{bmatrix} = \left[\frac{N}{2h}\right]^{\frac{1}{2}} \begin{bmatrix} H_{11k} & 0 & \cdots & 0 \\ H_{21k} & H_{22k} & \cdots & 0 \\ \cdots & \cdots & \cdots & \cdots \\ H_{M1k} & H_{M2k} & \cdots & H_{MMk} \end{bmatrix} \begin{bmatrix} \zeta_{1k} \\ \zeta_{2k} \\ \vdots \\ \zeta_{Mk} \end{bmatrix} \tag{3-29a}$$

That is, we can write

$$X_{pk} = \left[\frac{N}{2h}\right]^{\frac{1}{2}} \sum_{q=1}^{M} H_{pqk}\zeta_{qk} \tag{3-29b}$$

$$\bar{X}_{r\ell} = \left[\frac{N}{2h}\right]^{\frac{1}{2}} \sum_{s=1}^{M} \bar{H}_{rs\ell}\bar{\zeta}_{s\ell} \tag{3-29c}$$

where the bar denotes complex conjugate.

Then,

$$E[X_{pk}\overline{X}_{r\ell}] = \frac{N}{2h} E[\sum_{q=1}^{M}\sum_{s=1}^{M} H_{pqk}\overline{H}_{rs\ell}\zeta_{qk}\overline{\zeta}_{s\ell}] \tag{3-30a}$$

Moving the expectation operator inside, we can write

$$E[X_{pk}\overline{X}_{r\ell}] = \frac{N}{2h} \sum_{q=1}^{M}\sum_{s=1}^{M} H_{pqk}\overline{H}_{rs\ell}E[\zeta_{qk}\zeta_{s\ell}] \tag{3-30b}$$

Making use of properties of complex random number as given in terms of ξ's and η's by Eqs. (3-28a) and (3-28b), it can be easily seen that

$$E[\zeta_{qk}\overline{\zeta}_{s\ell}] = \delta_{qs}\delta_{k\ell} \tag{3-30c}$$

where δ_{qs} and $\delta_{k\ell}$ are Kronecker delta functions; substituting (3-30c) into (3-30b), we get

$$E[X_{pk}\overline{X}_{r\ell}] = \frac{N}{2h} \sum_{q=1}^{M}\sum_{s=1}^{M} H_{pqk}\overline{H}_{rs\ell}\delta_{qs}\delta_{k\ell} \tag{3-31a}$$

$$= \frac{N}{2h} \sum_{q=1}^{M} H_{pqk}\overline{H}_{rq\ell}\delta_{k\ell} \tag{3-31b}$$

Taking the inverse Fourier Transform of Eq. (3-24), we get

$$X_{pk} = \sum_{n=0}^{N-1} f_{pn}\mathrm{EXP}[-j\,\frac{2\pi kn}{N}] \tag{3-32a}$$

Therefore,

$$X_{p(N-k)} = \sum_{n=0}^{N-1} f_{pn}\mathrm{EXP}[-j\,\frac{2\pi(N-k)n}{N}]$$

$$= \sum_{n=0}^{N-1} f_{pn}\mathrm{EXP}[j\,\frac{2\pi kn}{N}] \tag{3-32b}$$

Since f_{pn} is real, comparing Eqs. (3-32a) and (3-32b), we see that

$$X_{p(N-k)} = \overline{X}_{pk} \tag{3-33}$$

Thus, it is only necessary to generate $\frac{N}{2}$ values of X for each time series because the other half of the values of X are just the complex conjugate of the first half of the values of X.

Now, it is necessary to show that time series represented by Eq. (3-24) do indeed have the proper power and cross-spectral densities.

From Eq. (3-24)

$$f_{pn} = \frac{1}{N} \sum_{k=0}^{N-1} X_{pk} \text{EXP}[j \frac{2\pi nk}{N}]$$

Since f_{pn} is real, taking the complex conjugate on both sides of the above equation, we can write

$$f_{pn} = \frac{1}{N} \sum_{k=0}^{N-1} X_{pk} \text{EXP}[-j \frac{2\pi nk}{N}]. \tag{3-34a}$$

Thus, the cross correlation between time series p and time series r is given by

$$R_{pr}(n,m) = E[f_{pn} f_{rm}] \tag{3-34a}$$

where, n and m stand for the time indices of process p and process r respectively.

Substituting for f_{pn} and f_{rm} from Eq. (3-24) and Eq. (3-24a) respectively in Eq. (3-34a), we get

$$R_{pr}(n,m) = E[\frac{1}{N^2} \sum_{k=0}^{N-1} \sum_{\ell=0}^{N-1} X_{pk} \overline{X}_{r\ell} \text{EXP}[j \frac{2\pi(kn-\ell m)}{N}]] \tag{3-34b}$$

Moving the expectation sign inside

$$R_{pr}(n,m) = \frac{1}{N^2} \sum_{k=0}^{N-1} \sum_{\ell=0}^{N-1} E[X_{pk} X_{r\ell}] \times \text{EXP}[j \frac{2\pi(kn-\ell m)}{N}]. \quad (3\text{-}34c)$$

From Eq. (3-31b) one obtains

$$E[X_{pk} \overline{X}_{r\ell}] = \frac{N}{2h} \sum_{q=1}^{M} H_{pqk} \overline{H}_{rq\ell} \delta_{k\ell}.$$

Substituting this in Eq. (3-34c)

$$R_{pr}(n,m) = \frac{1}{2hN} \sum_{k=0}^{N-1} \sum_{\ell=0}^{N-1} \{ \sum_{q=1}^{M} H_{pqk} \overline{H}_{rq\ell} \delta_{k\ell} \} \times \text{EXP}[j \frac{2\pi(kn-\ell m)}{N}]. \quad (3\text{-}34d)$$

Unless $k = \ell$, Eq. (3-34d) is zero.

Hence,

$$R_{pr}(n,m) = \frac{1}{2hN} \sum_{k=0}^{N-1} \sum_{q=1}^{M} H_{pqk} \overline{H}_{rqk} \text{EXP}[j \frac{2\pi k(m-n)}{N}]. \quad (3\text{-}34e)$$

That is, the correlation is a function of the time lag which proves that the process is stationary.

Finally we can write Eq. (3-34e) as

$$R_{pr}(m-n) = \frac{1}{2hN} \sum_{k=0}^{N-1} \sum_{q=1}^{M} H_{pqk} \overline{H}_{rqk} \text{EXP}[j \frac{2\pi k(m-n)}{N}]. \quad (3\text{-}35)$$

The spectral density function is the inverse Fourier Transform of Eq. (3-35). That is

$$G_{prk} = 2h \sum_{k=0}^{N-1} R_{pr}(m-n) \text{EXP}[-j \frac{2\pi k(m-n)}{N}] \quad (3\text{-}36a)$$

$$= \sum_{q=1}^{M} H_{pqk} \overline{H}_{rqk} \quad (3\text{-}36b)$$

which is equal to the elements of the spectral matrix between the process p and process q.

Thus, we see that the assumed form of the time series given by Eq. (3-24) has the same spectral density as the target spectral density function.

Simulation of Strong Wind Turbulence

In order to check the two simulation techniques described above namely the trigonometric model and Fast Fourier Transform model, we generated six correlated time series representing the fluctuating part of wind velocities. These six series represent the three components of the wind at two different spatial locations. Each simulation technique was checked by comparing the spectra of the simulated data to the spectra used to generate the data. The input spectra used for these time series are based on wind velocity measurements made by several investigators [16, 17, 18]. These spectra will not be discussed here in detail. Under strong wind conditions turbulence is due to mechanical mixing caused by frictional effects. In this case, the turbulence can be considered a stationary random process with zero mean and a Gaussian distribution.

The following expressions for the spectra were used for this simulation:

$$\frac{nC_{11}(n)}{u^{*2}} = \frac{87.56f_1}{((1.0 + 1.5\ (19.6f_1)^{0.845})^{1.945}} \qquad (3\text{-}37)$$

$$\frac{nC_{22}(n)}{u^{*2}} = \frac{24.23f_1}{((1.0 + 1.5\ (7.368f_1)^{0.781})^{2.134}} \qquad (3\text{-}38)$$

$$\frac{nC_{33}(n)}{u^{*2}} = \frac{3.36f_1}{1 + 10f_1^{5/3}} \tag{3-39}$$

$$\frac{nC_{44}(n)}{u^{*2}} = \frac{272.2f_2}{((1.0 + 1.5\ (39.3f_2)^{0.845})^{1.972}} \tag{3-40}$$

$$\frac{nC_{55}(n)}{u^{*2}} = \frac{46.46f_2}{((1.0 + 1.5\ (11.06f_2)^{0.781})^{2.1}} \tag{3-41}$$

$$\frac{nC_{66}(n)}{u^{*2}} = \frac{3.36f_2}{1 + 10f_2^{5/3}} \tag{3-42}$$

$$\frac{nC_{13}(n)}{u^{*2}} = -\frac{12.5f_1}{(1.0 + 7.5f_1)^{8/3}} \tag{3-43}$$

$$\frac{nC_{46}(n)}{u^{*2}} = -\frac{12.5f_2}{(1.0 + 7.5f_2)^{8/3}} \tag{3-44}$$

$$C_{14}(n) = (C_{11}(n)C_{44}(n))^{\frac{1}{2}}(\exp(-19\Delta f))^{\frac{1}{2}}\cos\ (2\pi\Delta f) \tag{3-45}$$

$$Q_{14}(n) = (C_{11}(n)C_{44}(n))^{\frac{1}{2}}(\exp(-19\Delta f))^{\frac{1}{2}}\sin\ (2\pi\Delta f) \tag{3-46}$$

$$C_{25}(n) = (C_{22}(n)C_{55}(n))^{\frac{1}{2}}(\exp(-13\Delta f))^{\frac{1}{2}}\cos\ (4\pi\Delta f) \tag{3-47}$$

$$Q_{25}(n) = (C_{22}(n)C_{55}(n))^{\frac{1}{2}}(\exp(-13\Delta f))^{\frac{1}{2}}\sin\ (4\pi\Delta f) \tag{3-48}$$

$$C_{36}(n) = (C_{33}(n)C_{66}(n))^{\frac{1}{2}}(\exp(-13\Delta f))^{\frac{1}{2}}\cos\ (4\pi\Delta f) \tag{3-49}$$

$$Q_{36}(n) = (C_{33}(n)C_{66}(n))^{\frac{1}{2}}(\exp(-13\Delta f))^{\frac{1}{2}}\sin\ (4\pi\Delta f) \tag{3-50}$$

$$C_{34}(n) = (C_{13}(n)C_{46}(n))^{\frac{1}{2}}(\exp(-16\Delta f))^{\frac{1}{2}}\cos\ (3\pi\Delta f) \tag{3-51}$$

$$C_{16} = C_{34} \tag{3-52}$$

$$Q_{34}(n) = (C_{13}(n)C_{46}(n))^{\frac{1}{2}}(\exp(-16\Delta f))^{\frac{1}{2}}\sin\ (3\pi\Delta f) \tag{3-53}$$

$$Q_{16}(n) = Q_{34}(n) \tag{3-54}$$

where C_{ij} and Q_{ij} represent the co-spectrum and quadrature-spectrum parts of the spectral density function respectively.

Note that $C_{ij} = C_{ji}$

and $Q_{ij} = -Q_{ji}$

The elements of the components of the spectral matrix, which have not been listed above, have been assumed to be zero. The following actual values were used for simulation

$z_1 = 100$ ft, $z_2 = 50$ ft

$v_1 = 60$ ft/sec., $v_2 = 50.974$ ft/sec.

$f_1 = nz_1/v_1$, $f_2 = nz_2/v_2$

$u^{*2} = (5.212)^2 = 27.1649$ ft^2/sec^2

$f = n\Delta z/\bar{v} = n\ (100 - 50)/(60.0 + 50.974)/2$

where $\bar{v}$ = average velocity

n = frequency in cycles per sec.

Suffix 1 or 2 refers to the station at 100 ft or 50 ft respectively.

Results

Fig. 3-a shows a set of six simulated correlated time series based on the trigonometric model. Time series one, two and three represent the wind velocities in the mean wind, cross wind and vertical direction respectively at a height of 100 ft. Time series four, five and six are similar simulations for a spatial position 50 ft. below the first point. Series one and four are positively correlated, while series three and six are negatively correlated to one and four. Series two and five, the series representing the cross wind, are positively correlated to each other but uncorrelated to the other four series. For these series, velocities were calculated every second

for 2048 seconds. The number of frequencies used, equal to N in the analysis, was 600.

Fig. 3-b shows a similar set of simulated time series based on the Fast Fourier Transform method. It is interesting to note the similarity of the outcome. The number of frequencies used, equal to N in the analysis, has to be the same as the number of time points that is 2048.

A comparison between the spectra used to generate the simulated data and the spectra of the simulated data is presented in Figures 4-a through 9-a for the trigonometric model and in Figures 4-b through 9-b for the FFT model. Figures 8-a and 9-a are respectively the co- and quad-spectra between time series one and time series four based on trigonometric model. Figures 8-b and 9-b are the FFT counter part. In each case the solid line represents the original spectrum and the dashed line represents the spectrum of the simulated time series. The spectra were calculated from the simulated data using the "Cooley-Tukey" method of calculating the correlation function first, and then the "Tukey window" was used for smoothing purposes. As can be seen the comparison between the actual spectra and the simulated spectra is quite good in all cases. We did not consider it necessary to show all 36 possible power and cross-spectra. The agreement looks the worst for the quad-spectrum between series one and four (Figures 9-a and 9-b). The vertical scale for this comparison, however, is very expanded and about all we can conclude is that both the original and simulated spectra are very close to zero. Also,

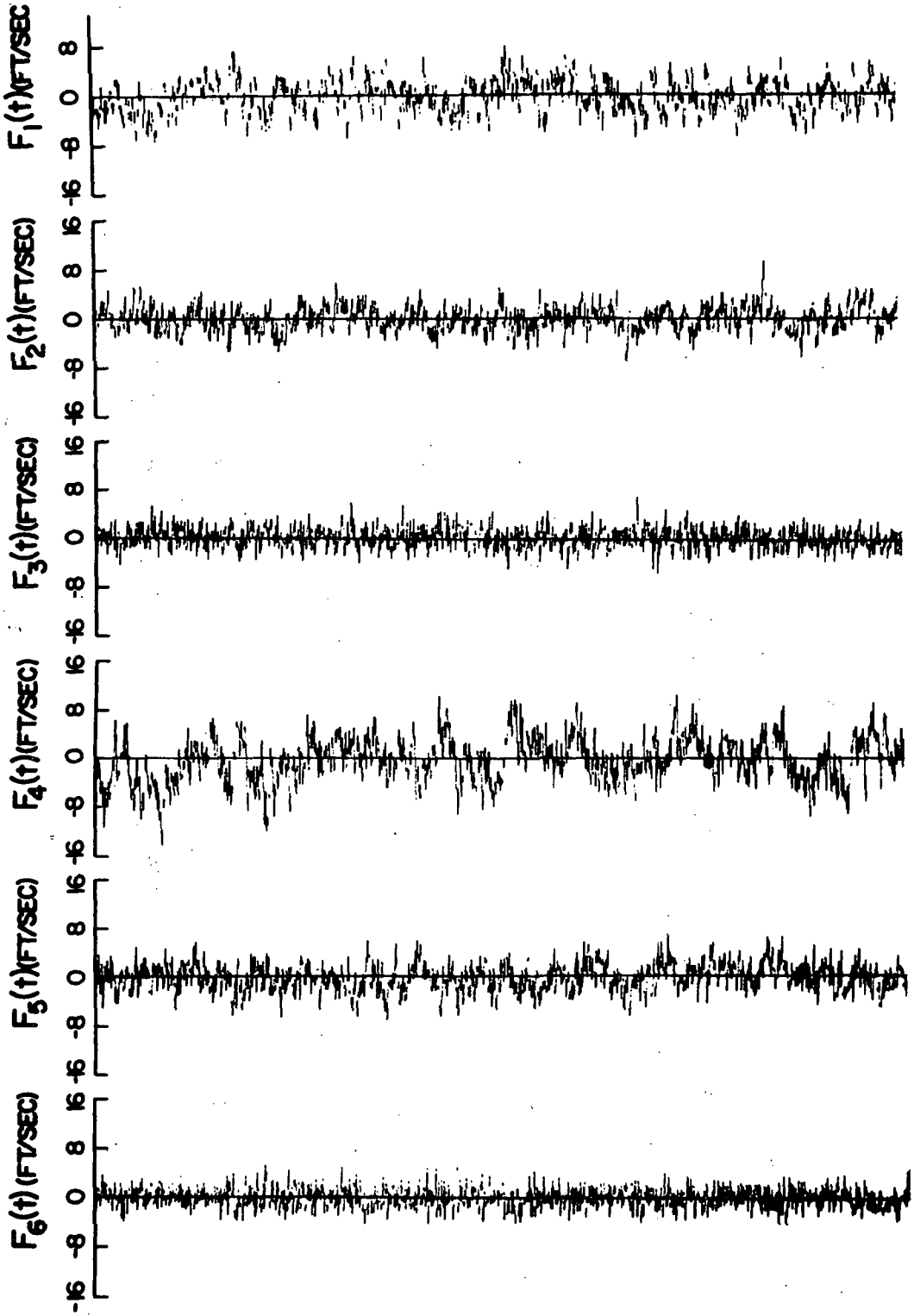

FIG 3A. SIMULATED WIND VELOCITIES BY TRIGONOMETRIC MODEL

THE TOTAL RECORD LENGTH IS 2048 SECONDS

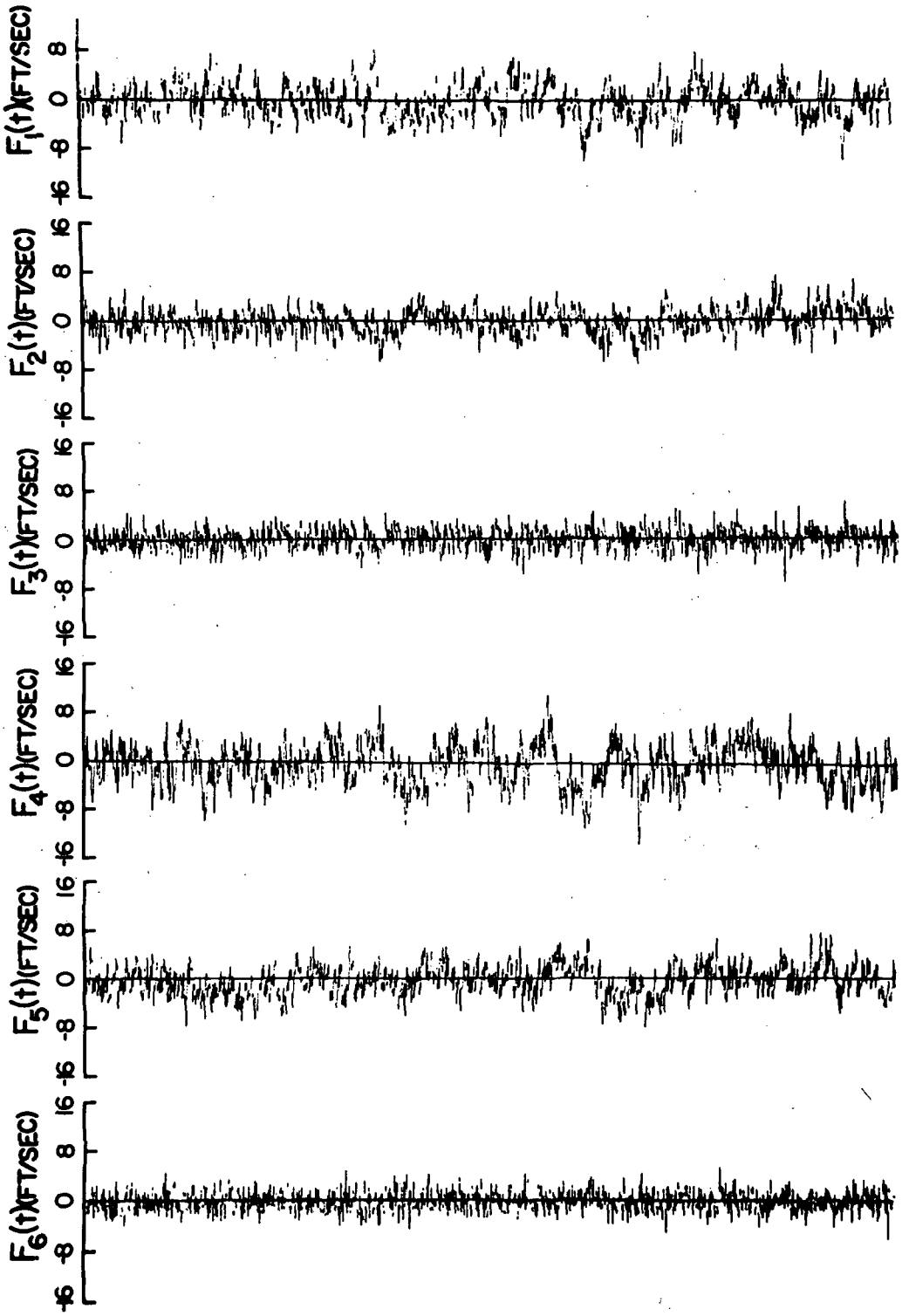

FIG 3a. SIMULATED WIND VELOCITIES BY FFT METHOD

THE TOTAL RECORD LENGTH IS 2048 SECONDS

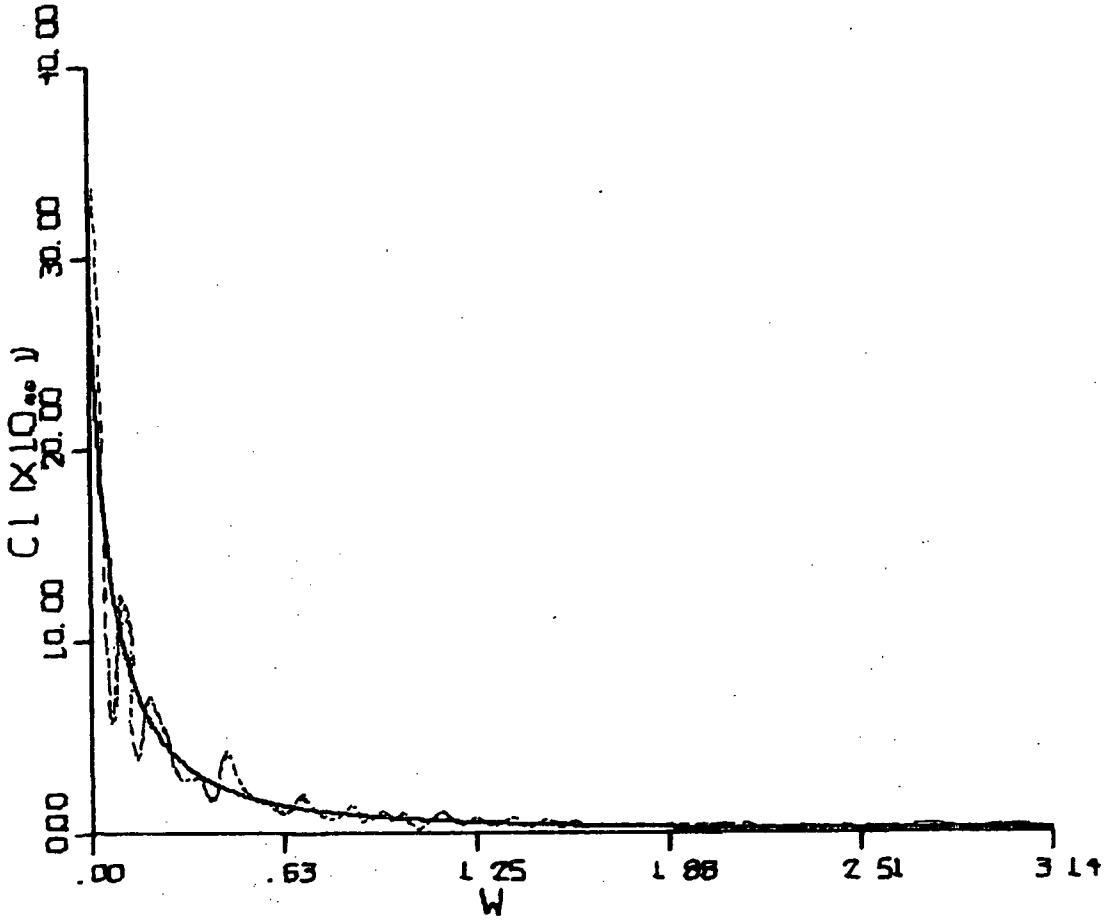

Fig. 4a. Comparison between the original $G_{11}(w)$ and the spectrum of the first simulated time series based on trigonometric model. (Vert. Scale: 100(M^2/sec)/in; Horz. Scale: 0.53(rad/sec)/in)

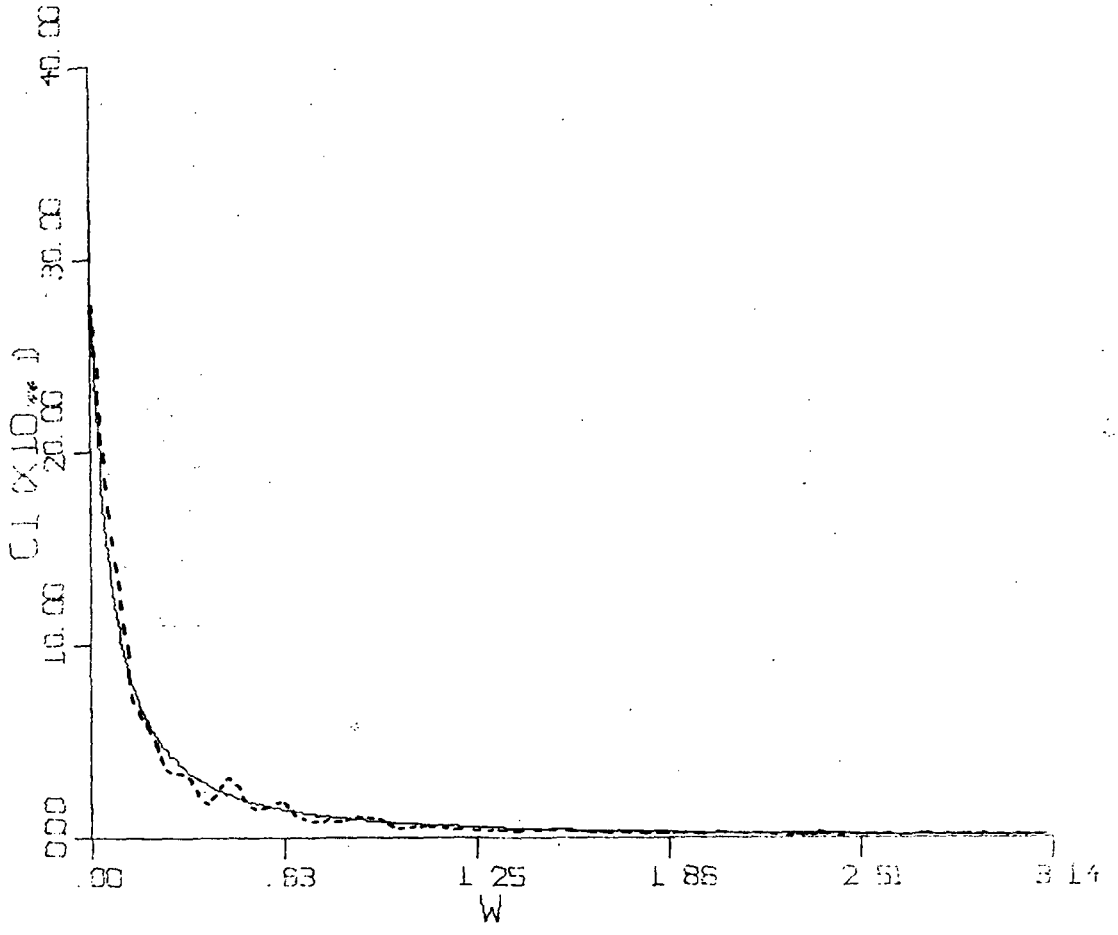

Fig 4b. Comparison between the original $G_{11}(w)$ and the spectrum of the first simulated time series based on FFT model. (Vert. Scale: $100(M^2/sec)/in$; Horz. Scale: $0.63(rad/sec)/in$)

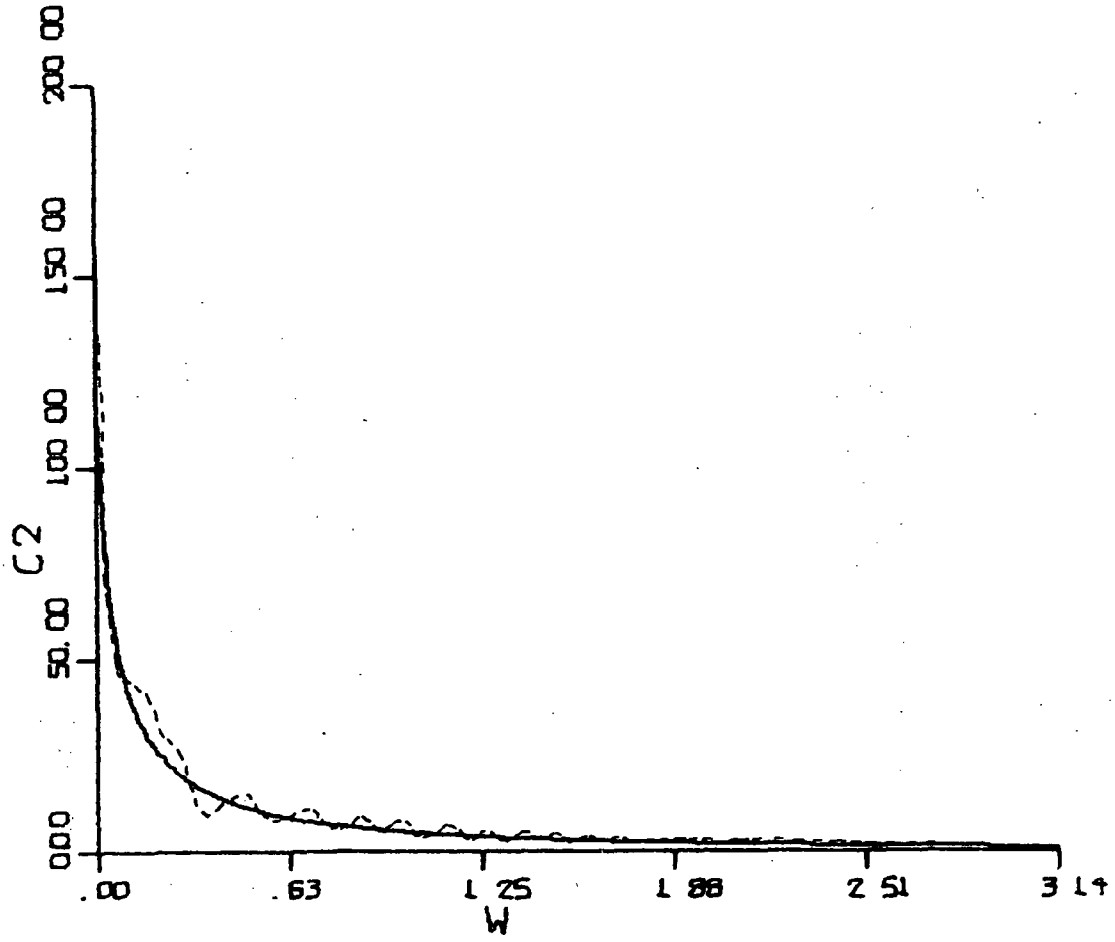

Fig. 5a. Comparison between the original $G_{22}(w)$ and the spectrum of the second simulated time series based on trigonometric model. (Vert. Scale: (50 M^2)/sec)/in; Horz. Scale: 0.63(rad/sec)/in)

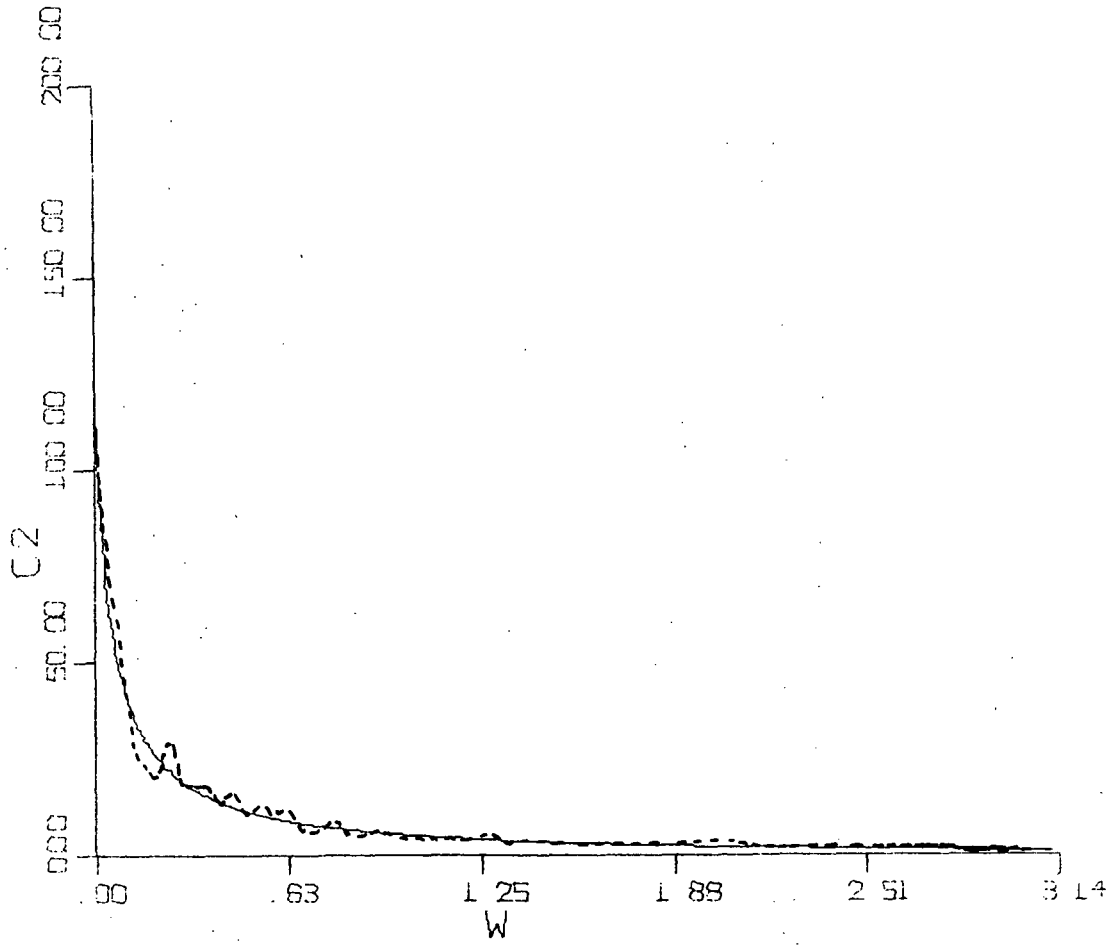

Fig. 5b. Comparison between the original $G_{22}(w)$ and the spectrum of the second simulated time series based on FFT model. (Vert. Scale: $(50M^2/sec)/in$; Horz. Scale: 0.63 (rad/sec)/in)

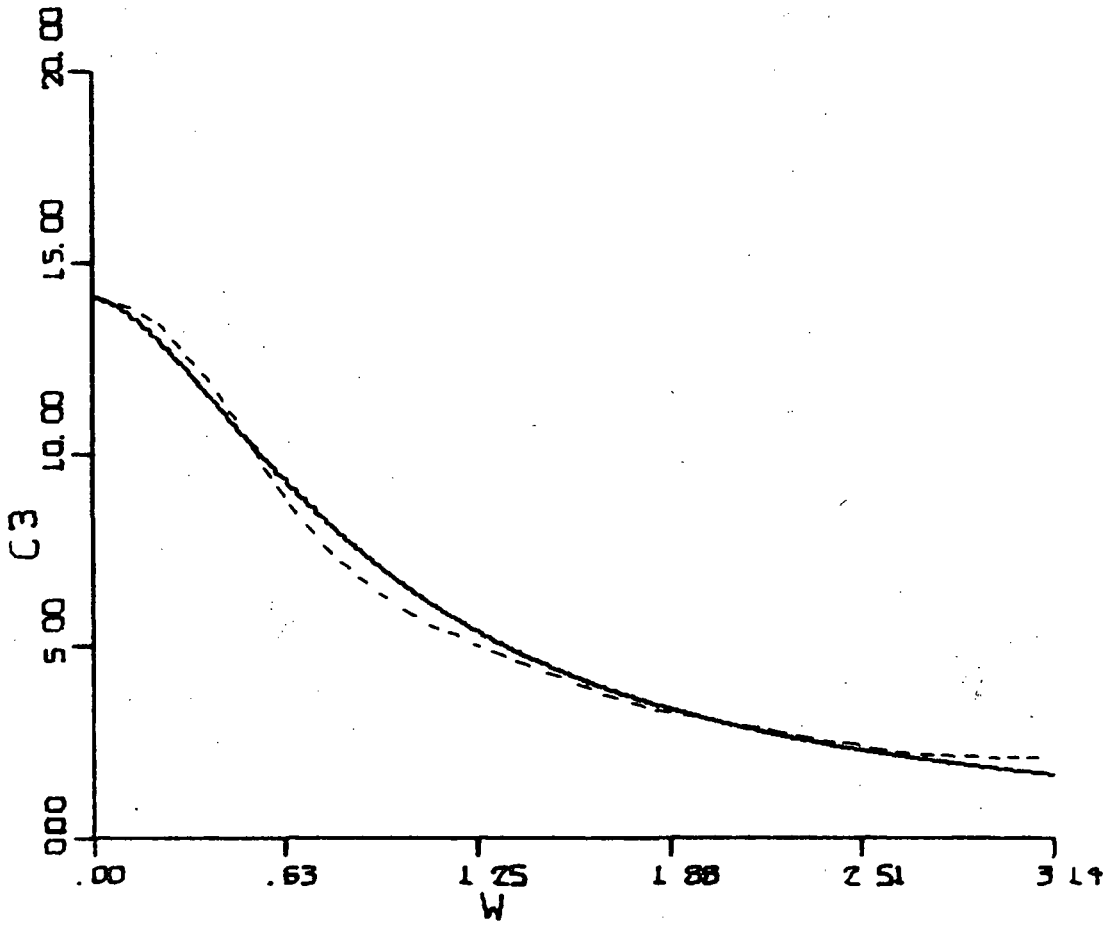

Fig. 6a. Comparison between the original $G_{33}(w)$ and the spectrum of the third simulated time series based on trigonometric model. (Vert. Scale: (5 M^2/sec)/in; Horz. Scale: 0.63(rad/sec)/in)

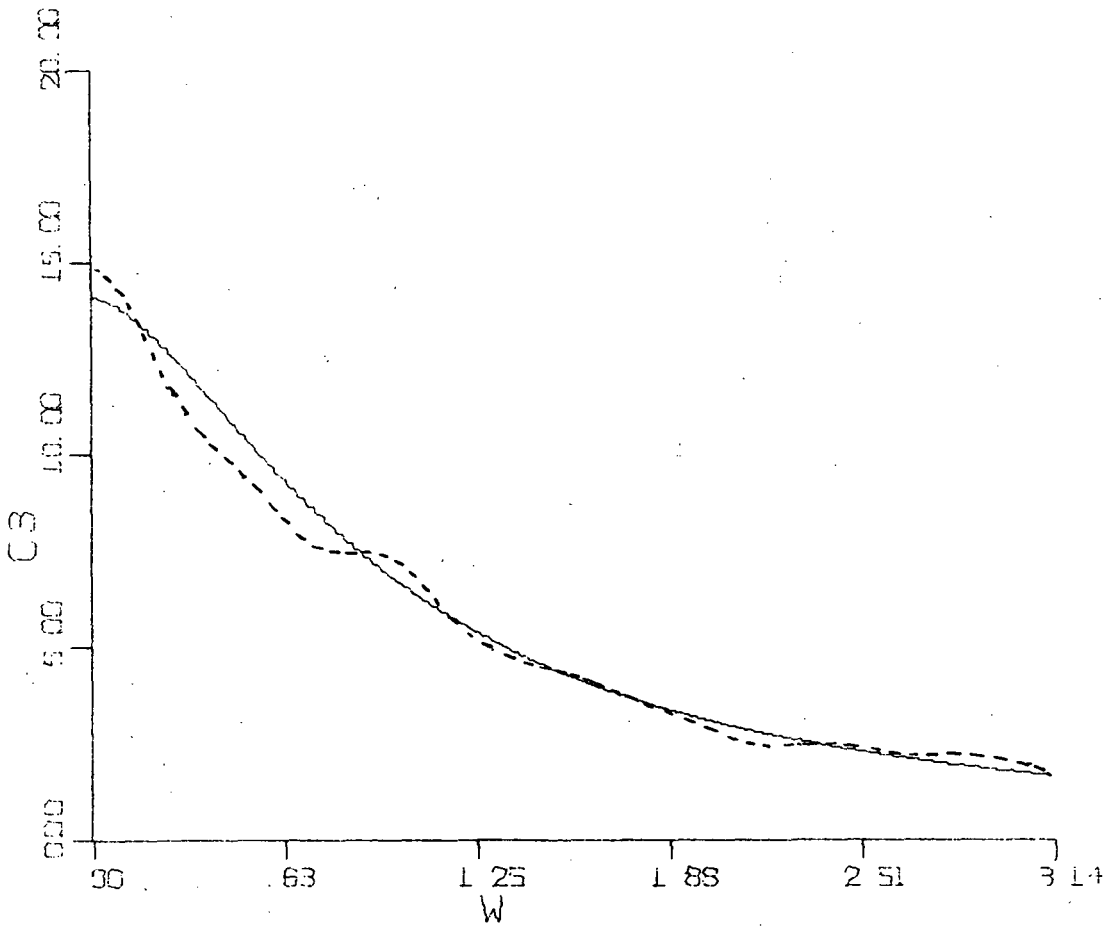

Fig. 6b. Comparison between the original $G_{33}(w)$ and the spectrum of the third simulated time series based on FFT model. (Vert. Scale: $5(M^2/sec)/in$; Horz. Scale: 0.63 (rad/sec)/in)

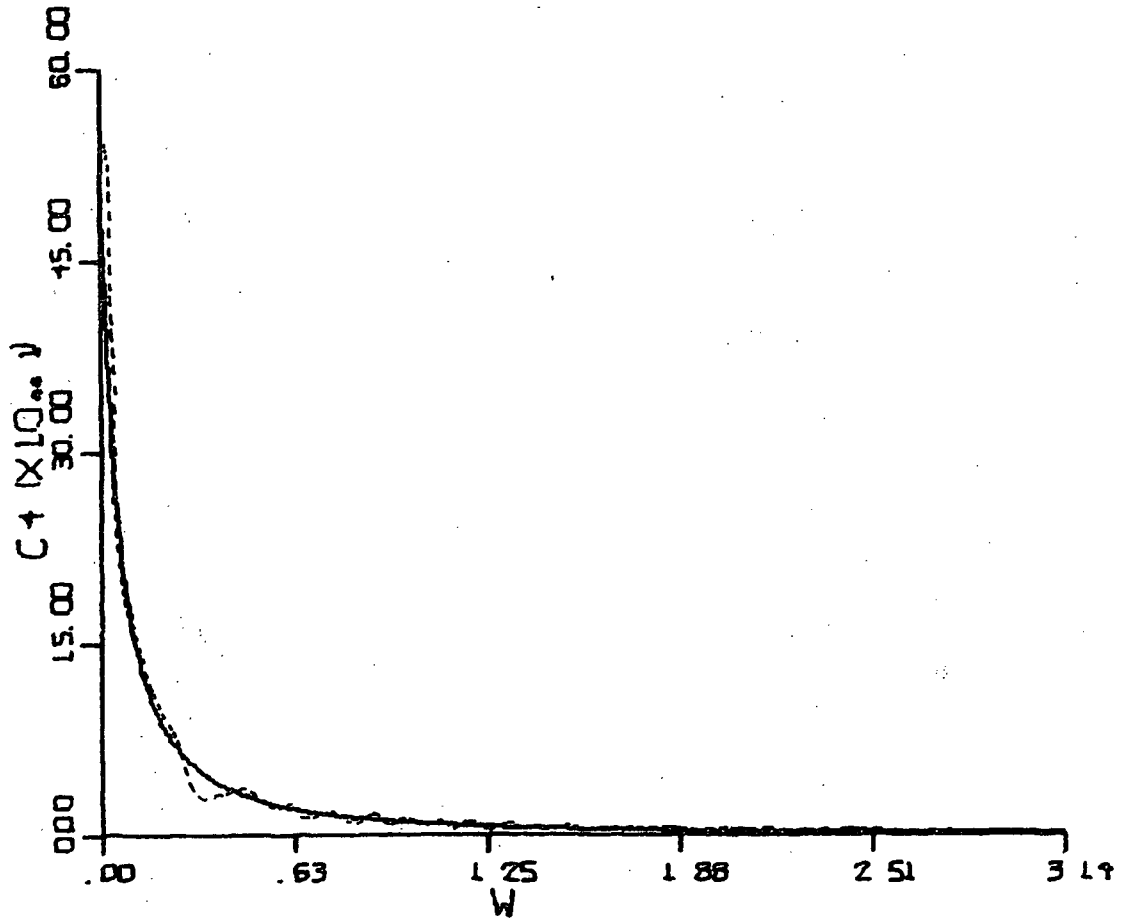

Fig. 7a. Comparison between the original $G_{44}(w)$ and the spectrum of the fourth simulated time series based on trigonometric model. (Vert. Scale: (150 M^2/sec)/in; Horz. Scale: 0.63(rad/sec)/in)

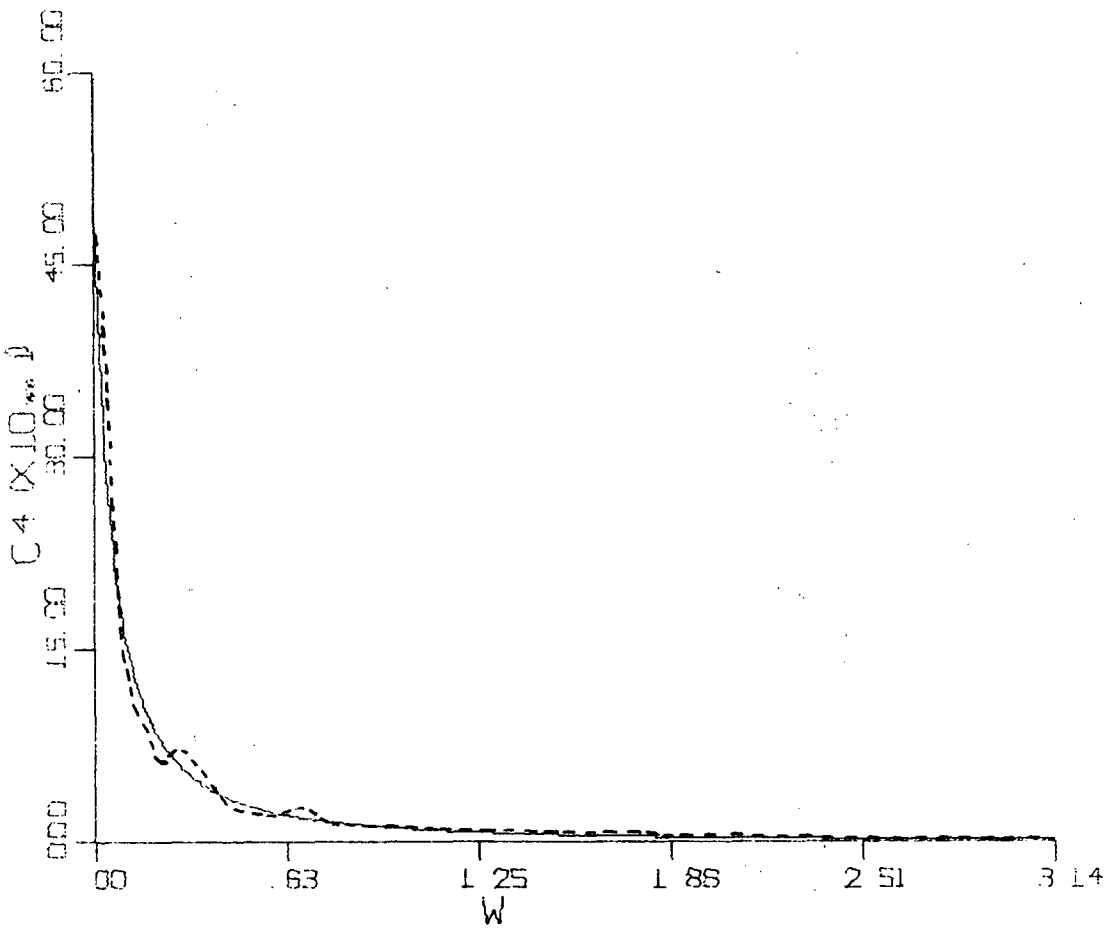

Fig. 7b. Comparison between the original $G_{44}(w)$ and the spectrum of the fourth simulated time series based on FFT model. (Vert. Scale: 150(M^2/sec)/in; Horz. Scale: 0.63(rad/sec)/in)

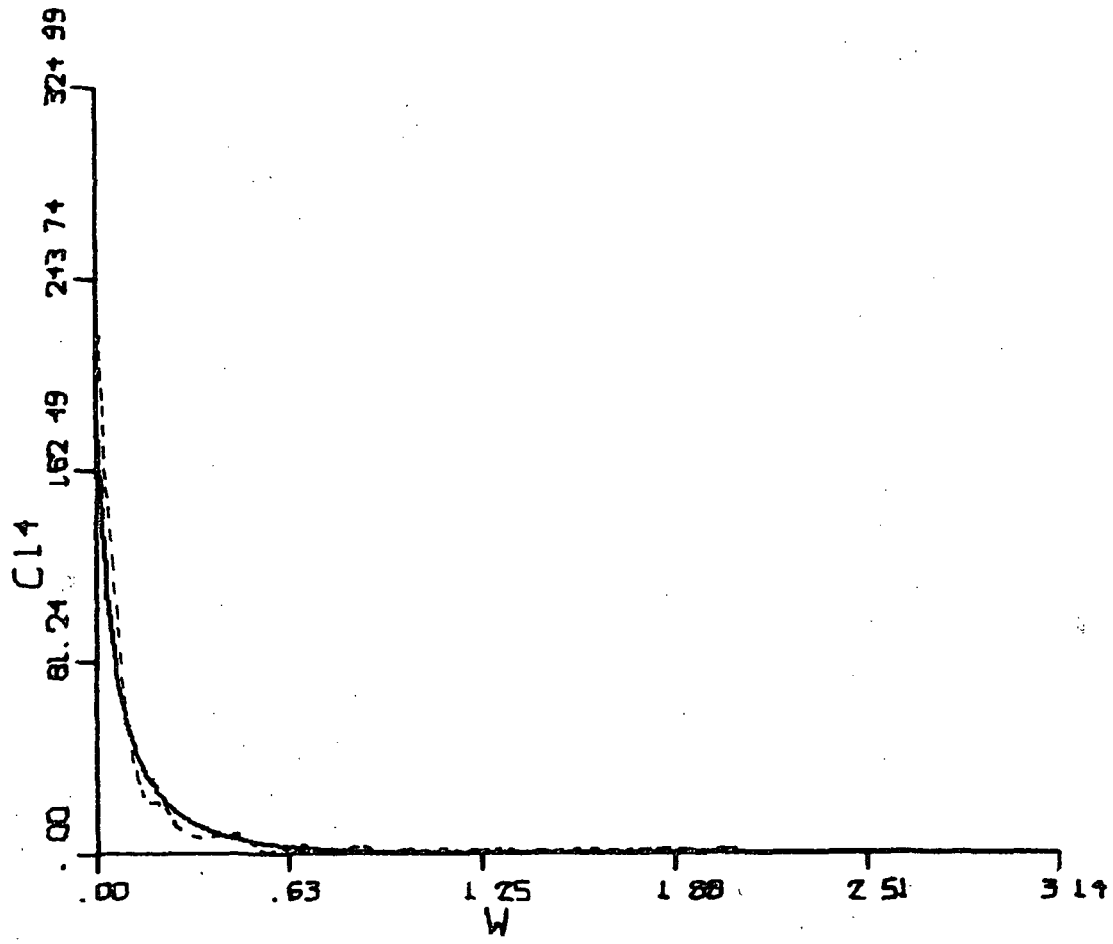

Fig. 8a. Comparison between the original $C_{14}(w)$ and the co-spectrum between simulated time series one and four based on trigonometric model. (Vert. Scale: 81.25 (M^2/sec)/in; Horz. Scale: 0.63 (rad/sec)/in)

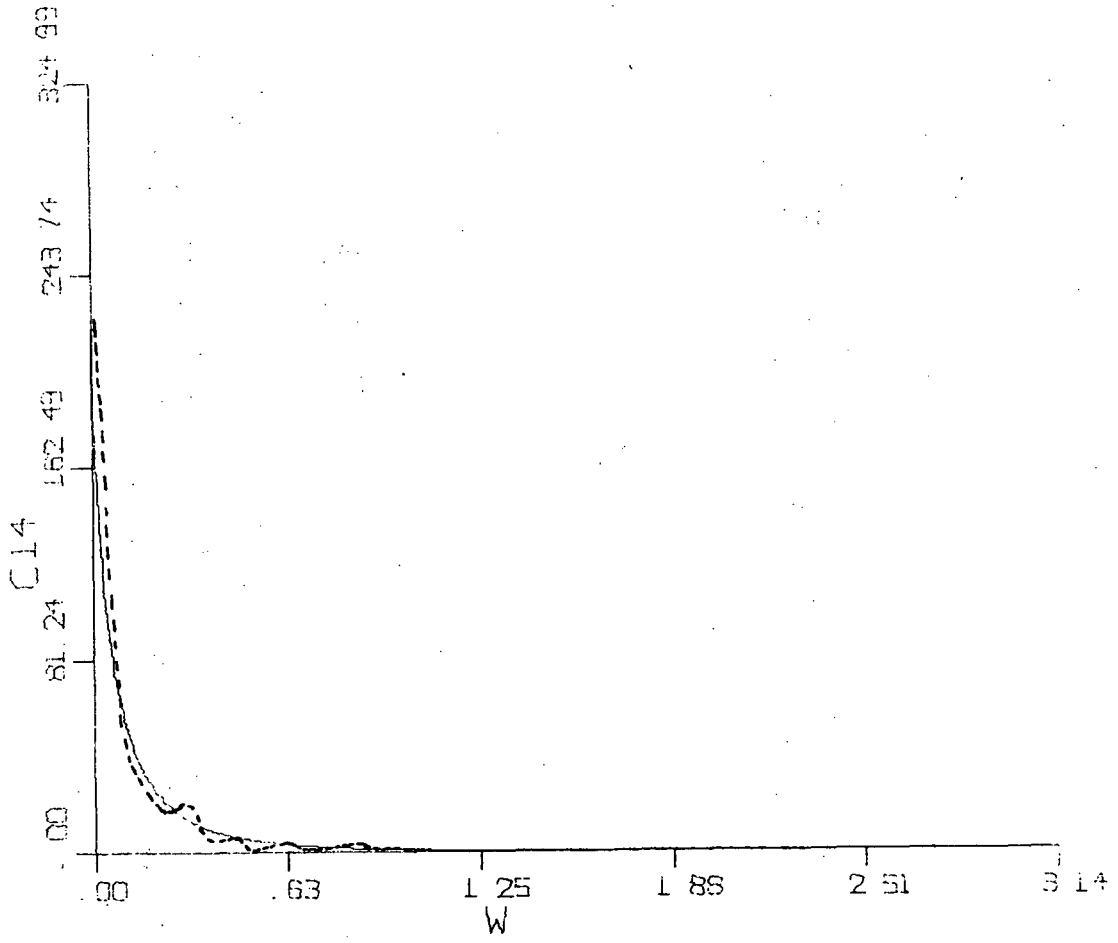

Fig. 8b. Comparison between the original $C_{14}(w)$ and the co-spectrum between simulated time series one and four based on FFT model. (Vert. Scale: 81.25(M^2/sec)/in; Horz. Scale: 0.63(rad/sec)/in)

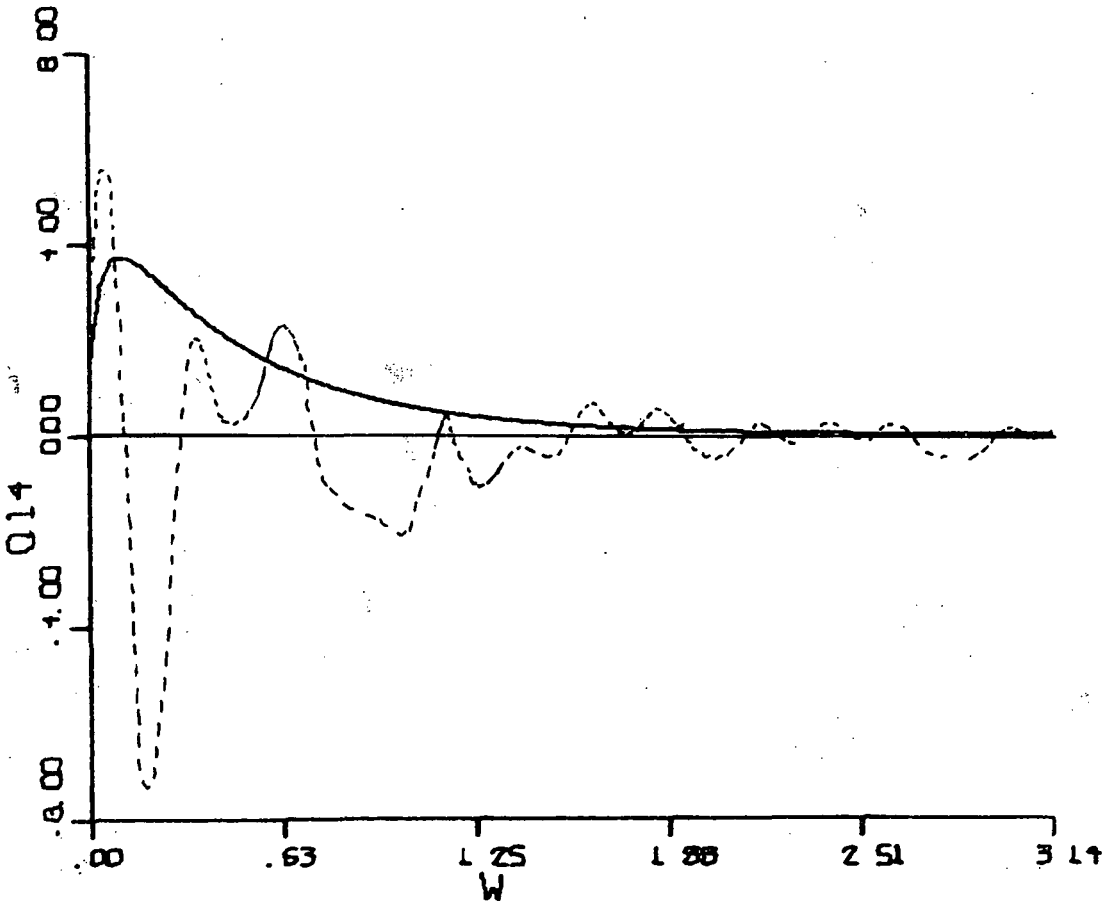

Fig. 9a. Comparison between the original $Q_{14}(w)$ and the quad-spectrum between simulated time series one and four based on trigonometric model. (Vert. Scale: 4.0(M^2/sec)/in; Horz. Scale: 0.63(rad/sec)/in)

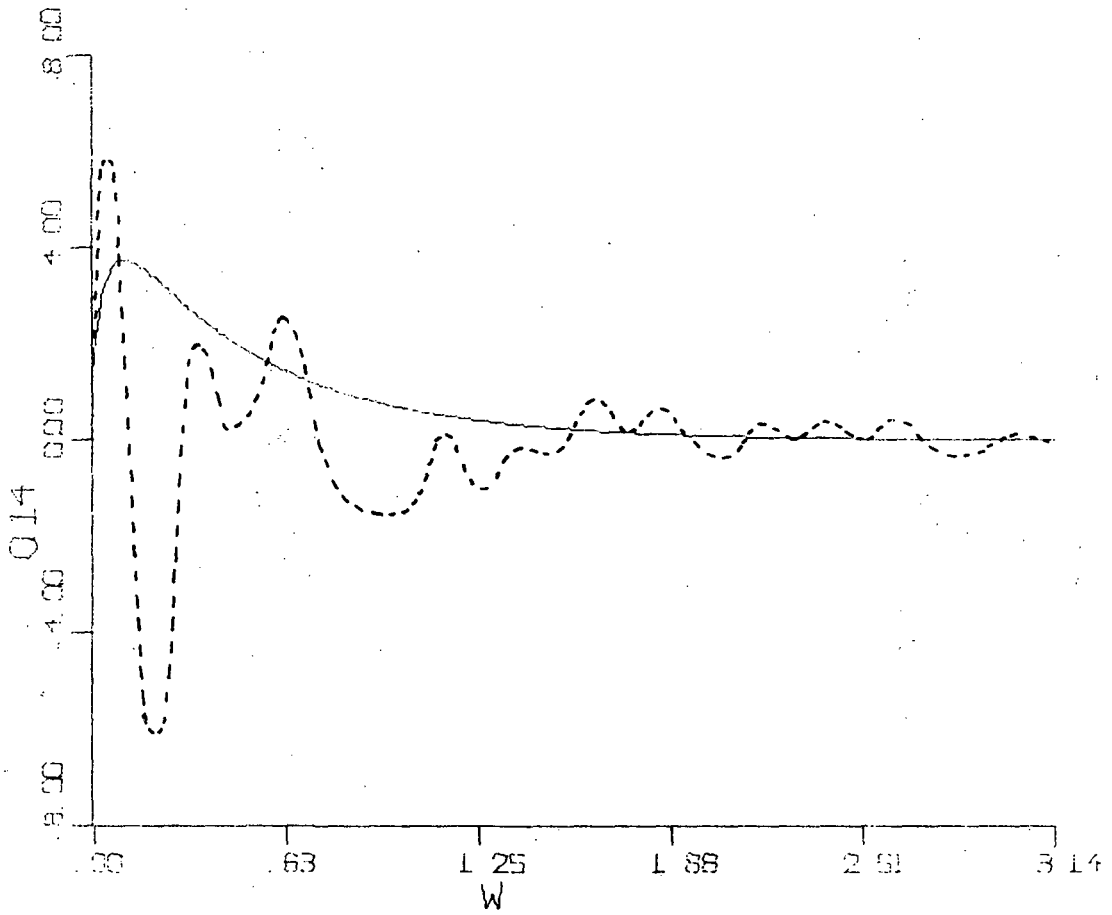

Fig. 9b. Comparison between the original $\overline{Q_{14}(w)}$ and the quad-spectrum between simulated time series one and four based on FFT model. (Vert. Scale: 4.0(M^2/sec)/in; Horz. Scale: 0.63 rad/sec)/in)

it is interesting to note that, in general, the comparison between the simulated spectra and the actual spectra looks better in the case of FFT approach.

Comment

Considering the above results we feel that both the simulation methods presented work very well. The only drawback we see is the amount of computer storage that is necessary. It is noted that FFT method works about twenty times faster in terms of computer time compared to trigonometric model. But FFT approach has a drawback in that the number of time points is equal to the frequency points and we can't restart the simulation at any given time t. It has to start with t = 0. Also, the time interval is related to frequency intervals. The trigonometric approach does not suffer from these disadvantages. Here, we can start the simulation beyond any given time and also the time interval is not dependent on the frequency discretization. Because of the presence of sine and cosine functions in the trigonometric model, it can be very useful in the response analysis of linear system. Thus, we see that whereas the Fast Fourier Simulation method has a tremendous advantage in terms of computer time, trigonometric model is more useful in certain cases.

CHAPTER IV

APPLICATIONS OF THE SIMULATION TECHNIQUE

Example 1. Forced oscillations of a free standing latticed tower.

To show the application of the simulation method for a linear problem the dynamic response of a three-legged, latticed steel tower, shown in Figure 10, due to wind load in the y direction was investigated. The tower was idealized as a space truss, and the structural members were assumed to resist axial loads only.

For the dynamic analysis, the tower was modeled mathematically as a discrete system of fourteen masses lumped at the panel points. Horizontal loads were assumed to be applied at the panel points, and secondary stresses were assumed to be small.

The assumptions made in deriving this analytical model are summarized below:

1. The tower is a linear elastic space truss;
2. Motion in two orthogonal horizontal directions are uncoupled;
3. Vertical motions are negligible;
4. Loads are applied only at panel points;
5. Secondary stresses are negligible;
6. Masses are concentrated at centroids of planes at panel points;
7. The base of the tower is rigid; and

8. The deformations are small enough to be geometrically linear. Under these assumptions, the column elements of the flexibility matrix were computed by successively applying a unit load horizontally at each panel point in y direction. The flexibility coefficients are shown in Table 2. The mass matrix is diagonal.[37]

After the flexibility and mass matrices for the tower had been computed, the natural frequencies and mode shapes were obtained in the usual manner as described in the following section.

The equation of motion for an undamped, multi-degree of freedom, discrete mass systems are given by

$$M\ddot{\bar{y}} + K\bar{y} = \bar{F}(t) \qquad (4\text{-}1)$$

where M = mass matrix,

K = stiffness matrix of the system,

$\bar{F}(t)$ = forcing function vector of the system,

$\bar{y}$ = displacement vector,

and,

$\ddot{\bar{y}}$ = acceleration vector of the system.

When the system is vibrating harmonically at a natural frequency, $\bar{F}(t)$ is zero and the displacement vector may be written as

$$y = \bar{A}_n \sin(w_n t) \qquad (4\text{-}2)$$

where $\bar{A}_n$ = displacement vector of the n-th mode

w_n = n-th natural frequency.

Eq. (4-1) then becomes

$$-w_n^2 M\bar{A}_n \sin(w_n t) + K\bar{A}_n \sin(w_n t) = \bar{0} \qquad (4\text{-}3)$$

Dividing Eq. (4-3) by $w_n^2 \sin(w_n t)$ and rearranging terms, then

$$M\bar{A}_n = \frac{1}{w_n^2} K\bar{A}_n \tag{4-4}$$

Premultiplying both sides of Eq. (4-4) by the inverse of K

$$K^{-1}M\bar{A}_n = \frac{1}{w_n^2} K^{-1}K\bar{A}_n \tag{4-5}$$

and replacing K^{-1} by S, the flexibility matrix of the system, and $K^{-1}K = I$ = identity matrix, then

$$SM\bar{A}_n = \frac{1}{w_n^2} \bar{A}_n \tag{4-6}$$

Denoting D = SM as the dynamical matrix and $\lambda_n = \frac{1}{w_n^2}$, the standard algebraic eigen value problem is obtained as

$$D\bar{A}_n = \lambda_n \bar{A}_n \tag{4-7}$$

The computed first three eigen values and their corresponding eigen vectors are shown in Table 3. Three natural periods were 0.496 sec., 0.158 sec., and 0.080 sec. in the y direction.

After having determined the modal shape and natural frequencies, we will proceed to do the dynamical analysis as follows: Let the masses M_j, concentrated at points 1, 2, 3, ... j, k, ... r of the system be subject to disturbing forces.

$$F_j(t) = F_{aj} + F_{oj}(t) \tag{4-8}$$

where $F_{aj} = 0.5\rho C_{xj} S_j v_{aj}^2$ -- the static wind loading acting at the point under consideration, v_{aj} is the average value of the longitudinal component of the velocity at this point,

$F_{oj}(t) = F_{aj}\left(\frac{2v_{oj}(t)}{v_{aj}} + \frac{v_{oj}^2(t)}{v_{aj}^2}\right)$ is the disturbing force relevant

for the pulsating part of the velocity $v_{oj}(t)$,

ρ is the air density,

C_{xj} is the drag coefficient of the construction at the level j,

and S_j is the area of the projection of the structure at the level j on the plane perpendicular to the direction of the wind.

Now, let

$$y_k = \sum_{i=1}^{r} q_i(t)\alpha_{yi}(x_k) \tag{4-9}$$

where y_k = dynamic displacement

$\alpha_{yi}(x_k)$ = modes of natural oscillation

$q_i(t)$ = generalized coordinates.

Then the equation of motion for the i th mode is

$$\ddot{q}_i(t) + (u + iv)w_i^2 q_i(t) = \frac{Q_i(t)}{M_{ig}} \tag{4-10}$$

where $u = \dfrac{4 - r_o^2}{4 + r_o^2}$;

$$iv = \frac{4r_o}{4 + r_o^2}\sqrt{-1}; \quad r_o = \frac{\delta}{\pi}$$

The generalized force $Q_i(t) = \sum_{j=1}^{r} F_j(t)\alpha_{yi}(x_j)$, and the generalized mass $M_{ig} = \sum_{j=1}^{r} M_j\alpha_{yi}^2(x_j)$ where

w_i = i th natural circular frequency of the system

δ = logarithmic damping decrement of oscillation

Neglecting the square term in the expression for the disturbing force, which is very small compared to the first term, we can write

$$F_{oj}(t) = F_{aj}\left(\frac{2v_{oj}(t)}{v_{aj}}\right) \tag{4-11}$$

Now,

$$Q_i(t) = \sum_{j=1}^{N} \{F_{aj}\alpha_{yi}(x_j)[1 + \frac{2v_{oj}(t)}{v_{aj}}]\} \tag{4-12}$$

Then

$$\overline{Q_i}(t) = \text{mean generalized force} = \Sigma F_{aj}\alpha_{yi}(x_j) \tag{4-13}$$

$B_{Qi}(\tau)$ = correlative function of the generalized force = $E[Q_i(t)Q_i(t + \tau)]$

$$B_{Qi}(\tau) = E[\sum_{j=1}^{N}\sum_{k=1}^{N} \{F_{aj}\alpha_{yi}(x_j)(1 + \frac{2v_{oj}(t)}{v_{aj}})\} \times \{F_{ak}\alpha_{yi}(x_k)(1 + \frac{2v_{ok}(t + \tau)}{v_{aj}})\}] \tag{4-14a}$$

Multiplying these two expressions and moving the expectation sign inside

$$B_{Qi}(\tau) = \sum_{j=1}^{N}\sum_{k=1}^{N} F_{aj}F_{ak}\alpha_{yi}(x_j)\, y_i(x_k) + 4\sum_{j=1}^{N}\sum_{k=1}^{N} F_{aj}F_{ak}\alpha_{yi}(x_j)\, y_i(x_k) \times E[\frac{v_{oj}(t)v_{ok}(t + \tau)}{v_{aj}v_{ak}}] \tag{4-14b}$$

$B_{QiQ\ell}(\tau)$ = Cross correlative function for the generalized force = $E[Q_i(t)Q_\ell(t + \tau)]$

$$B_{QiQ\ell} = E[\sum_{j=1}^{N}\sum_{k=1}^{N} \{F_{aj}\alpha_{yi}(x_j)(1 + \frac{2v_{oj}(t)}{v_{aj}})\} \times \{F_{ak}\alpha_{y\ell}(x_k)(1 + \frac{2v_{ok}(t + \tau)}{v_{ak}})\}] \tag{4-15a}$$

$$B_{Qi Q\ell} = \sum_{j=1}^{N} \sum_{k=1} F_{aj} F_{ak} \alpha_{yi}(x_j) \alpha_{y\ell}(x_k)$$

$$+ \sum_{j=1}^{N} \sum_{k=1}^{N} F_{aj} F_{ak} \alpha_{yi}(x_j) \alpha_{y\ell}(x_k) E\left[\frac{v_{oj}(t) v_{ok}(t+\tau)}{v_{aj} v_{ak}}\right] \quad (4\text{-}15b)$$

Taking the Fourier Transform of the correlative and cross correlative functions we get

$S_{Qi}(w)$ = spectrum of the i th generalized force

$$= \sum_{j=1}^{N} \sum_{k=1}^{N} F_{aj} F_{ak} \alpha_{yi}(x_j) \alpha_{yi}(x_k)$$

$$\int_{-\infty}^{\infty} \left(1 + 4 \frac{E[v_{oj}(t) v_{ok}(t+\tau)]}{v_{aj} v_{ak}}\right) e^{-iw\tau} d\tau \quad (4\text{-}16a)$$

Assuming the mean wind to be invarient with time

$$S_{Qi}(w) = \sum_{j=1}^{N} \sum_{k=1}^{N} F_{aj} F_{ak} \alpha_{yi}(x_j) \alpha_{yi}(x_k)$$

$$x \left(\delta(w) + \frac{4}{v_{aj} v_{ak}} Sv_{oj} v_{ok}\right) \quad (4\text{-}16b)$$

where $Sv_{oj}v_{ok}$ is the cross-spectrum of the fluctuating velocities at points j and k. Note that $S_{Qi}(w)$ will be complex because $Sv_{oj}v_{ok}$ might have real and imaginary parts.

However, the imaginary part can be neglected if this turns out to be very small compared to the real part.

Similarly,

$S_{Qi Q\ell}(w)$ = cross-spectrum of the generalized force

$$S_{Qi Q\ell}(w) = \sum_{j=1}^{N} \sum_{k=1}^{N} F_{aj} F_{ak} \alpha_{yi}(x_j) \alpha_{y\ell}(x_k)$$

$$x \left(\delta(w) + \frac{4}{v_{aj} v_{ak}} Sv_{oj} v_{ok}\right) \quad (4\text{-}17)$$

For considering the dynamic effect, we don't consider the static deflection and in such cases the spectral density for the fluctuating part only will be

$$S_{Qi}(w) = \sum_{j=1}^{N} \sum_{k=1}^{N} F_{aj}F_{ak}\alpha_{yi}(x_j)\alpha_{yi}(x_k)$$

$$x \left(\frac{4}{v_{aj}v_{ak}} Sv_{oj}v_{ok}\right) \qquad (4\text{-}18)$$

and,

$$S_{QiQ\ell}(w) = \sum_{j=1}^{N} \sum_{k=1}^{N} F_{aj}F_{ak}\alpha_{yi}(x_j)\alpha_{y\ell}(x_k)$$

$$x \left(\frac{4}{v_{aj}v_{ak}} Sv_{oj}v_{ok}\right) \qquad (4\text{-}19)$$

Now, to find the expression for the transfer function of the system, let

$$Q_i(t) = e^{jwt}$$

and, $q_i(t) = \Phi_i(w)e^{jwt}$

where $\Phi_i(w)$ is the transfer function.

Substituting these expressions in Eq. (4-10) we get

$$-w^2\Phi_i(w)e^{jwt} + (u + iv)w_i^2\Phi_i(w)e^{jwt} = \frac{e^{jwt}}{M_{ig}}$$

$$\text{or, } \Phi_i(w) = \frac{1}{M_{ig}[-w^2 + (u + iv)w_i^2]}$$

$$\Phi_i(w) = \frac{-w^2 + (u - iv)w_i^2}{M_{ig}(-w^2 + (u + iv)w_i^2)(-w^2 + (u - iv)w_i^2}$$

$$\Phi_i(w) = \frac{-w^2 + (u - iv)w_i^2}{M_{ig}[w^4 - 2uw^2w_i^2 + w_i^4]} \qquad (4\text{-}20)$$

Since $u^2 + v^2 = 1$

$$|\Phi_i(w)|^2 = \frac{1}{M_{ig}{}^2[w^4 - 2uw^2w_i{}^2 + w_i{}^4]} \tag{4-21}$$

Then,

$S_{qi}(w)$ = spectrum of the generalized coordinate

$$S_{qi}(w) = S_{Qi}(w)|\Phi_i(w)|^2$$

$$S_{qi}(w) = \frac{S_{Qi}(w)}{M_{ig}{}^2(w^4 - 2uw^2w_i{}^2 + w_i{}^2)} \tag{4-22}$$

and using the relation

$$S_{qiq\ell}(w) = S_{QiQ\ell}(w)\Phi_i(w)\overline{\Phi}_\ell(w)$$

we get the cross-spectrum of the generalized coordinate as

$$S_{qiq\ell}(w) = \frac{S_{QiQ\ell}(w)[w^4 - u(w_i{}^2 + w_\ell{}^2)w^2 + iv(w_i{}^2 - w_\ell{}^2) + w_i{}^2w_\ell{}^2]}{M_{ig}M_{\ell g}(w^4 - 2uw_i{}^2w^2 + w_i{}^4)(w^4 - 2uw_\ell{}^2w^2 + w_\ell{}^4)} \tag{4-23}$$

Now, for the motion of any point k

$$y_k(t) = \sum_{i=1}^{r} q_i(t)\alpha_{yi}(x_k)$$

Similarly for any point ℓ

$$y_\ell(t) = \sum_{s=1}^{r} q_s(t)\alpha_{ys}(x_\ell)$$

Then correlation function between $y_k(t)$ and $y_\ell(t)$

$$R_{y_ky_\ell}(\tau) = \sum_{i=1}^{r}\sum_{s=1}^{r} R_{qiqs}(\tau)\alpha_{yi}(x_k)\alpha_{ys}(x_\ell) \tag{4-24}$$

Then the spectral density of the dynamic displacement

$$Sy_ky_\ell = \int_{-\infty}^{\infty} Ry_ky_\ell(\tau)e^{-iw\tau}d\tau$$

$$Sy_k y_\ell = \sum_{i=1}^{r} \sum_{s=1}^{r} \alpha_{yi}(x_k)\alpha_{ys}(x_\ell)S_{qiqs} \tag{4-25a}$$

$$Sy_k y_\ell = \sum_{i=1}^{r} \sum_{s=1}^{r} \alpha_{yi}(x_k)\alpha_{ys}(x_\ell)\Phi i(w)\overline{\Phi}(w)S_{QiQ\ell} \tag{4-25b}$$

$$\begin{aligned} Sy_k y_\ell = & \sum_{i=1}^{r} \sum_{s=1}^{r} \alpha_{yi}(x_k)\alpha_{ys}(x_\ell) \\ & \times \sum_{j=1}^{N} \sum_{k=1}^{N} F_{aj}F_{ak}\alpha_{yi}(x_j)\alpha_{ys}(x_k)\frac{4Sv_{oj}v_{ok}}{v_{aj}v_{ak}} \\ & \times \frac{[w^4 - u(w_i^2 + w_s^2)w^2 + iv(w_i^2 - w_s^2) + w_i^2 w_s^2]}{M_{ig}M_{sg}(w^4 - 2uw_i^2 w^2 + w_i^4)(w^4 - 2uw_s^2 w^2 + w_s^4)} \end{aligned} \tag{4-26}$$

when $k = \ell$, it gives the power spectrum of the displacement.

Thus, having obtained the expressions for cross and power spectrum, we can simulate the displacement at any point. Thus the spectral density function of the displacement being known, FFT simulation method was used to simulate the displacement of the top of the tower shown in Fig. 10 whose important parameters are listed in Tables 1-3. The value of the co-efficient of drag was taken to be 0.6 and one percent of the critical damping was used.

Fig. 11 shows the simulated samples of the displacement and the generalized forces. The first three samples are the time histories of the generalized force for the 1st, 2nd and 3rd mode of motion respectively and the fourth sample shows the time history of the normalized displacement of the top of the tower due to all the three modes combined together.

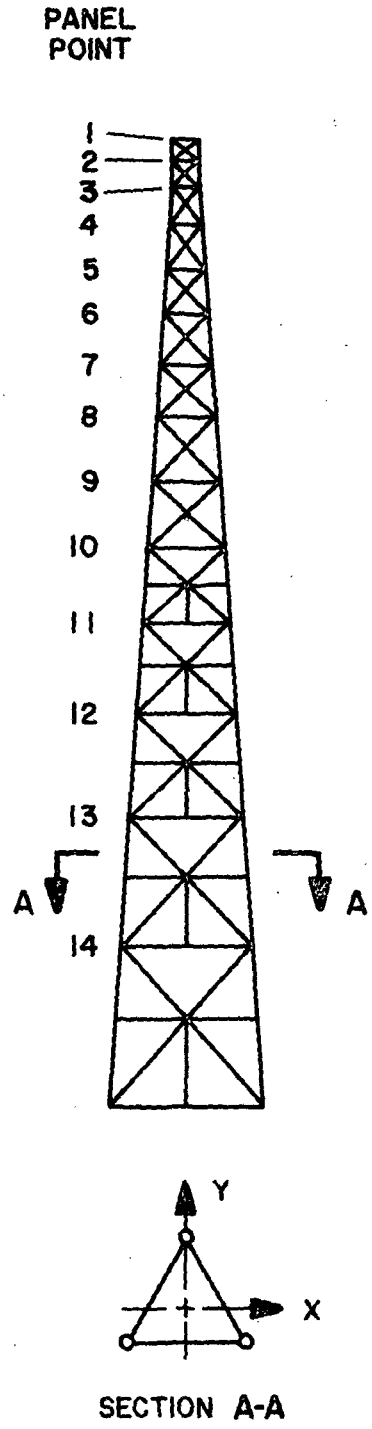

Fig. 10. Latticed steel tower subjected to turbulent wind load.

TABLE 1

CONCENTRATED MASSES AND PROJECTED AREAS

Panel Point	Elev. (ft)	Projected Area (sq. ft.)	D.L. (lb.) at Panel Point
1	150	2.87	1810
2	147	5.22	510
3	143	8.06	750
4	137	8.75	810
5	130	10.32	920
6	123	11.97	1790
7	115	14.12	1190
8	107	16.76	1360
9	97	19.30	2940
10	87	23.32	1900
11	75	28.08	3580
12	61	32.35	2940
13	45	43.45	5670
14	25	60.37	5240

NOTE: 1. Values for projected area are for one face only.

2. Values for D.L.(Dead Load) are for entire tower.

TABLE 2

FLEXIBILITY COEFFICIENTS IN Y DIRECTION
(inch/kip)

	1	2	3	4	5	6	7	8	9	10	11	12	13	14
1	0.4113													
2	0.3890	0.3702												
3	0.3599	0.3441	0.3231											
4	0.3190	0.3066	0.2900	0.2652										
5	0.2762	0.2665	0.2537	0.2344	0.2119									
6	0.2382	0.2307	0.2205	0.2053	0.1875	0.1697								
7	0.2001	0.1943	0.1864	0.1747	0.1610	0.1473	0.1317							
8	0.1667	0.1622	0.1562	0.1471	0.1366	0.1261	0.1140	0.1020						
9	0.1308	0.1276	0.1233	0.1168	0.1092	0.1016	0.0930	0.0843	0.0736					
10	0.1006	0.0983	0.0953	0.0907	0.0854	0.0800	0.0739	0.0678	0.0602	0.0526				
11	0.0708	0.0694	0.0674	0.0645	0.0612	0.0578	0.0539	0.0501	0.0453	0.0404	0.0347			
12	0.0440	0.0432	0.0422	0.0406	0.0388	0.0370	0.0349	0.0328	0.0302	0.0276	0.0245	0.0209		
13	0.0223	0.0220	0.0216	0.0209	0.0202	0.0194	0.0186	0.0177	0.0167	0.0156	0.0143	0.0128	0.0112	
14	0.0062	0.0062	0.0061	0.0060	0.0060	0.0059	0.0058	0.0057	0.0056	0.0054	0.0053	0.0051	0.0049	0.0048

Symmetrical about diagonal

TABLE 3

COMPUTED NORMALIZED MODE SHAPES
(Normalized with respect to bottom panel)

Y DIRECTION			
Panel Point	First Mode	Second Mode	Third Mode
1	39.93	-5.60	1.78
2	38.31	-4.73	1.23
3	36.15	-3.59	0.52
4	33.00	-2.00	-0.41
5	29.50	-0.38	-1.14
6	26.22	0.93	-1.56
7	22.71	2.10	-1.63
8	19.47	2.95	-1.44
9	15.82	3.61	-0.90
10	12.56	3.83	-0.21
11	9.18	3.72	0.63
12	5.96	3.13	1.29
13	3.19	2.20	1.56
14	1.00	1.00	1.00

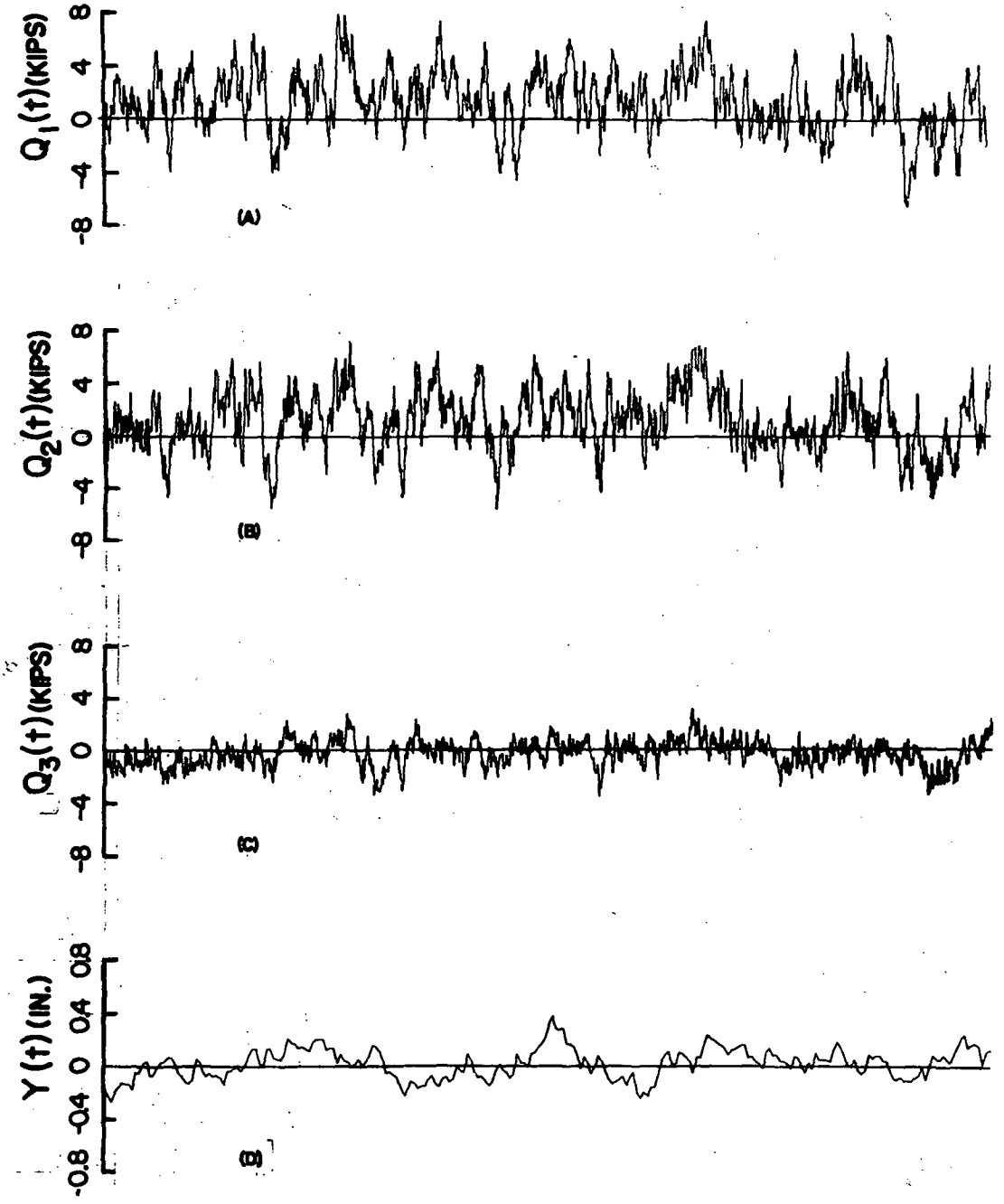

FIG. 11. GENERALIZED FORCES AND DISPLACEMENT FOR LATTICED TOWER:

(A) GENERALIZED FORCE FOR FIRST MODE
(B) GENERALIZED FORCE FOR SECOND MODE
(C) GENERALIZED FORCE FOR THIRD MODE
(D) NORMALIZED DYNAMIC DISPLACEMENT OF THE TOP OF THE TOWER

Example 2. Nonlinear Random Vibration of String

One of the most significant applications of the simulation technique is for simulating random generalized forces. The necessity of simulating random generalized forces arises when the dynamic response analysis is performed in time domain for the purpose of obtaining information beyond second-order statistics or when the structure is nonlinear and therefore an approximate random response is sought by simulating the excitation. In order to assert the validity of the preceding discussion, the problem of nonlinear vibration of a string will be considered in this example followed by the problem of nonlinear vibration of a plate in the next example.

The governing differential equation for nonlinear vibration of a string is

$$\rho\frac{\partial^2 u}{\partial t^2} + C\frac{\partial u}{\partial t} = [T_o + \frac{AE}{2L}\int_o^L (\frac{\partial u}{\partial x})^2 dx]\frac{\partial^2 u}{\partial x^2} + f(x,t) \qquad (4\text{-}27)$$

where ρ is mass per unit length, C is the linear viscous damping, T_o is the initial tension, f(x,t) is force per unit length of string, A is the cross-sectional area of string, and the boundary conditions are

$$u(o,t) = u(L,t) = 0 \qquad (4\text{-}28)$$

Assuming an approximate solution of the form,

$$u(x,t) = \sum_{n=1}^{M} b_n(t)\sin\frac{n\pi}{L}x \qquad (4\text{-}29)$$

one obtains

$$\sum_{n=1}^{M} (\rho \ddot{b}_n + C\dot{b}_n)\sin\frac{n\pi x}{L}$$

$$= [T_o + \frac{AE}{2L}\int_o^L (\sum_{n=1}^{M} b_n \frac{n\pi}{L}\cos\frac{n\pi}{L})^2 dx]$$

$$x\ [-\Sigma b_n \sin\frac{n\pi x}{L} \cdot (\frac{n\pi}{L})^2] + f(x,t) \qquad (4\text{-}30)$$

or,

$$\sum_{h=1}^{M} [\rho \ddot{b}_n + C\dot{b}_n + (T_o + \frac{AE}{4L}\sum_{n=1}^{M} b_k{}^2(\frac{n\pi}{L})^2(\frac{n\pi}{L})^2 b_n]$$

$$x \sin\frac{n\pi x}{L} = f(x,t) \qquad (4\text{-}31)$$

Multiplying both sides of Eq. (4-31) by $\sin\frac{m\pi x}{L}$ and integrating, one obtains

$$\rho \ddot{b}_n + C\dot{b}_n + [T_o + \frac{AE}{4L}\sum_{k=1}^{M} b_k{}^2(\frac{k\pi}{L})^2](\frac{n\pi}{L})^2 b_n$$

$$= \int_o^L f(x,t)\sin\frac{n\pi x}{L}\,dx \qquad (4\text{-}32a)$$

Dividing by ρ throughout, we get

$$\ddot{b}_n + 2\beta\dot{b}_n + [\frac{T_o}{\rho} + \frac{AE}{4\rho L}\sum_{k=1}^{M} b_k{}^2(\frac{k\pi}{L})^2](\frac{n\pi}{L})^2 b_n$$

$$= \frac{2}{\rho L}\int_o^L f(x,t)\sin\frac{n\pi x}{L}dx \qquad (4\text{-}32b)$$

where $\beta = \frac{C}{2\rho}$

or,

$$b_n + 2\beta\dot{b}_n + [\frac{T_o}{4\rho L^2} + \frac{AE}{16\rho L^3}\sum_{k=1} b_k{}^2(\frac{k\pi}{L})^2](2n\pi)^2 b_n$$

$$= \frac{2}{\rho L}\int_o f(x,t)\sin\frac{n\pi x}{L}dx \qquad (4\text{-}32c)$$

Assuming that the fundamental frequency of the corresponding linear spring is 0.1 Hz or $\frac{T_o}{\rho L^2} = 4\ \text{sec}^{-2}$, we can write Eq. (4-32c) as

$$\ddot{b}_n + 2\beta\dot{b}_n + [1 + \frac{AE}{4T_o}\sum_{k=1}^{M}(\frac{k\pi}{L})^2 b_k{}^2](2n\pi)^2 b_n = \frac{8L}{T_o}\int_o^L f(x,t)\sin\frac{m\pi x}{L}dx \qquad (4\text{-}33)$$

The right-hand side of Eq. (4-33) is the random generalized forces to be simulated.

Let $f_m(t) = \int_o^L f(t,x_1)\sin\frac{m\pi x_1}{L}dx_1$

$$f_n(t+\tau) = \int_o^L f(t+\tau,x_2)\sin\frac{n\pi x_2}{L}dx_2$$

Then,

$R_{mn}(\tau)$ = correlation function of the generalized force

$R_{mn}(\tau) = E[f_m(t)f_n(t+\tau)]$

$$R_{mn}(\tau) = \int_o^L\int_o^L E[f(t,x_1)f(t+\tau,x_2)] \times \sin\frac{m\pi x_1}{L}\sin\frac{n\pi x_2}{L}dx_1dx_2$$

$$R_{mn}(\tau) = \int_o^L\int_o^L R(\tau,x_1,x_2)\sin\frac{m\pi x_1}{L}\sin\frac{n\pi x_2}{L}dx_1dx_2 \qquad (4\text{-}34)$$

where $R(\tau,x_1,x_2)$ is the correlation function of the actual force.

Taking the Fourier Transform of Eq. (4-34) we get

$$S_{mn}(w) = \int_o^L\int_o^L S(w,x_1,x_2)\sin\frac{m\pi x_1}{L}\sin\frac{n\pi x_2}{L}dx_1dx_2 \qquad (4\text{-}35)$$

where $S_{mn}(w)$ and $S(w,x_1,x_2)$ are the spectral density functions of the

generalized force and actual force respectively.

For the particular case we take (Ref. [8]),

$$S(w,x_1,x_2) = S_0(w)e^{-\alpha|w||x_1-x_2|} \tag{4-36}$$

where

$$S_0(w) = \left[\frac{a^2}{a^2 + w^2}\right]\frac{\sigma_f^2}{\pi} \tag{4-37}$$

α and a are constants and σ_f gives the standard deviation of the actual force.

Substituting Eq. (4-36) in Eq. (4-35)

$$S_{mn}(w) = \int_0^L \int_0^L S_0(w)e^{-\alpha|w||x_1-x_2|}\sin\frac{m\pi x_1}{L}\sin\frac{n\pi x_2}{L}dx_1dx_2$$

$$= S_0(w)I_{mn} \tag{4-38}$$

where $I_{mn} = \int_0^L \int_0^L e^{-\alpha|w||x_1-x_2|}\sin\frac{m\pi x_1}{L}\sin\frac{n\pi x_2}{L}dx_1dx_2$

or,

$$I_{mn} = \int_0^L \sin\frac{m\pi x_1}{L}\left[e^{-\alpha|w|x_1}\int_0^{x_1} e^{\alpha|w|x_2}\sin\frac{n\pi x_2}{L}dx_2\right.$$

$$\left. + e^{\alpha|w|x_1}\int_{x_1}^L e^{-\alpha|w|x_2}\sin\frac{n\pi x_2}{L}dx_2\right]dx_1$$

$$= \int_0^L \sin\frac{m\pi x_1}{L}\left[\frac{2\alpha|w|\sin\frac{n\pi x_1}{L}}{(\alpha w)^2+(\frac{n\pi}{L})^2} + \frac{e^{\alpha|w|(x-L)}(\frac{n\pi}{L})(-1)^{n+1}}{(w)^2 + (\frac{n\pi}{L})^2}\right]$$

$$x\, dx_1 + \int_0^L \frac{\sin\frac{m\pi x_1}{L}e^{-\alpha|w|x_1}(\frac{n\pi}{L})dx_1}{(\alpha w) + (\frac{n\pi}{L})^2}$$

$$= \frac{1}{(\alpha w)^2 + (\frac{n\pi}{L})^2}\{\alpha|w|L \cdot \delta_{mn}$$

$$+ (\frac{n\pi}{L})(-1)^{n+1} e^{-\alpha|w|L} \frac{e^{\alpha|w|L}(\frac{m\pi}{L})(-1)^{m+1} + (\frac{m\pi}{L})}{(\alpha w)^2 + (\frac{m\pi}{L})^2}$$

$$+ (\frac{n\pi}{L}) \frac{e^{-\alpha|w|L}(\frac{m\pi}{L})(-1)^{m+1} + (\frac{m\pi}{L})}{(\alpha w)^2 + (\frac{m\pi}{L})^2}$$

which can be further simplified as

$$I_{mn} = \frac{1}{(\alpha w)^2 + (\frac{n\pi}{L})^2}\{\alpha|w|L \cdot \delta_{mn}$$

$$+ \frac{(\frac{m\pi}{L})(\frac{n\pi}{L})}{(\alpha w)^2 + (\frac{m\pi}{L})^2}[1 + (-1)^{m+n} + e^{-\alpha|w|L}((-1)^{m+1} + (-1)^{n+1})]\} \tag{4-39}$$

So,

$$S_{mn}(w) = \frac{a^2}{a^2 + w^2} \frac{\sigma_f^2}{\pi} \times \frac{1}{(\alpha w)^2 + (\frac{n\pi}{\tau})^2}\{\alpha|w|L \cdot \delta_{mn}$$

$$+ \frac{(\frac{m\pi}{L})(\frac{n\pi}{L})}{(\alpha w)^2 + (\frac{m\pi}{L})^2}[1 + (-1)^{m+n} + e^{-\alpha|w|L}((-1)^{m+1} + (-1)^{n+1})]\} \tag{4-40}$$

A numerical example was carried out for the case where $\beta = 0.1 \times 2\pi$ sec^{-1}, $a = 4\pi$ sec^{-1}, $\alpha L = 0.7$ sec, $\frac{T_o}{AE} = 0.05$, $L = 25$ in., $T_o =$

100 lb., $\rho = \frac{1}{25}$ lb/in, $E = 3\times10^7$ psi.

From the derived expression for the spectral density function, the generalized forces for 1st, 2nd and 3rd modes were simulated by the FFT method. They are shown in Fig. 12. Equations of motion (4-33) for n = 1, 2, and 3 were reduced to six first order differential equations which were solved numerically by using the Modified Predictor-Corrector method. Fig. 13 shows the simulated samples of the displacement at the midspan. The first three time series are the generalized displacement histories for the 1st, 2nd, and 3rd modes of motion respectively. The fourth one gives the actual displacement due to all three modes of motion at the center of the string. The root mean square $\sigma_{\hat{u}}$ of nondimensional response

$$\hat{u}(\tfrac{L}{2},t) = u(\tfrac{L}{2},t)/(\tfrac{L}{10})$$

at the midspan is plotted as a function of the root mean square $\sigma_{\hat{f}}$ of nondimensional forcing function

$$\hat{f}(x,t) = f(x,t)/(\tfrac{T_o}{L})$$

in Fig. 14. The total number of 2000 time points with time increment of 0.025 sec. were used for response calculation. For the sake of comparison, the response of the linear string was also plotted on the Fig. 14.

Conclusion

By comparing the results with the one obtained by Shinozuka [8] for the same problem, it is found that they are very close. This demonstrates the usefullness of the FFT simulation method. It is very

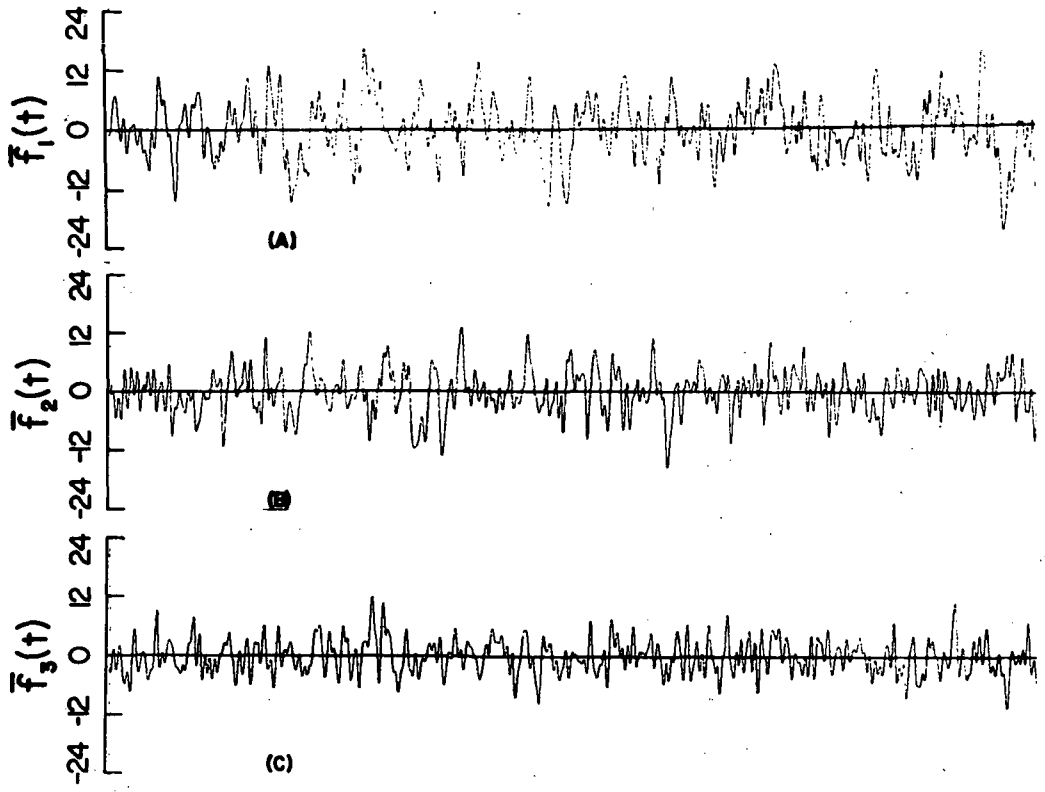

FIG. 12. GENERALIZED FORCES FOR NONLINEAR STRING:

(A) NONDIMENSIONAL GENERALIZED FORCE FOR 1ST MODE

(B) NONDIMENSIONAL GENERALIZED FORCE FOR 2ND MODE

(C) NONDIMENSIONAL GENERALIZED FORCE FOR 3RD MODE

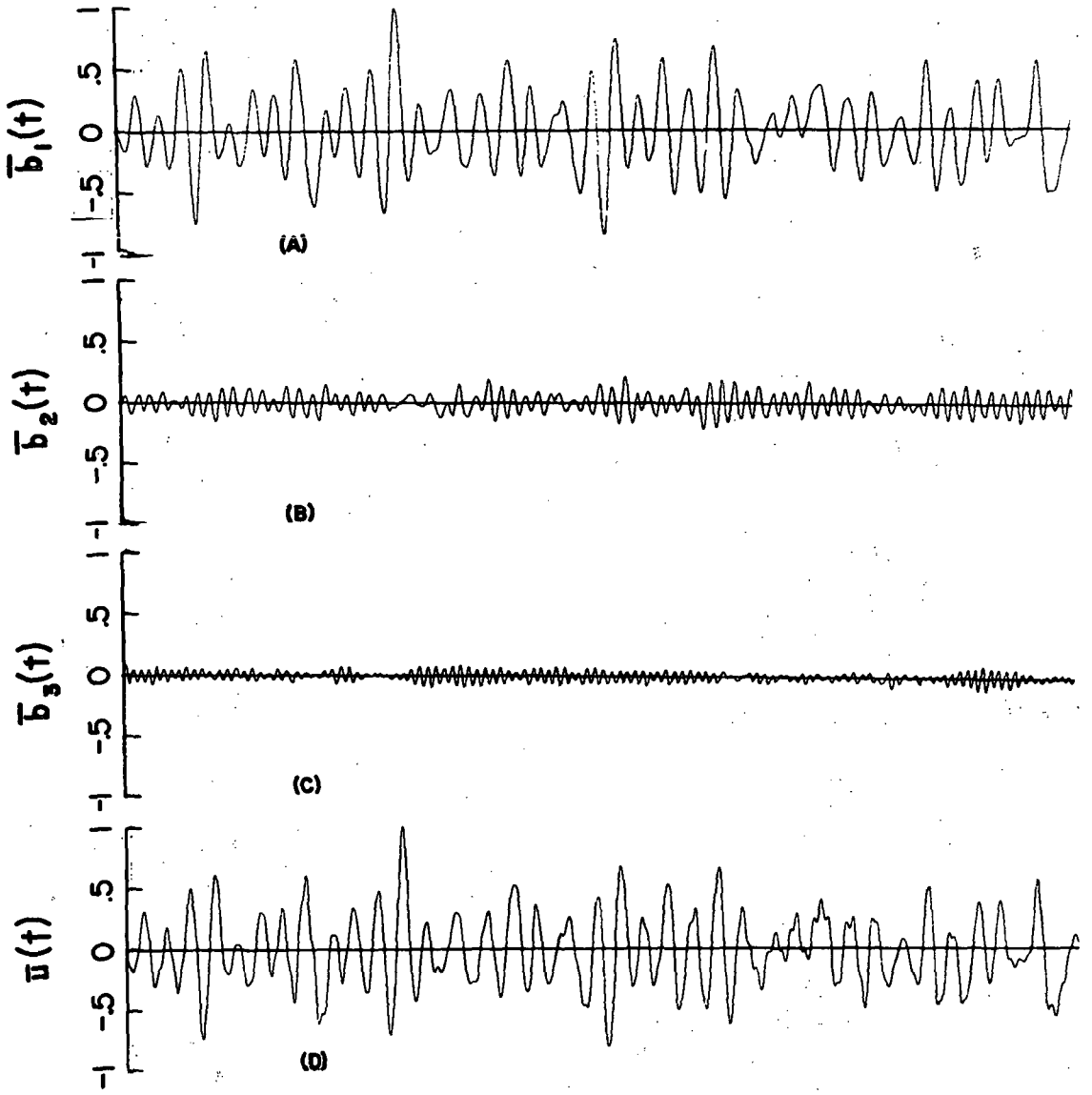

FIG. 13. DISPLACEMENT TIME HISTORIES FOR NONLINEAR STRING:

(A) NONDIMENSIONAL GENERALIZED DISPLACEMENT FOR 1ST MODE

(B) NONDIMENSIONAL GENERALIZED DISPLACEMENT FOR 2ND MODE

(C) NONDIMENSIONAL GENERALIZED DISPLACEMENT FOR 3RD MODE

(D) NONDIMENSIONAL DISPLACEMENT TIME HISTORY AT THE CENTER OF THE STRING

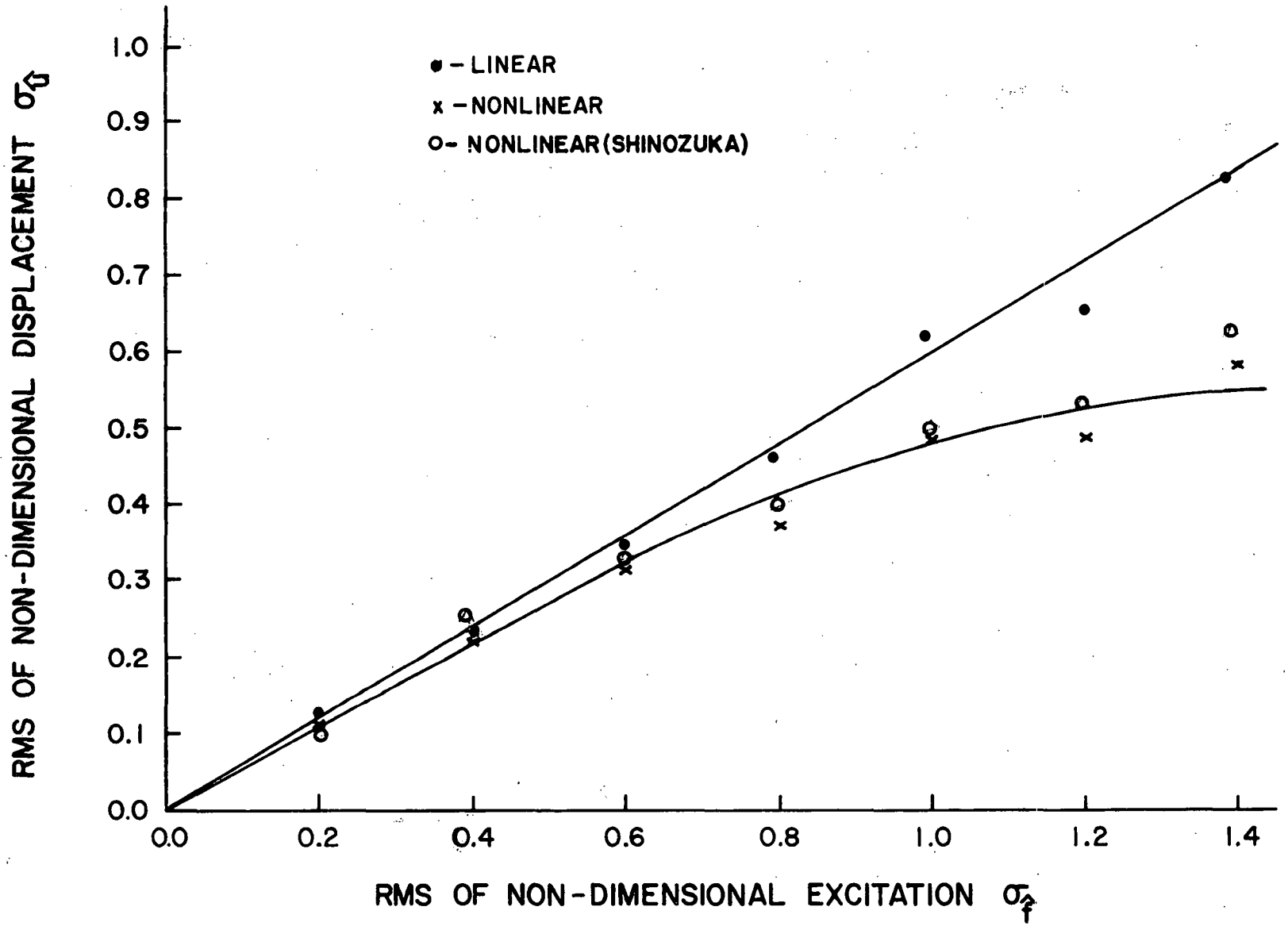

Fig. 14. Comparison between linear and nonlinear response of a string by FFT method.

interesting to note that total computer time for 2048 simulated points was less than 2 minutes which shows the advantage of time-saving due to FFT method. To simulate the same number of points using trigonometric model takes about 30 minutes of computer time.

Example 3. Nonlinear Panel Response Due to Turbulent Boundary Layer.

The random vibration of a flexible plate immersed in a fluid flow on one side and backed by a fluid filled cavity on the other side has been considered in this analysis (Fig. 15). The nonlinear plate stiffness, induced in the plate by out-of-plane bending and the mutual interaction between the external and internal fluid flow, is included. The same problem has been considered by Shinozuka [1] where he used multidimensional simulation method to find the deflection at the center of the plate. In the present work, the FFT simulation approach has been used to do the response analysis at the center of plate. The results are compared with the ones obtained in Ref. [1].

The deflection w of a simply supported plate having geometric nonlinearity is described, in dimensionless form, by two partial differential equations

$$\nabla^4\bar{w} = \bar{\Phi}_{yy}\bar{} + \bar{\Phi}_{xx}\bar{w}_{yy}\bar{} - 2\bar{\Phi}_{xy}\bar{} - \bar{w}_{xy}\bar{}$$
$$- \beta\bar{w}_t - \bar{w}_{tt}\bar{} + \bar{p} + \bar{p}^e + \bar{p}^c \qquad (4\text{-}41)$$

$$\nabla^4\bar{\Phi} = 12(1-\nu^2)\{\bar{w}_{xy}^2\bar{} - \bar{w}_{xx}\bar{w}_{yy}\bar{}\} \qquad (4\text{-}42)$$

with boundary conditions

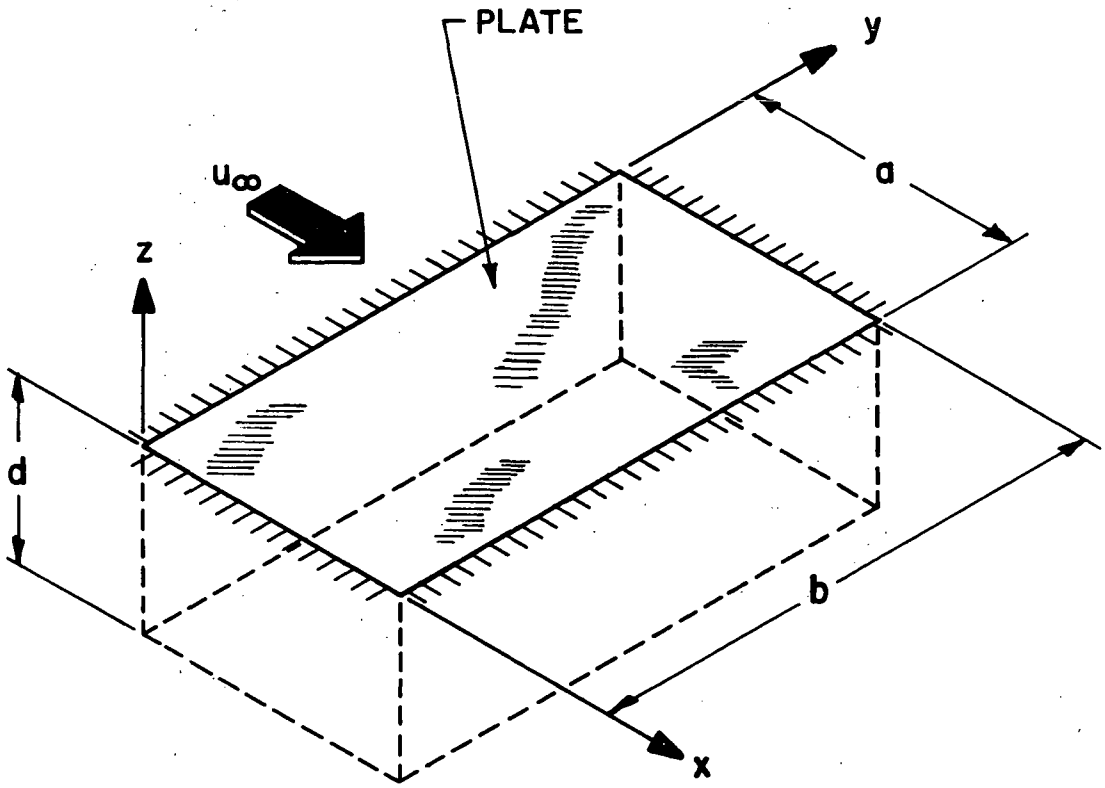

Fig. 15. Problem geometry for nonlinear plate vibration due to turbulent boundary layer pressure.

$$\bar{w}(0,\bar{y},\bar{t}) = \bar{w}(1,\bar{y},\bar{t}) = 0$$
$$\bar{w}(\bar{x},0,\bar{t}) = \bar{w}(\bar{x},1,\bar{t}) = 0 \qquad (4\text{-}43)$$
$$\bar{w}_{\bar{x}\bar{x}}(\bar{x},0,\bar{t}) = \bar{w}_{\bar{x}\bar{x}}(\bar{x},1,\bar{t}) = 0$$
$$\bar{w}_{\bar{y}\bar{y}}(0,\bar{y},\bar{t}) = \bar{w}_{\bar{y}\bar{y}}(1,\bar{y},\bar{t}) = 0$$

where $\bar{x} = x/a$, a = plate length

$\bar{y} = y/b$, b = plate width

$\bar{w} = w/h$, h = plate thickness

$\bar{\Phi}$ = nondimensional airy stress function for membrane stresses

ν = Poisson's ratio

$\bar{t}$ = nondimensional time = $\frac{t}{ab}\sqrt{\frac{D}{\rho}}$ where

$D = Eh^3/12(1-\nu^2)$, plate stiffness

E = modulus of elasticity

β = damping co-efficient

$\bar{p} = \frac{a^2b^2}{hD} p(\bar{x},\bar{y},\bar{t})$ where $p(\bar{x},\bar{y},\bar{t})$ is turbulent pressure

$\bar{p}_e = \frac{a^2b^2}{hD} p^e(\bar{x},\bar{y},\bar{t})$ where $p^e(\bar{x},\bar{y},\bar{t})$ is fluid pressure due to external flow

$\bar{p}_c = \frac{a^2b^2}{hD} \bar{p}^c(\bar{x},\bar{y},\bar{t})$ where $p_c(\bar{x},\bar{y},\bar{t})$ is fluid pressure due to cavity flow

In solving Eqs. (4-41) and (4-42), the plate deflection $\bar{w}$ is expanded in terms of the normal modes of the corresponding linear plate:

$$\bar{w}(\bar{x},\bar{y},\bar{t}) = \sum_m \sum_n b_{mn}(\bar{t}) \sin m\pi\bar{x} \sin n\pi\bar{y} \qquad (4\text{-}44)$$

where $b_{mn}(\bar{t})$ is the modal amplitude.

After the stress function $\bar{\Phi}$ is evaluated [19], the assumed modal solution is satisfied in the Galerkin sense by computing its integral which is average weighted in turn by each term of Eq. (4-44). The result is a system of simultaneous nonlinear integral-differential equations for $b_{mn}(t)$ which involve the following generalized forces

$$\bar{F}_{mn}(\bar{t}) = \frac{a^2b^2}{hD}\int_0^1\int_0^1 p(\bar{x},\bar{y},\bar{t})\sin m\pi\bar{x}\sin n\pi\bar{y}d\bar{x}d\bar{y} \qquad (4\text{-}45a)$$

$$\bar{F}^e_{mn}(\bar{t}) = \frac{a}{h\rho_\infty U_\infty{}^2}\int_0^1\int_0^1 p^e(\bar{x},\bar{y},\bar{t})\sin m\pi\bar{x}\sin n\pi\bar{y}d\bar{x}d\bar{y} \qquad (4\text{-}45b)$$

$$\bar{F}^c_{mn}(\bar{t}) = \frac{a}{h\rho_\infty a_c{}^2}\int_0^1\int_0^1 p^c(\bar{x},\bar{y},\bar{t})\sin m\pi\bar{x}\sin n\pi\bar{y}d\bar{x}d\bar{y} \qquad (4\text{-}45c)$$

where ρ_∞ = free stream density

U_∞ = mean external flow velocity

a_c = velocity of sound, cavity flow

To promote computation ease, a two mode approximation corresponding to x coordinate and one mode approximation corresponding to y coordinate to Eq. (4-44) has been assumed. Then the solution for $\bar{\Phi}$ [19] satisfying Eq. (4-42) is given by

$$\begin{aligned}\bar{\Phi} = {} & \frac{\pi^2Eh^3}{16D(1-\nu^2)\alpha^2}\{[(1+\nu\alpha^2)b_{11}{}^2 + (4+\nu\alpha^2)b_{21}{}^2]\bar{y}^2 \\ & + [(\alpha^2+\nu)b_{11}{}^2 + (\alpha^2+4\nu)b_{21}{}^2]\alpha^2\bar{x}^2\} \\ & + \frac{Eh^2\alpha^2}{4D}\{[\frac{b_{11}{}^2}{8}\cos 2\pi\bar{x} - b_{11}b_{21}\cos\pi\bar{x} \\ & + \frac{b_{11}b_{21}}{9}\cos 3\pi x + \frac{b_{21}{}^2}{32}\cos 4\pi\bar{x}] + [\frac{b_{11}{}^2 + 4b_{21}{}^2}{8\alpha^u} \\ & + \frac{9b_{11}b_{21}}{(1+4\alpha^2)^2}\cos\pi\bar{x} - \frac{b_{11}b_{21}}{(9+4\alpha^2)^2}\cos 3\pi\bar{x}]\cos 2\pi\bar{y}\}\end{aligned} \qquad (4\text{-}46)$$

where $\alpha = \frac{a}{b}$

Substituting Eq. (4-46) and Eq. (4-44) into Eq. (4-41) we get the following set of equations

$$\ddot{b}_1 + \beta_1\dot{b}_1 + (C_{10} + C_{11}b_1^2 + C_{12}b_2^2)b_{11} = 4(\bar{F}_1 + \lambda C\bar{F}_1^c + \lambda\bar{F}_1^e) \tag{4-47a}$$

$$\ddot{b}_2 + \beta_2\dot{b}_2 + (C_{20} + C_{21}b_1^2 + C_{22}b_2^2)b_{21} = 4(\bar{F}_2 + \lambda C\bar{F}_2^c + \lambda\bar{F}_2^e) \tag{4-47b}$$

where $b_1 \equiv b_{11}$, $b_2 \equiv b_{21}$, $\bar{F}_1 \equiv \bar{F}_{11}$, $\bar{F}_2 \equiv \bar{F}_{21}$, etc.

$$C_{10} = (\alpha + \frac{1}{\alpha})^2\pi^4$$

$$C_{20} = (\alpha + \frac{4}{\alpha})^2\pi^4$$

$$C_{11} = \frac{3}{4}\pi^4[(1-\nu^2)(\alpha^2 + \frac{1}{\alpha^2}) + 2(2\nu + \alpha^2 + \frac{1}{\alpha^2})]$$

$$C_{12} = \frac{3}{4}\pi^4\{(1-\nu^2)[4(\alpha^2 + \frac{1}{\alpha^2}) + \frac{81\alpha^2}{(1+4\alpha^2)^2} + \frac{\alpha^2}{(9+4\alpha^2)^2}] + 2(5\nu + \alpha^2 + \frac{4}{\alpha^2})\}$$

$$C_{21} = C_{12}$$

$$C_{22} = \frac{3}{4}\pi^4[(1-\nu^2)(\alpha^2 + \frac{16}{\alpha^2}) + 2(8\nu + \alpha^2 + \frac{16}{\alpha^2})]$$

β_1 and β_2 are the damping coefficients for the first and second mode respectively. The generalized aerodynamic force of the external flow is given by

$$\bar{F}_m^e = \sum_r Q_{rm} \tag{4-48}$$

where Q_{rm} is given in references [20] and [21]. For high mach

numbers, Eq. (2-48) can be approximated to

$$\bar{F}_m^e(\bar{t}) = \sum_r [E_{rm} b_r(\bar{t}) + P_{rm1} \dot{b}_r(\bar{t})] \qquad (4\text{-}49)$$

where

$$E_{rm} = \frac{rm}{2M(m^2-r^2)}[1 - (-1)^{r+m}] \quad \text{for } r \neq m$$

$$= 0 \quad \text{for } r = m$$

$$P_{rm} = \frac{\sqrt{D}}{4MbU_\infty\sqrt{\rho}} \quad \text{for } r = m$$

$$= 0 \quad \text{for } r \neq m, \text{ M = mach no.}$$

Again based on Ref. [21], the generalized cavity force is given by

$$\bar{F}_m^c = -\frac{a}{\pi^4 d}\frac{m[1 - (-1)^m]}{m^2}\sum_{r=1} r\frac{[1 - (-1)^r]}{r^2} b_r \qquad (4\text{-}50)$$

Thus having obtained the approximate expressions for the generalized forces due to external flow and cavity flow, we proceed to find the generalized forces due to turbulent pressure fluctuations as follows by using the FFT simulation technique: the semi-empirical formula of cross-spectral density for subsonic boundary layer turbulence is given by [22]

$$S(w,k_1,k_2) = \frac{\left\{0.715 \times 10^{-6} \frac{q^2\zeta}{\pi^2 U_\infty} \times [3.7\exp(-2\frac{w\zeta}{U_\infty}) + 0.8\exp(-0.47\frac{w\zeta}{U_\infty}) - 3.4\exp(-8\frac{w\zeta}{U_\infty})](\frac{w}{U_c})^2\right\}}{[(0.1\frac{w}{U_c})^2 + (\frac{w}{U_c} + k_1)^2][(0.715\frac{w}{U_c})^2 + k_2^2]} \qquad (4\text{-}51)$$

$$\text{for } 0 \leq w < \infty$$

where, w = freq. in radians, k_1 and k_2 are wave numbers in the x and y

directions respectively. $U_c = 0.65\ U_\infty$, q = dynamic pressure = $\rho U_\infty^2/2$, ζ = boundary layer thickness.

Let $\xi_1 = x_2 - x_1$

$\xi_2 = y_2 - y_1$

Then the spectral density function

$$S(w,\xi_1,\xi_2) = \int_{-\infty}^{\infty}\int_{-\infty}^{\infty} e^{j\xi_1 k_1} e^{j\xi_2 k_2} s(w,k_1,k_2)\,dk_1\,dk_2$$

$$= 10^{-5}\left(\frac{q^2\zeta}{\pi^2 U_\infty}\right) C_0 \int_{-\infty}^{\infty} \frac{e^{j\xi_1 k_1}\left(\frac{0.1w}{U_c}\right)dk_1}{\left[\left(\frac{0.1w}{U_c}\right)^2 + \left(\frac{|w|}{U_c} + k_1\right)^2\right]}$$

$$\times \int_{-\infty}^{\infty} \frac{e^{j\xi_2 k_2}\left(\frac{0.715w}{U_c}\right)dk_2}{\left[\left(\frac{0.715w}{U_c}\right)^2 + k_2^2\right]}$$

$$= C_0 \times 10^{-5}\left(\frac{q^2\zeta}{\pi^2 U_\infty}\right) e^{-|\xi_1|\frac{0.1w}{U_c}} e^{-|\xi_2|\frac{0.715w}{U_c}} e^{-\frac{j|w|\xi_1}{U_c}} \qquad (4\text{-}52)$$

where $C_0 = 3.7\exp\left(-2\frac{w\zeta}{U_\infty}\right) + 0.8\exp\left(-0.47\frac{w\zeta}{U_\infty}\right) - 3.4\exp\left(-8\frac{w\zeta}{U_\infty}\right)$

Now, the generalized force due to turbulent pressure fluctuation is given as

$$\bar{F}_{m_1 m_2}(t) = \frac{a^2 b^2}{hD}\int_0^1\int_0^1 p(\bar{x}_1,\bar{y}_1,\bar{t})\sin m_1\pi\bar{x}_1 \sin m_2\pi\bar{y}, d\bar{x}_1, d\bar{y}_1 \qquad (4\text{-}53a)$$

$$\bar{F}_{n_1 n_2}(\bar{t}+\tau) = \frac{a^2 b^2}{hD}\int_0^1\int_0^1 p(\bar{x}_2,\bar{y}_2,\bar{t}+\tau)\sin n_1\pi\bar{x}_2 \sin n_2\pi\bar{y}_2 d\bar{x}_2 d\bar{y}_2 \qquad (4\text{-}53b)$$

Then

$$E[\bar{F}_{m_1m_2}(\bar{t})\bar{F}_{n_1n_2}(\bar{t}+\bar{\tau})] = (\frac{a^2b^2}{hD})^2\int_0^1\int_0^1\int_0^1\int_0^1 E[p(\bar{x}_1,\bar{y}_1,\bar{t})p(\bar{x}_2,\bar{y}_2,\bar{t}+\bar{\tau})] \times \sin m_1\pi\bar{x}_1 \sin m_2\pi\bar{y}_1 \sin n_1\pi\bar{x}_2 \sin n_2\pi\bar{y}_2 d\bar{x}_1 d\bar{y}_1 d\bar{x}_2 d\bar{y}_2$$

or,

$$R_{m_1m_2n_1n_2}(\bar{\tau}) = (\frac{a^2b^2}{hD})^2\int_0^1\int_0^1\int_0^1\int_0^1 R_p(\bar{x}_1,\bar{x}_2,\bar{y}_1,\bar{y}_2,\bar{\tau}) \times \sin m_1\pi\bar{x}_1 \sin m_2\pi\bar{y}_1 \sin n_1\pi\bar{x}_2 \sin n_2\pi\bar{y}_2 d\bar{x}_1 d\bar{x}_2 d\bar{y}_1 d\bar{y}_2 \quad (4\text{-}54)$$

where $R_{m_1m_2n_1n_2}(\tau)$ is the cross correlation function of the generalized force and $R_p(\bar{x}_1,\bar{x}_2,\bar{y}_1,\bar{y}_2,\bar{\tau})$ is the cross correlation function of the turbulent pressure fluctuations.

Taking the Fourier Transform of both sides of Eq. (4-54) we get

$$S_{m_1m_2n_1n_2}(\bar{w}) = (\frac{a^2b^2}{hD})^2\int_0^1\int_0^1\int_0^1\int_0^1 S(w,\bar{\xi}_1,\bar{\xi}_2) \times \sin m_1\pi\bar{x}_1 \sin m_2\pi\bar{y}_1 \sin n_1\pi\bar{x}_2 \sin n_2\pi\bar{y}_2 d\bar{x}_1 d\bar{x}_2 d\bar{y}_1 d\bar{y}_2 \quad (4\text{-}55)$$

where $S_{m_1m_2n_1n_2}(\bar{w})$ and $S(\bar{w},\bar{\xi}_1,\bar{\xi}_2)$ are the spectral density functions of the generalized forces and turbulent pressure fluctuations respectively and $\bar{w}$ is the nondimensional frequency.

Nondimensionalizing Eq. (4-52) with respect to w, ξ_1 and ξ_2 and substituting in Eq. (4-55) for $S(w,\bar{\xi}_1,\bar{\xi}_2)$ we get

$$S_{m_1m_2n_1n_2}(\bar{w}) = \left(\frac{a^2b^2}{hD}\right)^2 10^{-5}\left(\frac{q^2\zeta}{\pi^2 U_\infty}\right)\frac{1}{ab}\sqrt{\frac{D}{\rho}}c_o$$

$$\times \int_o^1\int_o^1\int_o^1\int_o^1 e^{-|\bar{x}_2-\bar{x}_1|\frac{0.1wa}{U_c}} e^{-|\bar{y}_2-\bar{y}_1|\frac{0.715wb}{U_c}}$$

$$\times e^{-j(x_2-x_1)\frac{aw}{U_c}} \sin m_1\pi\bar{x}_1 \sin m_2\pi\bar{y}_1 \sin n_1\pi\bar{x}_2$$

$$\times \sin n_2\pi\bar{y}_2 d\bar{x}_1 d\bar{x}_2 d\bar{y}_1 d\bar{y}_2 \qquad (4\text{-}56)$$

In order to solve the integral in Eq. (4-56) we proceed as follows:

let

$$I_{m_1n_1} = \int_o^1\int_o^1 e^{-|\bar{x}_2-\bar{x}_1|\frac{0.1wa}{U_c}} e^{-j(\bar{x}_2-\bar{x}_1)\frac{aw}{U_c}}$$

$$\sin m_1\pi\bar{x}_1 \sin n_1\pi\bar{x}_2 d\bar{x}_1 d\bar{x}_2 \qquad (4\text{-}57a)$$

$$I_{m_2n_2} = \int_o^1\int_o^1 e^{-|\bar{y}_2-\bar{y}_1|\frac{0.715wa}{U_c}}$$

$$\sin m_2\pi\bar{y}_1 \sin n_2\pi\bar{y}_2 d\bar{y}_1 d\bar{y}_2 \qquad (4\text{-}57b)$$

then

$$I_{m_1n_1} = \int_o^1 e^{j\frac{wa}{U_c}x_1} \sin m_1\pi x_1 \left[e^{-\frac{0.1wa}{U_c}x_1}\right.$$

$$\times \int_o^{\bar{x}_1} e^{\frac{0.1wa}{U_c}\bar{x}_2} e^{-j\frac{wa}{U_c}\bar{x}_2} \sin n_1\pi\bar{x}_2 d\bar{x}_2$$

$$\left. + e^{\frac{0.1wa}{U_c}\bar{x}_1} \int_{\bar{x}_1}^1 e^{-\frac{0.1wa}{U_c}\bar{x}_2} e^{-j\frac{wa}{U_c}\bar{x}_2}\right.$$

$$\left. \times \sin n_1\pi\bar{x}_2 d\bar{x}_2\right] d\bar{x}_1 \qquad (4\text{-}58)$$

Evaluating the integrals inside the square bracket separately:

$$\int_0^{\bar{x}_1} e^{\frac{0.1wa}{U_c}\bar{x}_2} e^{-j\frac{wa}{U_c}\bar{x}_2} \sin n_1\pi\bar{x}_2 d\bar{x}_2$$

$$= \int_0^{\bar{x}_1} e^{\frac{0.1wa}{U_c}\bar{x}_2} \cos \frac{wa}{U_c}\bar{x}_2 \sin n_1\pi\bar{x}_2 d\bar{x}_2$$

$$-j\int_0^{\bar{x}_1} e^{\frac{0.1wa}{U_c}\bar{x}_2} \sin \frac{wa}{U_c}\bar{x}_2 \sin n_1\pi\bar{x}_2 d\bar{x}_2$$

$$= \int_0^{\bar{x}_1} e^{\frac{0.1wa}{U_c}\bar{x}_2} \cos \frac{wa}{U_c}\bar{x}_2 \sin n_1\pi\bar{x}_2 d\bar{x}_2$$

$$-j\int_0^{\bar{x}_1} e^{\frac{0.1wa}{U_c}\bar{x}_2} \frac{1}{2}\{\cos (n_1\pi - \frac{wa}{U_c})\bar{x}_2 - \cos (n_1\pi + \frac{wa}{U_c})\bar{x}_2\} d\bar{x}_2$$

$$= \frac{e^{\frac{0.1wa}{U_c}\bar{x}_1}}{2}\{\frac{\frac{0.1wa}{U_c}\sin (n_1\pi + \frac{wa}{U_c})\bar{x}_1 - (n_1\pi + \frac{wa}{U_c})\cos (n_1\pi + \frac{wa}{U_c})\bar{x}_1}{A}$$

$$+ \frac{\frac{0.1wa}{U_c}\sin (n_1\pi - \frac{wa}{U_c})\bar{x}_1 - (n_1\pi - \frac{wa}{U_c})\cos (n_1\pi - \frac{wa}{U_c})\bar{x}_1}{B}$$

$$+ \frac{1}{2}\frac{(n_1\pi + \frac{wa}{U_c})}{A} + \frac{1}{2}\frac{(n_1\pi - \frac{wa}{U_c})}{B}$$

$$-j\frac{1}{2}\{\frac{e^{\frac{0.1wa}{U_c}}}{B}(\frac{0.1wa}{U_c}\cos (n_1\pi - \frac{wa}{U_c})\bar{x}_1$$

$$+ (n_1\pi - \frac{wa}{U_c})\sin (n_1\pi - \frac{wa}{U_c})\bar{x}_1)$$

$$- \frac{0.1wa}{U_c} \frac{1}{B}\}$$

$$+ j\frac{1}{2}\{\frac{e^{\frac{0.1wa}{U_c}\bar{x}_1}}{A}(\frac{0.1wa}{U_c}\cos\ (n_1\pi + \frac{wa}{U_c})\bar{x}_1$$

$$+ (n_1\pi + \frac{wa}{U_c})\sin\ (n_1\pi + \frac{wa}{U_c})\bar{x}_1)$$

$$- \frac{0.1wa}{U_c} \frac{1}{A}\} \qquad (4\text{-}59a)$$

where, $A = (\frac{0.1wa}{U_c})^2 + (n_1\pi + \frac{wa}{U_c})^2$

$$B = (\frac{0.1wa}{U_c})^2 + (n_1\pi - \frac{wa}{U_c})^2$$

Integral Table [23] was used to evaluate the above integrals.

Now, we want to evaluate

$$\int_{\bar{x}_1}^{1} e^{\frac{-0.1wa}{U_c}\bar{x}_2} e^{-j\frac{wa}{U_c}\bar{x}_2} \sin n_1\pi\bar{x}_2 d\bar{x}_2$$

$$= \int_{\bar{x}_1}^{1} e^{\frac{-0.1wa}{U_c}\bar{x}_2} \cos \frac{wa}{U_c}\bar{x}_2 \sin n_1\pi\bar{x}_2 d\bar{x}_2$$

$$-j\int_{\bar{x}_1}^{1} e^{\frac{-0.1wa}{U_c}\bar{x}_2} \frac{1}{2}\{\cos\ (n_1\pi - \frac{wa}{U_c})\bar{x}_2 - \cos\ (n_1\pi + \frac{wa}{U_c})x_2\}dx_2$$

$$= \frac{C}{A} + \frac{D}{B}$$

$$-e^{\frac{-0.1wa}{U_c}\bar{x}_1}\{\frac{\frac{-0.1wa}{U_c}\sin\ (n_1\pi + \frac{wa}{U_c})\bar{x}_1 - (n_1\pi + \frac{wa}{U_c})\cos\ (n_1\pi + \frac{wa}{U_c})\bar{x}_1}{A}$$

$$+ \frac{\frac{-0.1wa}{U_c}\sin\ (n_1\pi - \frac{wa}{U_c})\bar{x}_1 - (n_1\pi - \frac{wa}{U_c})\cos\ (n_1\pi - \frac{wa}{U_c})\bar{x}_1}{B}\}$$

$$- \frac{j}{2}\left(\frac{E}{B}\right) - \frac{j}{2}\left(\frac{F}{A}\right)$$

$$+ \frac{j}{2}\frac{e^{-\frac{0.1w}{U_c}\bar{x}_1}}{B}\left\{-\frac{0.1wa}{U_c}\cos\left(n_1\pi - \frac{wa}{U_c}\right)\bar{x}_1 + \left(n_1\pi - \frac{wa}{U_c}\right)\sin\left(n_1\pi - \frac{wa}{U_c}\right)\bar{x}_1\right\}$$

$$- \frac{j}{2}\frac{e^{-0.1w\bar{x}_1}}{A}\left\{-\frac{0.1wa}{U_c}\cos\left(n_1\pi + \frac{wa}{U_c}\right)\bar{x}_1 + \left(n_1\pi + \frac{wa}{U_c}\right)\sin\left(n_1\pi + \frac{wa}{U_c}\right)\bar{x}_1\right\} \tag{4-59b}$$

where,

$$C = e^{-\frac{0.1wa}{U_c}}\left\{-\frac{0.1wa}{U_c}\sin\left(n_1\pi + \frac{wa}{U_c}\right) - \left(n_1\pi + \frac{wa}{U_c}\right)\cos\left(n_1\pi + \frac{wa}{U_c}\right)\right\}$$

$$D = e^{-\frac{0.1wa}{U_c}}\left\{-\frac{0.1wa}{U_c}\sin\left(n_1\pi - \frac{wa}{U_c}\right) - \left(n_1\pi - \frac{wa}{U_c}\right)\cos\left(n_1\pi - \frac{wa}{U_c}\right)\right\}$$

$$E = e^{-\frac{0.1wa}{U_c}}\left\{-\frac{0.1wa}{U_c}\cos\left(n_1\pi - \frac{wa}{U_c}\right) + \left(n_1\pi - \frac{wa}{U_c}\right)\sin\left(n_1\pi - \frac{wa}{U_c}\right)\right\}$$

$$F = e^{-\frac{0.1wa}{U_c}}\left\{-\frac{0.1wa}{U_c}\cos\left(n_1\pi + \frac{wa}{U_c}\right) + \left(n_1\pi + \frac{wa}{U_c}\right)\sin\left(n_1\pi + \frac{wa}{U_c}\right)\right\}$$

Multiplying Eq. (4-59a) by $e^{-\frac{0.1wa}{U_c}\bar{x}_1}$ and Eq. (4-59b) by $e^{-\frac{0.1wa}{U_c}\bar{x}_1}$ and adding them, we get

$$\left[e^{-\frac{0.1wa}{U_c}\bar{x}_1}\int_0^{x_1} e^{\frac{0.1wa}{U_c}\bar{x}_2} e^{-j\frac{wa}{U_c}\bar{x}_2}\sin n_1\pi\bar{x}_2 d\bar{x}_2\right.$$

$$\left. + e^{\frac{0.1wa}{U_c}\bar{x}_1}\int_{x_1}^{1} e^{-\frac{0.1wa}{U_c}\bar{x}_2} e^{-j\frac{wa}{U_c}\bar{x}_2}\sin n_1\pi\bar{x}_2 d\bar{x}_2\right.$$

$$= \frac{1}{A}\left\{\frac{0.1wa}{U_c}\sin\left(n_1\pi + \frac{wa}{U_c}\right)\bar{x}_1\right\}$$

$$+ \frac{1}{B}\{\frac{0.1wa}{U_c}\sin\ (n_1\pi - \frac{wa}{U_c})\bar{x}_1\}$$

$$+ \frac{1}{2A}\{(n_1\pi + \frac{wa}{U_c})e^{\frac{-0.1wa}{U_c}\bar{x}_1} + Ce^{\frac{0.1wa}{U_c}\bar{x}_1}\}$$

$$+ \frac{1}{2B}\{(n_1\pi - \frac{wa}{U_c})e^{\frac{-0.1wa}{U_c}\bar{x}_1} + De^{\frac{0.1wa}{U_c}\bar{x}_1}\}$$

$$+ j\frac{1}{A}\{\frac{0.1wa}{U_c}\cos\ (n_1\pi + \frac{wa}{U_c})\bar{x}_1\}$$

$$- j\frac{1}{B}\{\frac{0.1wa}{U_c}\cos\ (n_1\pi - \frac{wa}{U_c})\bar{x}_1\}$$

$$+ j\frac{1}{2A}\{\frac{-0.1wa}{U_c}e^{\frac{-0.1wa}{U_c}\bar{x}_1} + Fe^{\frac{0.1wa}{U_c}\bar{x}_1}\}$$

$$+ j\frac{1}{2B}\{\frac{0.1wa}{U_c}e^{\frac{-0.1wa}{U_c}\bar{x}_1} - Ee^{\frac{0.1wa}{U_c}\bar{x}_1}\} \qquad (4\text{-}59c)$$

Substituting Eq. (4-59c) in Eq. (4-58) and carrying out the integration, we get

$$I_{m_1n_1} = \{\frac{0.1wa}{2AU_c} + \frac{0.1wa}{2BU_c}\}\delta_{m_1n_1}$$

$$+ \{\frac{n_1\pi + \frac{wa}{U_c}}{4A} + \frac{n_1\pi - \frac{wa}{U_c}}{4B}\}e^{\frac{-0.1wa}{U_c}}\{\frac{C1}{A1} + \frac{D1}{B1}\}$$

$$+ \{\frac{C}{4A} + \frac{D}{4B}\}e^{\frac{0.1wa}{U_c}}\{\frac{C2}{A1} + \frac{D2}{B1}\}$$

$$+ \frac{0.1wa}{U_c}\{\frac{1}{4B} - \frac{1}{4A}\}e^{\frac{-0.1wa}{U_c}}\{\frac{E1}{A1} + \frac{F1}{B1}\}$$

$$+ e^{\frac{0.1wa}{U_c}}\{\frac{F}{4A} - \frac{E}{4B}\}\{\frac{G1}{A1} - \frac{G2}{B1}\}$$

$$+ j\ \frac{0.1wa}{2AU_c(m_1\pi + n_1\pi)}\{-\ (-1)^{m_1+n_1+\ 1}\}$$

$$+ j \frac{0.1wa}{2BU_c(m_1\pi + n_1\pi)}\{(-1)^{m_1+n_1} - 1\}$$

$$+ j \{\frac{n_1\pi + \frac{wa}{U_c}}{4A} + \frac{n_1\pi - \frac{wa}{U_c}}{4B}\}e^{\frac{-0.1wa}{U_c}}\{\frac{F1}{B1} + \frac{E1}{A1}\}$$

$$+ j \{\frac{C}{4A} + \frac{D}{4B}\}e^{\frac{0.1wa}{U_c}}\{\frac{G1}{A1} + \frac{G2}{B1}\}$$

$$+ j \frac{0.1wa}{U_c}\{\frac{1}{4B} - \frac{1}{4A}\}e^{\frac{-0.1wa}{U_c}}\{\frac{C1}{A1} + \frac{D1}{B1}\}$$

$$+ j \{\frac{F}{4A} - \frac{E}{4B}\}e^{\frac{0.1wa}{U_c}}\{\frac{C2}{A1} + \frac{D2}{B1}\} \qquad (4\text{-}60)$$

where

$$A1 = (\frac{0.1wa}{U_c})^2 + (m_1\pi + \frac{wa}{U_c})^2$$

$$B1 = (\frac{0.1wa}{U_c})^2 + (m_1\pi - \frac{wa}{U_c})^2$$

$$C1 = \frac{-0.1wa}{U_c}\sin(m_1\pi + \frac{wa}{U_c}) - (m_1\pi + \frac{wa}{U_c})\cos(m_1\pi + \frac{wa}{U_c}) + (m_1\pi + \frac{wa}{U_c})$$

$$D1 = \frac{-0.1wa}{U_c}\sin(m_1\pi - \frac{wa}{U_c}) - (m_1\pi - w)\cos(m_1\pi - \frac{wa}{U_c}) + (m_1\pi - \frac{wa}{U_c})$$

$$E1 = \frac{-0.1wa}{U_c}\cos(m_1\pi + \frac{wa}{U_c}) + (m_1\pi + \frac{wa}{U_c})\sin(m_1\pi + \frac{wa}{U_c}) + \frac{0.1wa}{U_c}$$

$$F1 = \frac{-0.1wa}{U_c}\cos(m_1\pi - \frac{wa}{U_c}) + (m_1\pi - \frac{wa}{U_c})\sin(m_1\pi - \frac{wa}{U_c}) + \frac{0.1wa}{U_c}$$

$$G1 = \frac{0.1wa}{U_c}\cos(m_1\pi + \frac{wa}{U_c}) + (m_1\pi + \frac{wa}{U_c})\sin(m_1\pi + \frac{wa}{U_c}) + \frac{0.1wa}{U_c}$$

$$C2 = \frac{0.1wa}{U_c}\sin(m_1\pi + \frac{wa}{U_c}) - (m_1\pi + \frac{wa}{U_c})\cos(m_1\pi + \frac{wa}{U_c}) + (m_1\pi + \frac{wa}{U_c})$$

$$D2 = \frac{0.1wa}{U_c}\sin(m_1\pi - \frac{wa}{U_c}) - (m_1\pi - \frac{wa}{U_c})\cos(m_1\pi - \frac{wa}{U_c}) + (m_1\pi + \frac{wa}{U_c})$$

$$G2 = \frac{0.1wa}{U_c}\cos(m_1\pi - \frac{wa}{U_c}) + (m_1\pi - \frac{wa}{U_c})\sin(m_1\pi - \frac{wa}{U_c}) - \frac{0.1wa}{U_c}$$

Now,

$$I_{m_2n_2} = \int_0^1 \int_0^1 e^{-|\bar{y}_2-\bar{y}_1|\frac{0.715wb}{U_c}} \sin m_2\pi\bar{y}_1 \sin n_2\pi\bar{y}_1 d\bar{y}_1 d\bar{y}_2$$

Carrying out the integration we get

$$I_{m_2n_2} = \frac{1}{\left(\frac{0.715wb}{U_c}\right)^2 + (n_2\pi)^2}\left[\frac{0.715wb}{U_c}\delta_{m_2n_2}\right.$$

$$+ \frac{(m_2\pi)(n_2\pi)}{\left(\frac{0.715wb}{U_c}\right)^2 + (m_2\pi)^2}\{1 + (-1)^{m_2+n_2} + e^{\frac{-0.715wb}{U_c}}$$

$$\left. \times \left((-1)^{m_2+1} + (-1)^{n_2+1}\right)\}\right] \qquad (4\text{-}61)$$

Then

$$S_{m_1m_2n_1n_2}(\bar{w}) = \left(\frac{a^2b^2}{hD}\right)^2 10^{-5}\left(\frac{q^2\zeta}{\pi^2U_\infty}\right)\frac{1}{ab}\frac{D_{C_o}}{\rho}\{I_{m_1n_1} + I_{m_2n_2}\} \qquad (4\text{-}62)$$

where $I_{m_1n_1}$ and $I_{m_2n_2}$ are given by Eq. (4-60) and Eq. (4-61) respectively.

Thus, the spectral density function of the generalized force due to turbulent pressure having been obtained, the generalized forces were simulated by using the FFT simulation technique.

As pointed out earlier, to work out a numerical example a two mode approximation in the x direction and one mode approximation in the y direction was taken. In order to compare the results with ones given in ref. [1], the following numerical values taken in [1] were used:

$a = 10$ in., $b = 20$ in.

$d = 5$ in., $\nu = 0.3$

$\rho = 0.1h$ lb/in^2, $E = 10^7$ psi

$U_c = 0.65\ U_\infty$, $\sigma_p = 0.0056\ q$

$\rho_\infty = \rho_c = 0.00089$ slugs/ft^3

$a_\infty = a_c = 995$ ft/sec

$U_\infty = 800$ ft/sec, $\zeta = 0.157$ in.

The thickness of the plate was varied in a way to adjust the nondimensional pressure, $\overline{p}$, for the convenience of illustration. The damping coefficients β_1 and β_2 were taken as 1 percent of the critical damping of the 1st and 2nd modes of linear plate, respectively.

In order to solve the equations (4-47a) and (4-47b), 4096 discrete values of both $\overline{F}_1(\overline{t})$ and $\overline{F}_2(\overline{t})$ were simulated from the derived expression for spectral density function using the FFT simulation technique. Eqs. (4-47a) and (4-47b) were reduced into four first order differential equations, and a modified predictor corrector method was used to solve for $b_1(\overline{t})$ and $b_2(\overline{t})$ with zero initial conditions. Fig. 16 shows the displacement time history at the center of the plate and the generalized forces for the first and second mode. The nondimensional R.M.S. response at the center of the plate versus the nondimensional R.M.S. pressure is plotted in Fig. 17 with and without the cavity effect. For the purpose of comparison, response corresponding to linear plate is also plotted in Fig. 17.

Conclusion

It is seen that the results obtained here compare very closely with the one given in Ref. [1] for the sub-sonic case. Results obtained in [1] are based on the multidimensional simulation analysis where

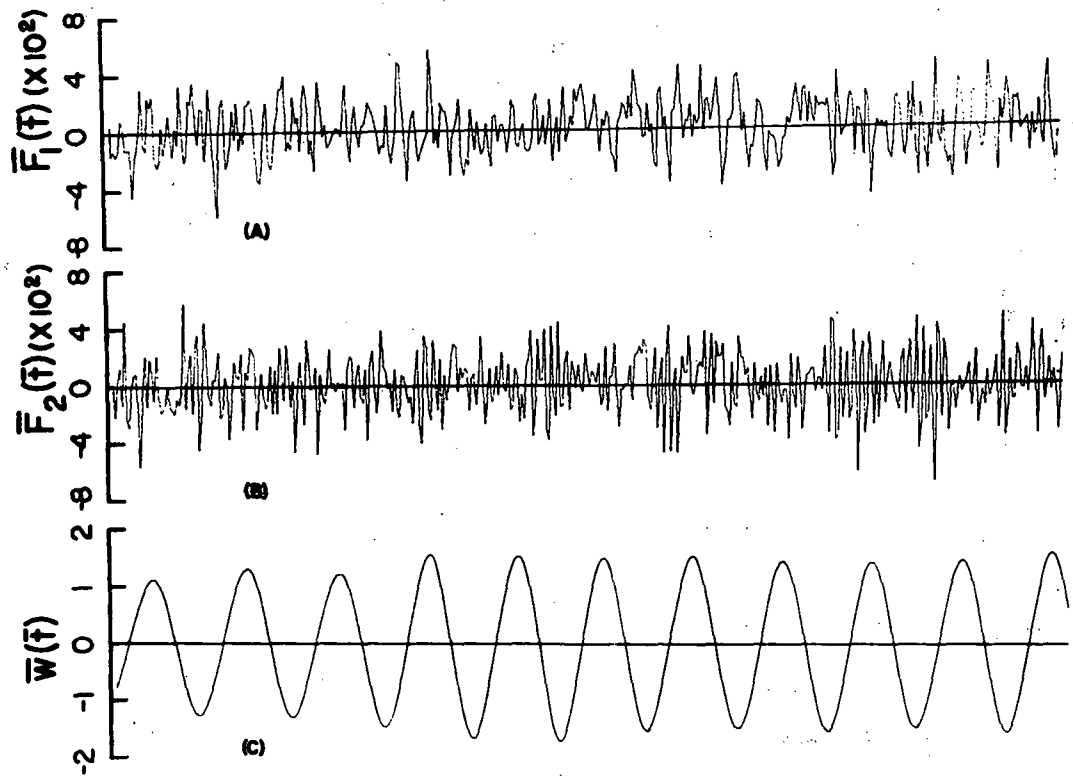

FIG. 16. GENERALIZED FORCES AND DISPLACEMENT FOR PLATE:

(A) NONDIMENSIONAL GENERALIZED FORCE FOR FIRST MODE
(B) NONDIMENSIONAL GENERALIZED FORCE FOR SECOND MODE
(C) NONDIMENSIONAL DISPLACEMENT AT THE CENTER OF THE PLATE

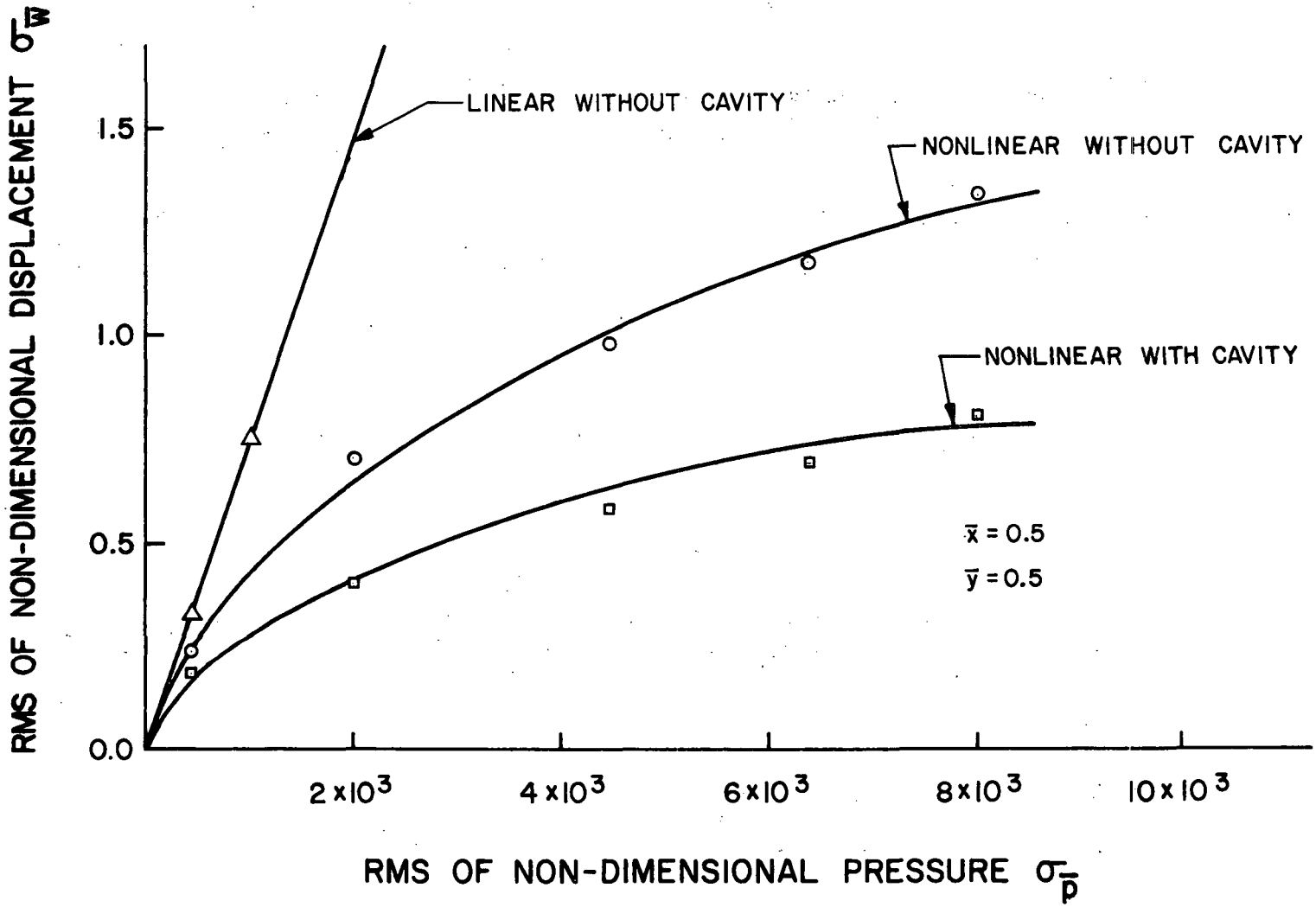

Fig. 17. Comparative study of plate response due to subsonic boundary layer pressure fluctuation by FFT method.

Shinozuka has taken only 100 frequency points which looks like a very small number considering the fact that turbulent pressure fluction takes place over a wide frequency range. From this point of view, our analysis seems more accurate because we have divided the spectrum into 4096 points. The total computer time to simulate 4096 values of both $\overline{F}_1(\overline{t})$ and $\overline{F}_2(\overline{t})$ and to obtain 4096 points for both $b_1(\overline{t})$ and $b_2(\overline{t})$ was only 3 minutes 30 seconds. It is needless to point out that the time required to simulate 4096 points for the generalized forces by using the trigonometric model of simulation will be much much more. This once again brings out the immense usefulness of FFT simulation approach wherever it is applicable.

CHAPTER V

CONCLUSIONS AND FUTURE EXTENSIONS

Two methods of simulation of a multivariate and multicorrelated random process have been presented and these methods have been applied to analyze some example problems of linear and nonlinear random vibration.

Comparing the two methods of simulation, we conclude that both the methods work very well. The only drawback is the amount of computer storage, which can become prohibitive if there are too many correlated processes to be simulated or if a very large number of discretized points are necessary for analysis. It is noted that FFT method works much faster in terms of computer time compared to the trigonometric model. This speed ratio is directly proportional to the number of series and discretized points to be simulated. For example, the time required to simulate the six components of wind turbulence, with each of the time series having 2048 discretized points, was twenty times less in the case of FFT method compared to the trigonometric approach. But FFT approach has a drawback in that the number of time points is equal to the number of frequency points and we cannot restart the simulation at any given time t. It has to start at t = 0. Also, the time interval is related to the frequency interval. The trigonometric approach does not suffer from these

disadvantages. Here, we can start the simulation beyond any given time and also the time interval is not dependent on the frequency discretization. Thus, we see that whereas the FFT method has a tremendous advantage in terms of computer time, the trigonometric method can be more useful in certain cases.

As to the usefulness and importance of the simulation technique, we conclude that it offers probably the best means of performing the nonlinear response analysis of random vibration problems when the spectral function for the forcing function is specified. In light of the review study in Chapter II, we feel that the simulation approach and particularly the FFT method gives a much faster solution with lesser number of constraints. It is noted that FFT method works as well as the ones in Ref. [1, 6, 8] for analyzing the nonlinear response and this approach is much faster than that of Shinozuka [1, 6, 8].

The methods of simulation presented here can be extended to include multidimensional homogeneous and nonhomogenous processes. For example, writing

$$
\begin{aligned}
f_m(t,x_1,x_2,\ldots x_n) &= \sum_{p=1}^{m} \sum_{k_1=1}^{N_1} \sum_{k_2=1}^{N_2} \cdots \sum_{k_n=1}^{N_n} \{a_{mp}(k_1,k_2\ldots k_n) \\
&\quad \times \cos\left[w_{1k_1} t + w_{2k_2} x_1 + \ldots + w_{nk_n} x_n + \alpha_{mp}(k_1,k_2\ldots k_n)\right] \\
&\quad + b_{mp}(k_1,k_2\ldots k_n) \\
&\quad \times \sin\left[w_{1k_1} t + w_{2k_2} x_1 + \ldots + w_{nk_n} x_n + \alpha_{mp}(k_1,k_2\ldots k_n)\right]
\end{aligned}
\qquad [5\text{-}1]
$$

one can simulate a multivariate multidimensional process using trigonometric method. Shinuzuka [6, 8] has already extended his trigonometric model to include the multidimensionality and the above proposed extension will not be much of a problem. But it will be really exciting to extend the FFT approach to a multivariate-multidimensional case. It does not seem very difficult particularly when the subroutine HARM can take care of up to 3-dimensional inverse Fourier Transform. We feel that it should work without trouble, but it does need a little closer look. It might be also interesting to extend the FFT approach to include the nonhomogeneous process by utilizing the concept of evolutionary power spectrum. This will be useful in simulating trasient and siesmic response and will also lead to considerable time saving over Shinozuka's method [8].

There are lots of other areas in which the simulation approach can be very useful and about which we have not discussed in this dissertation. For example, in the area of reliability analysis and in the response analysis of structures when the spatial variation of material properties are specified. These are some of the many areas, the simulation technique and particularly the FFT approach can be extended. These extensions look very practical.

REFERENCES

[1] Vaicatis, R., Jan, C. M. and Shinozuka, M., "Nonlinear Panel Response from a Turbulent Boundary Layer," AIAA Journal, Vol. 10, No. 7, July, 1972.

[2] Goto, H., Doki, K., and Akiyoshi, T., "Artificial Earthquake Waves by Computer," Proceeding of Japan Earthquake Engineering Symposium, 1966.

[3] Amin, M. and Ang, A. H. S., "Nonstationary Stochastic Model of Earthquake Motions," Journal of Engineering Mechanics Division, ASCE, Vol. 94.

[4] Liu, S. C., "Dynamics of Correlated Random Pulse Trains," Journal of Engineering Mechanics Div., ASCE, Vol. 96, Aug., 1970.

[5] Hoshiya, M. and Tieleman,H. W., "Two Stochastic Models for Simulation of Correlated Random Processes," V.P.I. Tech. Report, VPI=E-71-9, June, 1971.

[6] Shinozuka, M. and Jan, C. M., "Simulation of Multidimensional Random Processes II," Tech. Report No. 12, Columbia Univ., N.Y., April, 1971.

[7] Borgman, L. E., "Ocean Wave Simulation for Engineering Design," Journal of Waterways and Harbors Div., ASCE, Vol. No. WW4, November, 1969.

[8] Shinozuka, M., "Simulation of Multivariate and Multidimensional Random Processes," Journal of Acoustical Society of America, Vol. 49, No. 1, January, 1971.

[9] Ariarathan, S. T., "Random Vibration of Nonlinear Suspensions," Journal of Mechanical Engr. Science, Vol. 2, pp. 195-201 (1960).

[10] Caughey, T. K., "Derivation and Application of the Fokker-Planck Equation to Discrete Nonlinear Systems Subjected to White Random Excitation," Journal of Acoustical Society of America, Vol. 35, No. 11, 1963.

[11] Caughey, T. K., "Equivalent Linearization Technique," Journal of Acoustical Society of America, pp. 1706-1711 (1963)

[12] Crandall, S. H., "Perturbation Technique for Random Vibration of Nonlinear Systems," Journal of Acoustical Society of America, Vol. 35, No. 11, Nov., 1963.

[13] Tung, C. C., "The Effects of Runway Roughness on the Dynamic Response of Airplanes," Journal of Sound and Vibration, Vol. 5, pp. 164-172 (1967).

[14] Foss, K. A., "Coordinates Which Uncouple the Equations of Motion of Damped Linear Systems," Journal of Applied Mechanics, Vol. 25, pp. 361-364 (1958).

[15] Yang, I., "Stationary Random Response of Multidegree-of-Freedom Systems," Ph.D. Thesis, California Institute of Technology, submitted March 10, 1970.

[16] Blackadar,A. K., Dutton, J. A., Panofsky, H. A. and Chaplin, A., "Investigation of Turbulent Wind Field Below 150 M Altitude at the Eastern Test Range," NASA CR-1410, August, 1969.

[17] Panofsky, H. A., "Properties of Wind and Temperature at Round Hill, South Dartmouth, Massachusetts," Research and Development Tech. Report ECOM-0035-F, Penn. State Univ., Univ. Park, Penn., Aug., 1967.

[18] Fichtl, G. H. and Mcvehil, G. E., "Longitudinal and Lateral Spectra of Turbulence in the Atmospheric Boundary Layer," AGARD Conference Proceedings No. 48, NATO, Munich, Sept., 1969.

[19] Bolotin, V. V., Nonconservative Problems of the Theory of Elastic Stability, Pergamon Press, 1963, pp. 280-289.

[20] Dowell, E. H., "Generalized Aerodynamic Forces on a Flexible Plate Undergoing Transient Motion," Q. Appl. Math., Vol. 24, 1967.

[21] Dowell, E. H., "Transmission of Noise from Turbulent Boundary Layer Through a Flexible Plate into a Closed Cavity," Journal of Acoustical Society of America, Vol. 46, No. 1, 1969.

[22] Bull, M. K., "Wall-Pressure Fluctuation Associated with Subsonic Turbulent Boundary Layer Flow," J. Fluid Mech., Vol. 28, Part 4, 1967.

[23] Gradshteyn, I. S. and Ryzhik, I. M., Table of Integrals Series and Products, Academic Press, 1965.

[24] Bendat, J. S. and Piersol, A. G., Random Data: Analysis and Measurement Procedures, Wiley-Interscience, New York, 1971.

[25] Lin, Y. K., Probabilistic Theory of Structural Dynamics, McGraw-Hill Book Company, New York, 1967.

[26] Meirovitch, L., Analytical Methods in Vibration, The Macmillan Company, London, 1967.

[27] Dutton, J. A., Panofsky, H. A., Deaven, D. C., Kerman, B. R. and Mirabella, V., "Statistical Properties of Turbulence at the Kennedy Space Center for Aerospace Vehicle Design," NASA CR-1889, August 1971.

[28] McVehil, G. E. and Camnitz, H. G., "Ground Wind Characteristics at Kennedy Space Center," NASA CR-1418, Sept. 1969.

[29] Maestrello, L., "Measurement and Analysis of the Response Field of Turbulent Boundary Layer Excited Panels," J. of Sound and Vibration, 2, 1965, pp. 270-292.

[30] Shinozuka, M. and Wen, Y. K., "Monte Carlo Solution of Non-linear Vibrations," AIAA Paper No. 71-213, AIAA 9th Aerospace Science Meeting, New York, 1971.

[31] Fung, Y. C. and Barton, M. V., "Shock Response of a Nonlinear System," J. of Applied Mech., Sept., 1962.

[32] Gardener, N. J., "Response of Cooling Tower to Turbulent Wind," J. of Strc. Div. of ASCE, Oct., 1969.

[33] Vickery, B. J., "Wind Action on Simple Yielding Structures," J. of Engr. Mech. Div. of ASCE, April 1970.

[34] Beer, F. P., "On the Response of Linear System to Time-Dependent, Multidimensional Loadings," Journal of Applied Mechanics, March 1961.

[35] Shinozuka, M. and Astill, C. J., "Random Eigenvalue Problems in Structural Analysis," AIAA Journal, Vol. 10, No. 4, 1972.

[36] Hasselman, T. K. and Hart, G. C., "Modal Analysis of Random Structural Systems," J. of Engr. Mech. Div., ASCE, June 1972.

[37] Proceedings of Seminar on Wind Loads and Structures, sponsored by NSF, Japan Soc. for Promotion of Science and Univ. of Hawaii, Oct., 1970.

APPENDIX A

1. Random Variable and Probability Distribution Function

Let X be any random variable which varies with statistical regularity. Since X is a random variable, any function of X is also a random variable.

The first-order probability distribution function of X can be described by a graph as in Fig. A-1 which shows the probability density function p(X). The hatched area gives the probability that X lies between a and b. It is apparent that the probability is zero that X actually assumes any given value x. Also we have

$$\int_{-\infty}^{\infty} p(X)dX = 1. \qquad \text{(A-1)}$$

The cumulative distribution function (CDF) defines the probability of occurrence of a value of X less than or equal to a given value x, i.e.,

$$P(x) = \int_{-\infty}^{x} p(X)dx. \qquad \text{(A-2)}$$

According to fundamental theorem of integral calculus,

$$\frac{dP(x)}{dx} = p(x) \qquad \text{(A-3)}$$

wherever this derivative exists.

Properties of CDF

(1) CDF is a non-decreasing function of x

(2) P(x) varies between 0 and 1 as x varies from $-\infty$ to ∞. Thus $P(-\infty) = 0$ and $P(\infty) = 1$.

Several random variables $X_1, X_2, \ldots X_n$ are said to be jointly distributed if they are defined as functions on the same sample description

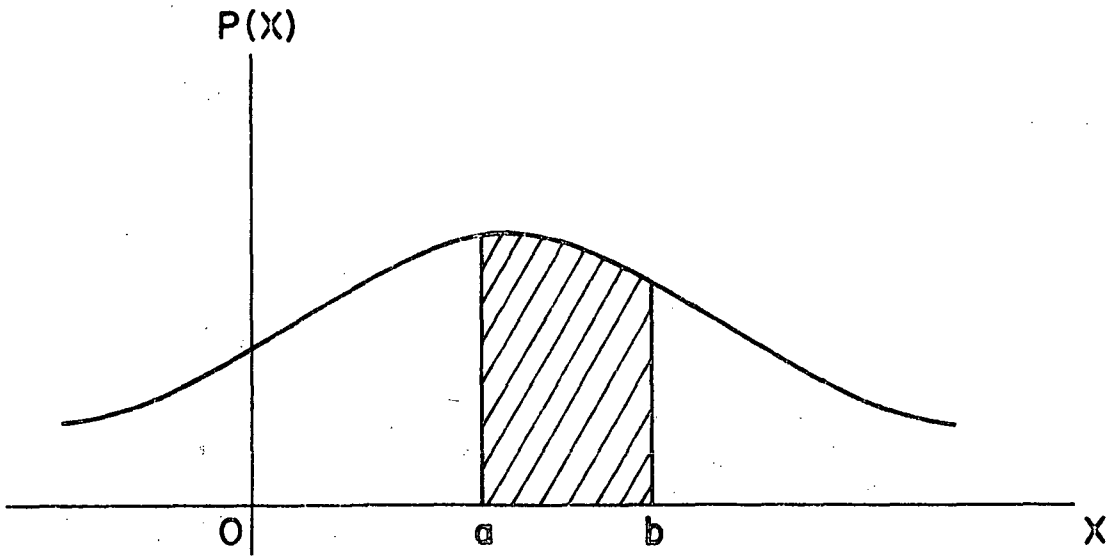

Fig. 1-A. PDF of Continuous Random Variable X.

space. We shall refer to $p(X_1, X_2,\ldots X_n)$ as the joint probability density of these random variables. Thus, the probability that $a_1 < X_1 < b_1$, $a_2 < X_2 < b_2,\ldots a_n < X_n < b_n$ is given by

$$\int_{a_1}^{b_1}\int_{a_2}^{b_2}\ldots\int_{a_n}^{b_n} p(X_1,X_2,\ldots X_n)dX_1dX_2\ldots dX_n . \tag{A-4}$$

Also,

$$\int_{-\infty}^{\infty}\int_{-\infty}^{\infty}\ldots\int_{-\infty}^{\infty} p(X_1,X_2,\ldots X_n)dX_1dX_2\ldots dX_n = 1 . \tag{A-5}$$

The joint probability distribution of two random variables X_1 and X_2 is given by

$$p(X_1,X_2) \tag{A-6}$$

and

$$p(a_1 < X_1 < b_1 \text{ and } a_2 < X_2 < b_2) .$$

$$= \int_{a_1}^{b_1}\int_{a_2}^{b_2} p(X_1,X_2)dX_1dX_2 \tag{A-7}$$

Supposing that X is now a random function of spacial coordinates $\underline{x}$ or time t, the first and joint probability distribution functions defined above are valid for any given values of $\underline{x}$ or t. That is, the probability that X ($\underline{x}$ or t) lies between a and b is given by

$$\int_a^b p(X(\underline{x}, \text{ or } t))dX(\underline{x} \text{ or } t) \tag{A-8}$$

and

$$P(x) = \int_{-\infty}^{\infty} p(X(\underline{x} \text{ or } t))dX(\underline{x} \text{ or } t) . \tag{A-9}$$

2. Mean, Mean Square, Variance and Standard Deviation

The ensemble average

$$\mu_X = E[X] = \int_{-\infty}^{\infty} X\, p(X)dX \qquad \text{(A-10)}$$

defines the mean of X or the expected value of X. The operator E is used to denote this kind of average. The mean square value of X is given by

$$E\,[X^2] = \int_{-\infty}^{\infty} X^2\, p(X)dX\,. \qquad \text{(A-11)}$$

An important statistical parameter is the variance of X which is the ensemble average of the square of the deviation from the mean. Thus the variance of X is given by

$$\sigma^2 = E\,[(X-\mu_X)^2] = \int_{-\infty}^{\infty} (X-\mu_X)^2\, p(X)dX\,. \qquad \text{(A-12)}$$

An alternate expression is

$$\sigma^2 = E[X^2] - \mu_X{}^2\,. \qquad \text{(A-13)}$$

When the mean is zero, the variance is identical with mean square. The square root of Eq. (13), that is σ, is called the standard deviation. The co-efficient of variation is defined by

$$V = \frac{\sigma}{\mu_X} \qquad \text{(A-14)}$$

which tells the degree of variation.

3. Random Process

Let us consider random functions X(t) and Y(t) in which t represents any variable, say, spacial co-ordinates or time.

For a random process, we may express the correlation between $X(t_1)$ and $X(t_2)$ by means of the autocorrelation function

$$R_X(t_1,t_2) = E[X(t_1)\,X(t_2)]$$

$$= \int_{-\infty}^{\infty}\int_{-\infty}^{\infty} X(t_1)\,X(t_2)\,p(X(t_1), X(t_2))dX(t_1)\,dX(t_2) \quad \text{(A-15)}$$

The prefix auto refers to the fact that $X(t_1)$ and $X(t_2)$ represents a product of values on the same sample at two different coordinates. If $X(t_1)$ and $X(t_2)$ are statistically independent, we have

$p(X(t_1), X(t_2)) = p(X(t_1))\,p(X(t_2))$ and hence

$$R_X(t_1, t) = E[X(t_1)]\,E[X_1 t_2)] \quad \text{(A-16)}$$

Cross correlation function is defined for two samples $X(t_1)$ and $Y(t_2)$ by

$$R_{XY}(t_1, t_2) = E[X(t_1)\,Y(t_2)]$$

$$= \int_{-\infty}^{\infty}\int_{-\infty}^{\infty} X(t_1)\,Y(t_2)\,p(X(t_1), Y(t_2))\,dX(t_1)\,dY(t_2) \quad \text{(A-17)}$$

Correlation coefficient is given by

$$\rho_{XY} = \frac{E[(X(t_1) - E[X(t_1)])\,(Y(t_2) - E[Y(t_2)])]}{\sigma_X(t_1)\,\sigma_Y(t_2)} \quad \text{(A-18)}$$

It can be shown that

$$-1 \leq \rho_{XY} \leq 1 \quad \text{(A-19)}$$

and the intermediate values of ρ_{XY} measure the degree of linear statistical dependence between $X(t_1)$ and $Y(t_2)$.

4. Stationary Random Process

A random process is said to be stationary if its probability distributions are invariant under a shift of the co-ordinates. In other words, the family of probability densities applicable at t_1 also applies at t_2. In particular, the first order probability density function p(X) becomes universal distribution independent of time. This implies that all the averages baseed on p(X), say, E[X] and σ^2, are constants independent of time.

For a stationary process, the autocorrelation or cross correlation functions become functions of the difference between t_1 and t_2 and independent of t_1 or t_2.

Therefore, for a stationary process, Equation (A-15) becomes

$$R_{X(\tau)} = E\,[X(t_1)\ X(t_1+\tau)],\ \tau = t_1 - t_2 \qquad \text{(A-20)}$$

and Equation (A-17) is

$$R_{XY(\tau)} = E\,[X(t_1)\ Y(t_1+\tau)],\ \tau = t_1 - t_2. \qquad \text{(A-21)}$$

APPENDIX B

Fast Fourier Transform

Restricting the limits to a finite time interval for the record $x(t)$, say in the range (o, T), the finite range Fourier Transform is defined as

$$X(f, T) = \int_{o}^{T} x(t) e^{-j2\pi ft} dt \qquad \text{(B-1)}$$

Assume now that time $x(t)$ is sampled at N equally spaced points a distance h apart, then for arbitrary f, the discrete version of Equation (B-1) becomes

$$X(f, T) = h \sum_{n=0}^{N-1} x_n \, \text{Exp}[-j\, 2\pi\, fnh] \qquad \text{(B-2)}$$

Selecting the discrete frequency values as

$$f_k = kf = \frac{k}{T} = \frac{k}{Nh} \qquad k = 0, 1, 2, \ldots N-1 \qquad \text{(B-3)}$$

At these frequencies, the transformed values give the Fourier components defined by

$$X_k = \frac{X(f_k, T)}{h} = \sum_{n=0}^{N-1} x_n \exp\left[-j \frac{2\pi kn}{N}\right]$$

$$k = 0, 1, 2 \ldots, N-1 \qquad \text{(B-4)}$$

where h has been included with $X(f_k, T)$ to have a scale factor of unity before the summation. Note that results are unique only out to

$k = \frac{N}{2}$ since the Nyquist cutoff frequency occurs at this point. Fast Fourier transform (FFT) methods are designed to compute these quantities, X_k, and can also be used to compute the co-efficients of the regular Fourier series Aq and Bq in the expression

$$x_n = x(nh) = Ao + \sum_{q=1}^{N/2} Aq \cos\left(\frac{2\pi qn}{N}\right) + \sum_{q=1}^{\frac{N}{2}-1} Bq \sin\left(\frac{2\pi qn}{N}\right) . \qquad \text{(B-5)}$$

To simplify the notation further, let

$$w(u) = \exp\left[-j \frac{2\pi u}{N}\right] . \qquad \text{(B-6)}$$

Observe that $w(N) = 1$ and for all u and v,

$$w(u + v) = w(u)\, w(v) . \qquad \text{(B-7)}$$

Also, let

$$X(k) = X_k \text{ and } x(n) = x_n \qquad \text{(B-8)}$$

Then Equation (B-4) becomes

$$X(k) = \sum_{n=0}^{N-1} x(n)\, w(kn), \quad k = 0, 1, 2, \ldots N-1 . \qquad \text{(B-9)}$$

Equations (B-4) and (B-9) should be studied so as to be easily recognized as the Fourier transform of x(n) when x(n) is expressed by a series of N terms. Such equations require a total of approximately N^2 complex multiply-add operations to compute all of the X(k) terms involved.

Fast Fourier Transform procedures are now based upon decomposing N into its composite (nonunity) factors, and carrying out Fourier transform over the smaller number of terms in each of the composite

factors. In particular, if N is the product of p factors such that

$$N = \prod_{i=1}^{p} r_i = r_1 r_2 \cdots r_p \tag{B-10}$$

where the r's are all integers greater than unity, then it can be proved [24] that X(k) in Equation (B-9) can be found by computing in an iterative fashion the sum of p terms,

$$\begin{aligned} &\frac{N}{r_1} \text{ Fourier transform requiring } 4r_1^2 \text{ real operations each,} \\ &\frac{N}{r_2} \text{ Fourier transform requiring } 4r_2^2 \text{ real operations each,} \\ &\vdots \\ &\frac{N}{r_p} \text{ Fourier transform requiring } 4r_p^2 \text{ real operations each.} \end{aligned} \tag{B-11}$$

Hence the total number of real operations becomes

$$4(Nr_1 + Nr_2 + Nr_3 + \cdots + Nr_p) = 4 \sum_{i=1}^{p} r_2 \tag{B-12}$$

The resulting speed ratio of these FFT procedures to the standard method is then

$$\text{speed ratio} = \frac{N^2}{4N \sum_{i=1}^{p} r_i} = \frac{N}{4 \sum_{i=1}^{p} r_i} \tag{B-13}$$

speed ratio for powers of two:

If $N = 2^p$, then $\sum_{i=1}^{p} r_i = 2p = 2 \log_2 N$

In this case, the speed ratio by equation (B-13) appears to be

$$\text{speed ratio} = \frac{N^2}{8Np} = \frac{N}{8p}$$

However, a doubling of the speed can be achieved in practice by noting that the values for w(kn), when N is a power of 2, all turn out to be +1 or -1, so as to yield a higher speed ratio of the order of

$$\text{speed ratio} = \frac{N}{4p} \tag{B-14}$$

For example, if $N = 2^{13} = 8192$, Equation (B-14) gives a speed ratio of $\frac{8192}{52} \simeq 158$.

APPENDIX C

Expanding Eq. (3-14), with $H(w_k)$ being a lower triangular matrix, one obtains

$$G_{mn} = H_{m_1}\overline{H}_{n_1} + H_{m_2}\overline{H}_{n_2} + \ldots. H_{mn}\overline{H}_{nn}, \text{ for } n < m,$$

$$G_{mm} = |H_{m_1}|^2 + |H_{m_2}|^2 + \ldots. |H_{mm}|^2 \qquad \text{(C-1)}$$

From Eqs. (3-22a), (3-22b), and (3-3) and (C-1) one can see that m th component process is simulated from $H_{mp}(w_k)$ (p = 1, ..., m) and the coherence between the m th component and n th component with n < m is generated by $H_{mp}(w_k)$ and $H_{np}(w_k)$ (p = 1, 2, ... n). When a vanishing minor is due to a zero mean square density of, say, the m th component process at a frequency w_k, then the elements of cross-spectral density associated with this component are also zero at this particular frequency. It is easy to show that a sufficient condition for this case is

$$H_{mn}(w_k) = 0, \text{ for } n = 1, 2, \ldots m$$

$$H_{nm}(w_k) = 0, \text{ for } n = m + 1, \ldots. M$$

The remaining elements of $H_{mn}(w_k)$ are then determined from the sub-matrix obtained by deleting the m th row and m th column from the matrix $G(w_k)$.

A coherence of unity between two component processes (the m th and the (m + 1) th) at a frequency w_k will also give rise to vanishing

principal minors. This implies a complete linear dependence at this frequency between the two processes and hence the existence of the transfer function $\beta(w_k)$ such that

$$G_{m+1,\, m+1}(w_k) = |\beta(w)|^2 G_{mm}(w_k)$$
$$G_{m,\, m+1}(w_k) = \beta(w) G_{mm}(w_k) \qquad \text{(C-2)}$$

Therefore, at this w_k, it can be shown that $G(w_k)$ will take the following form:

$$\begin{bmatrix} G_{11} \cdots G_{1j} & G_{1,j+1} \cdots G_{1M} \\ \cdots\cdots\cdots\cdots & \cdots\cdots\cdots \\ G_{j1} \cdots G_{jj} & G_{j,j+1} \cdots G_{jM} \\ G_{j+1,1} \cdots G_{j+1,j} & G_{j+1,j+1} \cdots G_{j+1,M} \\ \cdots\cdots\cdots\cdots & \cdots\cdots\cdots \\ G_{M1} \cdots G_{Mj} & G_{M,j+1} \cdots G_{MM} \end{bmatrix} =$$

$$\begin{bmatrix} G_{11} \cdots G_{1j} & \beta G_{ij} \cdots G_{1M} \\ \cdots\cdots\cdots\cdots & \cdots\cdots\cdots \\ G_{j1} \cdots G_{jj} & \beta G_{jj} \cdots G_{jM} \\ \bar{\beta} G_{j1} \cdots \bar{\beta} G_{jj} & |\beta|^2 G_{jj} \cdots \bar{\beta} G_{jM} \\ \cdots\cdots\cdots\cdots & \cdots\cdots\cdots \\ G_{M1} \cdots G_{Mj} & \beta G_{Mj} \cdots G_{MM} \end{bmatrix} \qquad \text{(C-3)}$$

In this case, $H(w_k)$ can be solved for a particular frequency in the following fashion.

First, reduce the size of both matrices $G(w_k)$ and $H(w_k)$ by deleting the $(j + 1)$ th row and $(j + 1)$ the column, then solve for the reduced $H(w_k)$ from the reduced $G(w_k)$, by the method mentioned in

Chapter III. Finally, the deleted elements of $H(w_k)$, as can be seen by direct substitution in Eq. (C-1), are given by

$$H_{j+1,p} = \overline{\beta} H_{jp}, \text{ for } p = 1, 2, \ldots j$$
$$H_{j+1,j+1} = 0, \qquad \text{(C-4)}$$
$$H_{p,j+1} = 0, \text{ for } p = j+2, \ldots M$$

If two component processes, again, say, the j th and (j + 1) th, are completely correlated, then $\beta(w)$ as defined for the previous case will reduce to a real constant β_0 independent of the frequency. This will lead to $D_p(w_k) = 0$, $p = j + 1, \ldots M$, for all frequencies. For this case, it is necessary to simulate only m - 1 component processes with the (j + 1) th removed from the system, since it can be obtained by

$$f_{j+1}(t) = \beta_0 f_j(t)$$

With the proper combination of the above procedures, it is possible to deal with the following situations:

(i) more than one component of $G(w_k)$ vanishes;

(ii) more than two components are completely coherent or correlated;

(iii) the combination thereof.

APPENDIX D

COMPUTER PROGRAM

This section of the report deals with the listing of some of the important input parameters in the computer programs included. On the left-hand column is the computer language (FORTRAN) symbol and on the right-hand side, just opposite, is the equivalent variable used in the derivation of the equations in Chapter III and Chapter IV.

Listing for Program for Simulation by Trigonometric Method:

K	KA, frequency index
$\alpha_{mp}(k)$	ALPHA(I,KK,KA), deterministic phase angles
W_u	WU, upper cut-off frequency
W_ℓ	WL, lower cut-off frequency
G_{mn}	S(I,J), element of spectral density function
H_{ji}	HHH(I,J), elements of lower triangular matrix
a_{mp}, b_{mp}	AA(I,KK,KA), BB(I,KK,KA), random Gaussian variables
Δw	DW, discretized frequency interval
m	KK, number of time series
ξ_p, η_p	V1, V2, random number generated by Gauss subroutine
Δt	DT, time interval
$f_m(t)$	F(I,JJJ), representation of time series

Listing for Program for Simulation by FFT Method:

K	KA, frequency index
G(I,J)	S(I,J), input spectral density function
H_{pqk}	HHH(I,J), elements of lower triangular matrix
η_{pk}, ξ_{pk}	Z1(K), Z2(K), independent Gaussian random numbers
ζ_p	XI(K), complex random number
h	DT, time interval
X_{pk}	DDX(I,KA), elements of complex random vector
f_{pn}	F(I,J), time series representation

Listing for Program for Nonlinear Response Analysis of String

σ_f	SIGF, standard deviation of the forcing function
L	TL, length of the string
α	ALPHA, a constant
T_o	TO, initial tension in the string
ρ	ROE, density per unit length
w_1, w_2, w_3	W1, W2, W3, natural frequency of vibration for 1st, 2nd and 3rd modes respectively
A	AR, area of cross section
$S_o(w)$	SO(KA), spectral density function of actual force
$S_{mn}(w)$	S(I,J), spectral density of the generalized force
$f_m(t)$	F(I,J), generalized force representation
$\dot{b}_n(t)$	AN(t), derivative of modal displacement
$b_n(t)$	BN(t), modal displacement

$\ddot{b}_n(t)$ ANPR(t), second derivative of the modal displacement

Listing for Program for Nonlinear Panel Response Problem:

β_1 BET1, percentage of critical damping for 1st mode of vibration

β_2 BET2, percentage of critical damping for 2nd mode of vibration

σ_p SIGP, r.m.s. pressure of boundary layer pressure fluctuations

U_∞ UINF, mean external flow velocity

a SA, plate length

b SB, plate width

ν GNU, Poisson's ratio

U_c UC, convectional speed

M CM, mack number

ρ ROE, plate density per unit area

d S1, cavity depth

u SV, sound velocity

ζ XSI, boundary layer thickness

$\frac{a}{b}$ ALP

D RIG, plate stiffness

λ^c DEMC, constant

λ DEM, constant

q	SQ, dynamic pressure
C_o	CONST, constant

```
C       SIMULATION OF MULTICORRELATED RANDOM PROCESSES BY TRIGONMETRIC
1       METHOD
        DIMENSION UU(6,6),TZ(2050),     C(6,6),Q(6,6),ALPHA(6,6,600)
       1,V(6,6) ,S(6,6), U(6,6), HH(6,6),HHH(6,6),    Y(6),X(6),A(6),B(6)
       1 ,AA(6,6,600),BB(6,6,600),W(600),WW(6),F(6,2048),F1(2048),
       1F2(2048),F3(2048),F4(2048),FF(2050),F5(2048),F6(2048)
        COMPLEX S ,HH,HHH,YYY,DD
        N=600
        WU=3.141592
        WL=0.00377
        XN=N
        DW=(WU-WL)/(XN-1.)
        DDW=SQRT(DW/6.28318)
        DT=1.
        KA=1
   14   XK=KA
        DO 7 I=1,6
        DO 7KK=1,I
    7   ALPHA(I,KK,KA)=0.0
        W(KA)=(XK-1.0)*DW+WL
C       INPUT SPECTRAL DENSITY FUNCTION
        DO 401 I=1,6
        DO 401 J=1,6
        C(I,J)=0.0
  401   Q(I,J)=0.0
        Z=30.48
        CU=6.198
        VU=0.845
        DU=(Z/18.0)**(-0.63)
        FMU=0.03*Z/18.0
        US=1.589
        Z=100.
```

```
      H =BU*(US**2)*CU*Z
      G=(120.0*FMU)*(1.+1.5*(W(KA)*Z/( 60.*2.0*3.14159*FMU))**VU)**(5.0
     1  /(3.0*VU))
      C(1,1)= H/G
      Z=15.24
      BU=(Z/18.0)**(-0.63)
      FMU=0.03*Z/18.0
      Z=50.
      H =BU*(US**2)*CU*Z
      G=(101.9*FMU)*(1.+1.5*(W(KA)*Z/(50.9*2.0*3.14159*FMU))**VU)**(5.0
     1  /(3.0*VU))
      C(4,4)= H/G
      Z=30.48
      CU=8.686
      VU=0.512
      BU=(Z/18.0)**(-0.35)
      FMU=0.1*(Z/18.0)**0.58
      Z=100.
      H =BU*(US**2)*CU*Z
      G=(120.0*FMU)*(1.+1.5*(W(KA)*Z/( 60.*2.0*3.14159*FMU))**VU)**(5.0
     1  /(3.0*VU))
      C(2,2)= H/G
      Z=15.24
      BU=(Z/18.0)**(-0.35)
      FMU=0.1*(Z/18.0)**0.58
      Z=50.
      H =BU*(US**2)*CU*Z
      G=(101.9*FMU)*(1.+1.5*(W(KA)*Z/(50.9*2.0*3.14159*FMU))**VU)**(5.0
     1  /(3.0*VU))
      C(5,5)= H/G
      Z=100.
      C(3,3)=((3.36*(US**2)*Z     )/(1.0+10.0*(W(KA)*Z/(2.0*3.14159*60.0
```

```
1 ))**(5.0/3.0)))/120.
 Z=50.
 C(6,6)=((3.36*(US**2)*Z     )/(1.0+10.0*(W(KA)*Z/(2.0*3.14159*50.97
1 ))**(5.0/3.0)))/101.94
 Z=100.
 H=(US**2)*12.5*Z
 G=-120.0*(1.0+6.0*W(KA)*Z/(2.0*3.14159*60.0))**(8./3.)
 C(1,3)=H/G
 C(3,1)=C(1,3)
 Z=50.
 H=(US**2)*10.0*Z
 G=-101.9*(1.0+6.0*W(KA)*Z/(2.0*3.14159*50.9))**(8./3.)
 C(4,6)=H/G
 C(6,4)=C(4,6)
 DELZ=50.
 DELF=0.0366
 E=0.7
 C(1,4)=(C(1,1)*C(4,4))**0.5*0.5*(EXP(-0.693*W(KA)*DELZ/(2.*
1 3.1416*55.5*DELF)))**0.5*(COS(W(KA)*DELZ*E/55.5))
 C(4,1)=C(1,4)
 Q(1,4)=(C(1,1)*C(4,4))**0.5*0.5*(EXP(-0.693*W(KA)*DELZ/(2.*
1 3.1416*55.5*DELF)))**0.5*(SIN(W(KA)*DELZ*E/55.5))
 Q(4,1)=-Q(1,4)
 E=1.5
 DELF=0.0448
 C(2,5)=(C(2,2)*C(5,5))**0.5*0.5*(EXP(-0.693*W(KA)*DELZ/(2.*
1 3.1416*55.5*DELF)))**0.5*(COS(W(KA)*DELZ*E/55.5))
 C(5,2)=C(2,5)
 Q(2,5)=(C(2,2)*C(5,5))**0.5*0.5*(EXP(-0.693*W(KA)*DELZ/(2.*
1 3.1416*55.5*DELF)))**0.5*(SIN(W(KA)*DELZ*E/55.5))
 Q(5,2)=-Q(2,5)
 C(3,6)=(C(3,3)*C(6,6))**0.5*0.5*(EXP(-0.693*W(KA)*DELZ/(2.*
```

```
     1 3.1416*55.5*DELF)))**0.5*(COS(W(KA)*DELZ*E/55.5))
      C(6,3)=C(3,6)
      Q(3,6)=(C(3,3)*C(6,6))**0.5*0.5*(EXP(-0.693*W(KA)*DELZ/(2.*
     1 3.1416*55.5*DELF)))**0.5*(SIN(W(KA)*DELZ*E/55.5))
      Q(6,3)=-Q(3,6)
      DELF=0.04
      E=1.0
      C(3,4)=(C(1,3)*C(4,6))**0.5*0.5*(EXP(-0.693*W(KA)*DELZ/(2.*
     1 3.1416*55.5*DELF))**0.5)*(COS(W(KA)*DELZ*E/55.5))*(-1.)
      C(4,3)=C(3,4)
      Q(3,4)=(C(1,3)*C(4,6))**0.5*0.5*(EXP(-0.693*W(KA)*DELZ/(2.*
     1 3.1416*55.5*DELF))**.5) *(SIN(W(KA)*DELZ*E/55.5))
      Q(4,3)=-Q(3,4)
      C(1,6)=C(3,4)
      C(6,1)=C(1,6)
      Q(1,6)=Q(3,4)
      Q(6,1)=-Q(1,6)
      DO 25 I=1,6
      DO 25 J=1,6
      C(I,J)=C(I,J)*2.0
      Q(I,J)=Q(I,J)*2.0
   25 S(I,J)=CMPLX(C(I,J),-Q(I,J))
C     BREAKING THE SPECTRAL MATRIX INTO THE UPPER AND LOWER TRIANGULAR
1     MATRIX
      DO 29 I=1,6
      DO 29 J=1,6
      HH(I,J)=CMPLX(0.0,0.0)
   29 HHH(I,J)=CMPLX(0.0,0.0)
      HH(1,1)=  CSQRT(S(1,1))
      HHH(1,1)=HH(1,1)
      DO 110 J=2,6
      HH(1,J) =    (S(1,J)/HH(1,1))
```

```
 110  HHH(J,1)= CONJG(HH(1,J))
      DO1120 I=2,6
      DD=CMPLX(0.0,0.0)
      M=I-1
      DO113 LP=1,M
 113  DD=DD+     (HH(LP,I)*CONJG(HH(LP,I)))
      YYY=S(I,I)-DD
      HH(I,I)= CSQRT(YYY)
      HHH(I,I)=HH(I,I)
      IF (I.EQ.6) GO TO1121
      NN=I+1
      MM=I-1
      DO1120 J=NN,6
      DD=CMPLX(0.0,0.0)
      DO222 LP=1,MM
 222  DD=DD+     (HH(LP,I)*CONJG(HH(LP,J)))
      HH(I,J)=       ((S(I,J)-DD)/HH(I,I))
      HHH(J,I)=CONJG(HH(I,J))
 1120 CONTINUE
 1121 CONTINUE
      DO 117 I=1,6
      DO 117 KK=1,6
      ALPHA(I,KK,KA)=0.0
      AA(I,KK,KA)=0.0
 117  BB(I,KK,KA)=0.0
C     RANDOM NUMBER NUMER GENERATOR SUBROUTINE GAUSS
      DO 123 KK=1,6
      CALL GAUSS(17,1.0,0.0,V1)
      CALL GAUSS(29,1.0,0.0,V2)
      DO 123 I=1,6
      AA(I,KK,KA)= (CABS(HHH(I,KK)))*V1*DDW
      BB(I,KK,KA)= (CABS(HHH(I,KK)))*V2*DDW
```

```
      IF(ABS(REAL(HHH(I,KK))).LT.0.00001) GO TO 2001
      ALPHA(I,KK,KA)=ATAN(AIMAG(HHH(I,KK))/REAL(HHH(I,KK)))
      GO TO 1233
 2001 ALPHA(I,KK,KA)=1.5708
 1233 IF(KA.GE.20) GO TO 123
      WRITE(6,2000) V1,V2
  123 CONTINUE
 3003 FORMAT(2I5)
 2000 FORMAT(2E16.8)
      IF(KA.EQ.600) GO TO 40
      KA=KA+1
      GO TO 14
   40 I=1
      XX=0.0
      YY=6.0
  100 TT=0.0
      DO 45 JJJ=1,2048
   45 F(I,JJJ)=0.0
      DO 46 JJJ=1,2048
      DO 47 KA=1,600
      DO 47 KK=1,I
   47 F(I,JJJ)=F(I,JJJ)+AA(I,KK,KA)*COS(W(KA)*TT+ALPHA(I,KK,KA))+
     1 BB(I,KK,KA)*SIN(W(KA)*TT+ALPHA(I,KK,KA))
      TT=TT+DT
46    FF(JJJ)=F(I,JJJ)
      DO225 J=1,2048
  225 TZ(J)=J-1
C     PLOTTING OF THE TURBULENCE TIME HISTORIES
      FF(2049)=16.0
      FF(2050)=-16.0
      CALL SCALE (TZ,2048,20.0,TZMIN,TX,1)
      CALL SCALE(FF,2050,4.0,FFMIN,FX,1)
```

```
      CALL AXIS (XX,YY,2HTZ,2,20.0,0.0,TZMIN,TX)
      CALL AXIS (XX,YY,2HFF,2,4.0,90.0,FFMIN,FX)
      CALL PLOT (XX,YY,-3)
      CALL LINE (TZ,FF,2048,1)
      XX=22.0
      YY=0.0
      IF(I.EQ.6) GO TO 111
      I=I+1
      GO TO 100
  111 CONTINUE
      DO 79 I=1,2048
      F1(I)=F(1,I)
      F2(I)=F(2,I)
      F3(I)=F(3,I)
      F4(I)=F(4,I)
      F5(I)=F(5,I)
   79 F6(I)=F(6,I)
      WRITE(10) F1
      WRITE(10) F2
      WRITE(10) F3
      WRITE(10) F4
      WRITE(10) F5
      WRITE(10) F6
      CALL PLOT (0.0,0.0,-4)
      STOP
      END
```

```
C       SIMULATION OF MULTICORRELATED RANDOM PROCESSES BY FFT METHOD
        DIMENSION UU(6,6),TZ(2050),    C(6,6),Q(6,6),A(2048,1,1)
       1,V(6,6) ,S(6,6), U(6,6), HH(6,6),HHH(6,6),    FF(2050)
       1,                          W(1025),WW(6),F(6,2048),F1(2048),
       1F2(2048),F3(2048),F4(2048),F5(2048),F6(2048)
       1 ,MV(3),INV(1024),Z1(6),Z2(6),DX(6),DDX(6,2048),XI(6),P(1024)
        COMPLEX S ,HH,HHH,YYY,DD,XI,DX,DDX,A
        XX=0.0
        YY=5.0
        N=1025
        WXX=SQRT(2.*2048.)
        WU=3.141592
        XN=N
        DW=(WU-WL)/(XN-1.)
        DDW=SQRT(DW*0.5)
        CT=1.
        KA=1
   14   XK=KA
        W(KA)=(XK-1.0)*DW+WL
C       INPUT SPECTRAL DENSITY FUNCTION
        DO 401 I=1,6
        DO 401 J=1,6
        C(I,J)=0.0
  401   Q(I,J)=0.0
        Z=30.48
        CU=6.198
        VU=0.845
        BU=(Z/18.0)**(-0.63)
        FMU=0.03*Z/18.0
        US=1.589
        Z=100.
        H =BU*(US**2)*CU*Z
```

```
      G=(120.0*FMU)*(1.+1.5*(W(KA)*Z/( 60.*2.0*3.14159*FMU))**VU)**(5.0
     1  /(3.0*VU))
      C(1,1)= H/G
      Z=15.24
      BU=(Z/18.0)**(-0.63)
      FMU=0.03*Z/18.0
      Z=50.
      H =BU*(US**2)*CU*Z
      G=(101.9*FMU)*(1.+1.5*(W(KA)*Z/(50.9*2.0*3.14159*FMU))**VU)**(5.0
     1  /(3.0*VU))
      C(4,4)= H/G
      Z=30.48
      CU=8.686
      VU=0.512
      BU=(Z/18.0)**(-0.35)
      FMU=0.1*(Z/18.0)**0.58
      Z=100.
      H =BU*(US**2)*CU*Z
      G=(120.0*FMU)*(1.+1.5*(W(KA)*Z/( 60.*2.0*3.14159*FMU))**VU)**(5.0
     1  /(3.0*VU))
      C(2,2)= H/G
      Z=15.24
      BU=(Z/18.0)**(-0.35)
      FMU=0.1*(Z/18.0)**0.58
      Z=50.
      H =BU*(US**2)*CU*Z
      G=(101.9*FMU)*(1.+1.5*(W(KA)*Z/(50.9*2.0*3.14159*FMU))**VU)**(5.0
     1  /(3.0*VU))
      C(5,5)= H/G
      Z=100.
      C(3,3)=((3.36*(US**2)*Z     )/(1.0+10.0*(W(KA)*Z/(2.0*3.14159*60.0
     1 ))**(5.0/3.0)))/120.
```

```
      Z=50.
      C(6,6)=((3.36*(US**2)*Z     )/(1.0+10.0*(W(KA)*Z/(2.0*3.14159*50.97
     1 ))**(5.0/3.0)))/101.94
      Z=100.
      H=(US**2)*12.5*Z
      G=-120.0*(1.0+6.0*W(KA)*Z/(2.0*3.14159*60.0))**(8./3.)
      C(1,3)=H/G
      C(3,1)=C(1,3)
      Z=50.
      H=(US**2)*10.0*Z
      G=-101.9*(1.0+6.0*W(KA)*Z/(2.0*3.14159*50.9))**(8./3.)
      C(4,6)=H/G
      C(6,4)=C(4,6)
      DELZ=50.
      DELF=0.0366
      E=0.7
      C(1,4)=(C(1,1)*C(4,4))**0.5*0.5*(EXP(-0.693*W(KA)*DELZ/(2.*
     1 3.1416*55.5*DELF)))**0.5*(COS(W(KA)*DELZ*E/55.5))
      C(4,1)=C(1,4)
      Q(1,4)=(C(1,1)*C(4,4))**0.5*0.5*(EXP(-0.693*W(KA)*DELZ/(2.*
     1 3.1416*55.5*DELF)))**0.5*(SIN(W(KA)*DELZ*E/55.5))
      Q(4,1)=-Q(1,4)
      E=1.5
      DELF=0.0448
      C(2,5)=(C(2,2)*C(5,5))**0.5*0.5*(EXP(-0.693*W(KA)*DELZ/(2.*
     1 3.1416*55.5*DELF)))**0.5*(COS(W(KA)*DELZ*E/55.5))
      C(5,2)=C(2,5)
      Q(2,5)=(C(2,2)*C(5,5))**0.5*0.5*(EXP(-0.693*W(KA)*DELZ/(2.*
     1 3.1416*55.5*DELF)))**0.5*(SIN(W(KA)*DELZ*E/55.5))
      Q(5,2)=-Q(2,5)
      C(3,6)=(C(3,3)*C(6,6))**0.5*0.5*(EXP(-0.693*W(KA)*DELZ/(2.*
     1 3.1416*55.5*DELF)))**0.5*(COS(W(KA)*DELZ*E/55.5))
```

```
      C(6,3)=C(3,6)
      Q(3,6)=(C(3,3)*C(6,6))**0.5*0.5*(EXP(-0.693*W(KA)*DELZ/(2.*
     1 3.1416*55.5*DELF)))**0.5*(SIN(W(KA)*DELZ*E/55.5))
      Q(6,3)=-Q(3,6)
      DELF=0.04
      E=1.0
      C(3,4)=(C(1,3)*C(4,6))**0.5*0.5*(EXP(-0.693*W(KA)*DELZ/(2.*
     1 3.1416*55.5*DELF))**0.5)*(COS(W(KA)*DELZ*E/55.5))*(-1.)
      C(4,3)=C(3,4)
      Q(3,4)=(C(1,3)*C(4,6))**0.5*0.5*(EXP(-0.693*W(KA)*DELZ/(2.*
     1 3.1416*55.5*DELF))**.5) *(SIN(W(KA)*DELZ*E/55.5))
      Q(4,3)=-Q(3,4)
      C(1,6)=C(3,4)
      C(6,1)=C(1,6)
      Q(1,6)=Q(3,4)
      Q(6,1)=-Q(1,6)
      DO 25 I=1,6
      DO 25 J=1,6
      C(I,J)=C(I,J)*2.0
      Q(I,J)=Q(I,J)*2.0
   25 S(I,J)=CMPLX(C(I,J),-Q(I,J))
C     BREAKING THE SPECTRAL MATRIX INTO THE UPPER AND LOWER TRIANGULAR
1     MATRIX
      DO 29 I=1,6
      DO 29 J=1,6
      HH(I,J)=CMPLX(0.0,0.0)
   29 HHH(I,J)=CMPLX(0.0,0.0)
      HH(1,1)=  CSQRT(S(1,1))
      HHH(1,1)=HH(1,1)
      DO 110 J=2,6
      HH(1,J) =    (S(1,J)/HH(1,1))
  110 HHH(J,1)= CONJG(HH(1,J))
```

```
      DO1120 I=2,6
      DD=CMPLX(0.0,0.0)
      M=I-1
      DO113 LP=1,M
  113 DD=DD+    (HH(LP,I)*CONJG(HH(LP,I)))
      YYY=S(I,I)-DD
      HH(I,I)= CSQRT(YYY)
      HHH(I,I)=HH(I,I)
      IF (I.EQ.6) GO TO1121
      NN=I+1
      MM=I-1
      DO1120 J=NN,6
      DD=CMPLX(0.0,0.0)
      DO222 LP=1,MM
  222 DD=DD+    (HH(LP,I)*CONJG(HH(LP,J)))
      HH(I,J)=      ((S(I,J)-DD)/HH(I,I))
      HHH(J,I)=CONJG(HH(I,J))
 1120 CONTINUE
 1121 CONTINUE
C     RANDOM NUMBER NUMER GENERATOR SUBROUTINE GAUSS
      DO 109 K=1,6
      CALL GAUSS(33,0.707,0.0,V2)
      CALL GAUSS(27,0.707,0.0,V3)
      Z2(K)=V2
  109 Z1(K)=V3
      DO 252 K=1,6
  252 XI(K)=CMPLX(Z1(K),Z2(K))
      DO 300 I=1,6
      DD=CMPLX(0.0,0.0)
      DO 309 J=1,I
  309 DD   =DD+HHH(I,J)*XI(J)
      DX(I)=DD
```

```
 300  DDX(I,KA)=DX(I)
      IF(KA.EQ.1025) GO TO 40
      KA=KA+1
      GO TO 14
 40   DO 600 I=1,6
      DO 600 N=1,1023
      K=1025+N
      J=1025-N
 600  DDX(I,K)=CONJG(DDX(I,J))
      DO 800 J=1,6
      DO 700 I=1,2048
 700  A(I,1,1)=DDX(J,I)
      MV(1)=11
      MV(2)=0
      MV(3)=0
C     SUBROUTINE TO PERFORM THE INVERSE FOURIER TRANSFORM
      CALL HARM(A,MV,INV,P,1,IFEER)
      DO225 I=1,2048
      FF(I)=REAL(A(I,1,1))/WXX
      F(J,I)=FF(I)
 225  TZ(I)=I-1
C     PLOTTING OF THE TURBULENCE TIME HISTORIES
      FF(2049)=16.0
      FF(2050)=-16.0
      CALL SCALE (TZ,2048,20.0,TZMIN,TX,1)
      CALL SCALE (FF,2050,4.0,FFMIN,FX,1)
      CALL AXIS (XX,YY,2HTZ,-2,20.,0.0,TZMIN,TX)
      CALL AXIS (XX,YY,2HFF,2,4.0,90.0,FFMIN,FX)
      CALL PLOT (XX,YY,-3)
      CALL LINE (TZ,FF,2048,1)
      XX=22.0
      YY=0.0
```

```
800   CONTINUE
      CALL PLOT (0.0,0.0,-4)
      STOP
      END
```

```
C       PROGRAM FOR RANDOM RESPONSE ANALYSIS OF A NONLINEAR STRING USING
1       FFT SIMULATION METHOD
        DIMENSION W(1025),SO(1025),S(3,3)
       1,FF(2050),F(3,2049), T(15),DX(6),DDX(3,2050)
       1 ,HH(4,4),HHH(4,4),AX(2048,1,1),INV(1024),Z1(6),Z2(6),Z3(6),
       1 XI(6),MV(3),P(1024),TZ(2050),
       1 A1PR(2048),A2PR(2048),A3PR(2048),B1PR(2048),B2PR(2048),B3PR(2048)
       1,A1MF(2048),A2MF(2048),A3MF(2048),B1MF(2048),B2MF(2048),B3MF(2048)
       1,A1CR(2048),A2CR(2048),A3CR(2048),B1CR(2048),B2CR(2048),B3CR(2048)
       1,G1(2048),G2(2048),G3(2048)
        COMMON    A1(2048),A2(2048),A3(2048),B3(2048),B1(2048),B2(2048),
       1 A1P(2048),A2P(2048),A3P(2048),B1P(2048),B2P(2043),B3P(2048),
       1 F1(2048),F2(2048),F3(2048)
        COMMON BETA1,BETA2,BETA3,W1,W2,W3,AR,TL,TO,E
        COMPLEX AX,XI,DZ,DX,DDX
        XX=0.0
        YY=3.0
        KKK=1
        SIG=0.2
 11     CONTINUE
        DO 239 I=1,3
        DO 239 KA=1,1025
 239    DDX(I,KA)=CMPLX(0.0,0.0)
        SIGF=(SIG**2)*3.14159*16.0/1.19
        N=257
        XN=N
        WXX=SQRT(2.*.025*2048)
        WU=10.0*3.14159
        WL=0.0
        DW=(WU-WL)/(XN-1.)
        A=4.0*3.14159
        TL=25.0
```

```
      ALPHA=0.7/25.0
      TO=100.0
      ROE=1.0/25.0
      E=3.0*10.0**7
      AR=TO/(0.05*E)
      W1=SQRT(((1.0*3.14159/TL)**2)*TO/ROE)
      W2=SQRT(((2.0*3.14159/TL)**2)*TO/ROE)
      W3=SQRT(((3.0*3.14159/TL)**2)*TO/ROE)
      BETA1=0.1*6.28318/W1
      BETA2=0.1*6.28318/W2
      BETA3=0.1*6.28318/W3
      KA=1
   14 XK=KA
      W(KA)=(XK-1.0)*DW+WL
      SO(KA)=(A/(A**2+W(KA)**2))*SIGF/3.14159
      JJJ=3
      DO 15 I=1,JJJ
      DO 15 J=1,JJJ
      YJ=  (ALPHA*W(KA))**2+(J*3.14159/TL)**2
      YI=  (ALPHA*W(KA))**2+(I*3.14159/TL)**2
      XIJ=I*J*(3.14159/TL)**2
      IF(I.EQ.J) GO TO 16
      S(I,J)=SO(KA)*XIJ*(1.0+(-1.0)**(I+J)+EXP(-ALPHA*W(KA)*TL)
     1 *((-1.)**(I+1)+(-1.)**(J+1)))/(YJ*YI)
      GO TO 15
C     SPECTRAL DENSITY FUNCTION OF THE GENERALIZED FORCE
   16 S(I,J)=(ALPHA*W(KA)*TL+XIJ/YI*(1.+(-1.)**(I+J)+EXP(-ALPHA*W(KA)*TL
     1 )*((-1.)**(I+1)+(-1.)**(J+1))))/YJ*SO(KA)
   15 CONTINUE
      DO 29 I=1,JJJ
      DO 29 J=1,JJJ
      HH(I,J)=0.0
```

```
29    HHH(I,J)=0.0
      HH(1,1)=    SQRT(S(1,1))
      HHH(1,1)=HH(1,1)
      DO 110 J=2,JJJ
      HH(1,J) =    ( S(1,J)/HH(1,1))
110   HHH(J,1)= HH(1,J)
      DO1120 I=2,JJJ
      DD=0.0
      M=I-1
      DO113 LP=1,M
113   DD=DD+     (HH(LP,I)*HH(LP,I))
      YYY= S(I,I)-DD
      HH(I,I)=  SQRT(YYY)
      HHH(I,I)=HH(I,I)
      IF (I.EQ.JJJ) GO TO 1121
      NN=I+1
      MM=I-1
      DO1120 J=NN,JJJ
      DD=0.0
      DO222 LP=1,MM
222   DD=DD+     (HH(LP,I)*HH(LP,J))
      HH(I,J)=      (( S(1,J)-DD)/HH(I,I))
      HHH(J,I)=HH(I,J)
1120  CONTINUE
1121  CONTINUE
      DO 109 K=1,JJJ
      CALL GAUSS(17,0.707,0.0,V3)
      CALL GAUSS(23,0.707,0.0,V2)
      Z2(K)=V2
109   Z1(K)=V3
      DO 252 K=1,JJJ
252   XI(K)=CMPLX(Z1(K),Z2(K))
```

```
      DO 300 I=1,JJJ
      DZ=CMPLX(0.0,0.0)
      DO 309 J=1,I
  309 DZ   =DZ+HHH(I,J)*XI(J)
      DX(I)=DZ
  300 DDX(I,KA)=DX(I)
      IF(KA.EQ.257)  GO TO 40
      KA=KA+1
      GO TO 14
   40 DO 600 I=1,JJJ
      DO 600 N=1,1023
      K=1025+N
      J=1025-N
  600 DDX(I,K)=CONJG(DDX(I,J))
      DO 800 J=1,JJJ
      DO 700 I=1,2048
  700 AX(I,1,1) =DDX(J,I)
      MV(1)=11
      MV(2)=0
      MV(3)=0
      CALL HARM(AX,MV,INV,P,1,IFEER)
C     SIMULATED GENERALIZED FORCE
      DO225 I=1,2048
      FF(I)=REAL(AX(I,1,1))*8.0*TL/(TC*WXX)
      F(J,I)=FF(I)
  225 TZ(I)=I-1
      FF(2049)=25.0
      FF(2050)=-25.0
      CALL SCALE (TZ,2048,20.0,TZMIN,TX,1)
      CALL SCALE (FF,2050,4.0,FFMIN,FX,1)
      CALL AXIS (XX,YY,2HTZ,-2,20.,0.0,TZMIN,TX)
      CALL AXIS (XX,YY,2HFF,2,4.0,90.0,FFMIN,FX)
```

```
      CALL PLOT (XX,YY,-3)
      CALL LINE (TZ,FF,2048,1)
      XX=22.0
      YY=0.0
  800 CONTINUE
      DO 801 I=1,2048
      F1(I)=F(1,I)
      F2(I)=F(2,I)
  801 F3(I)=F(3,I)
C     SIMLATED GENERALIZED FORCE
C     CALCULATION OF NONLINEAR RESPNSE BY MODIFIED PREDICTOR CORRECTOR
1     METHOD
C INITIAL CONDITIONS
      M=1
      H=0.025
      A1(1)=0.0
      B1(1)=0.0
      A2(1)=0.0
      B2(1)=0.0
      A3(1)=0.0
      B3(1)=0.0
C STARTING VALUES
      CALL FCT(M)
C PREDICTOR
      A1PR(2)= 4.0*H     *(2.0*A1P(1))/3.0
      B1PR(2)= 4.0*H     *(2.0*B1P(1))/3.0
      A2PR(2)= 4.0*H     *(2.0*A2P(1))/3.0
      B2PR(2)= 4.0*H     *(2.0*B2P(1))/3.0
      A3PR(2)= 4.0*H     *(2.0*A3P(1))/3.0
      B3PR(2)= 4.0*H     *(2.0*B3P(1))/3.0
C NO MODIFIER
      A1(2)=A1PR(2)
```

```
      B1(2)=B1PR(2)
      A2(2)=A2PR(2)
      B2(2)=B2PR(2)
      A3(2)=A3PR(2)
      B3(2)=B3PR(2)
      M=2
      CALL FCT(M)
C  CORRECTOR
      A1CR(2)=0.125*(9.0*A1(1)+ 3.0*H*(A1P(2)+2.0*A1P(1)))
      B1CR(2)=0.125*(9.0*B1(1)+ 3.0*H*(B1P(2)+2.0*B1P(1)))
      A2CR(2)=0.125*(9.0*A2(1)+ 3.0*H*(A2P(2)+2.0*A2P(1)))
      B2CR(2)=0.125*(9.0*B2(1)+ 3.0*H*(B2P(2)+2.0*B2P(1)))
      A3CR(2)=0.125*(9.0*A3(1)+ 3.0*H*(A3P(2)+2.0*A3P(1)))
      B3CR(2)=0.125*(9.0*B3(1)+ 3.0*H*(B3P(2)+2.0*B3P(1)))
C  FINAL VALUES
      A1(2)=A1CR(2)+9.0       *(A1PR(2)-A1CR(2))/121.0
      B1(2)=B1CR(2)+9.0       *(B1PR(2)-B1CR(2))/121.0
      A2(2)=A2CR(2)+9.0       *(A2PR(2)-A2CR(2))/121.0
      B2(2)=B2CR(2)+9.0       *(B2PR(2)-B2CR(2))/121.0
      A3(2)=A3CR(2)+9.0       *(A3PR(2)-A3CR(2))/121.0
      B3(2)=B3CR(2)+9.0       *(B3PR(2)-B3CR(2))/121.0
C THIRD POINT
      M=2
      WRITE(6,66)M,B1(M),B2(M),B3(M),F1(M),F2(M),F3(M)
      CALL FCT(M)
      A1PR(3)=4.0     *H*(2.0*A1P(2)-A1P(1))/3.0
      B1PR(3)=4.0     *H*(2.0*B1P(2)-B1P(1))/3.0
      A2PR(3)=4.0     *H*(2.0*A2P(2)-A2P(1))/3.0
      B2PR(3)=4.0     *H*(2.0*B2P(2)-B2P(1))/3.0
      A3PR(3)=4.0     *H*(2.0*A3P(2)-A3P(1))/3.0
      B3PR(3)=4.0     *H*(2.0*B3P(2)-B3P(1))/3.0
C MODIFIER
```

```
      A1MF(3)=A1PR(3)-112.0       *(A1PR(2)-A1CR(2))/121.0
      B1MF(3)=B1PR(3)-112.0       *(B1PR(2)-B1CR(2))/121.0
      A2MF(3)=A2PR(3)-112.0       *(A2PR(2)-A2CR(2))/121.0
      B2MF(3)=B2PR(3)-112.0       *(B2PR(2)-B2CR(2))/121.0
      A3MF(3)=A3PR(3)-112.0       *(A3PR(2)-A3CR(2))/121.0
      B3MF(3)=B3PR(3)-112.0       *(B3PR(2)-B3CR(2))/121.0
      A1(3)=A1MF(3)
      B1(3)=B1MF(3)
      A2(3)=A2MF(3)
      B2(3)=B2MF(3)
      A3(3)=A3MF(3)
      B3(3)=B3MF(3)
      M=3
      CALL FCT(M)
      A1CR(3)=0.125*(9.0*A1(2)+3.0*H*(A1P(3)+2.0*A1P(2)-A1P(1)))
      B1CR(3)=0.125*(9.0*B1(2)+3.0*H*(B1P(3)+2.0*B1P(2)-B1P(1)))
      A2CR(3)=0.125*(9.0*A2(2)+3.0*H*(A2P(3)+2.0*A2P(2)-A2P(1)))
      B2CR(3)=0.125*(9.0*B2(2)+3.0*H*(B2P(3)+2.0*B2P(2)-B2P(1)))
      A3CR(3)=0.125*(9.0*A3(2)+3.0*H*(A3P(3)+2.0*A3P(2)-A3P(1)))
      B3CR(3)=0.125*(9.0*B3(2)+3.0*H*(B3P(3)+2.0*B3P(2)-B3P(1)))
C FINAL VALUES
      A1(3)=A1CR(3)+9.0           *(A1PR(3)-A1CR(3))/121.0
      B1(3)=B1CR(3)+9.0           *(B1PR(3)-B1CR(3))/121.0
      A2(3)=A2CR(3)+9.0           *(A2PR(3)-A2CR(3))/121.0
      B2(3)=B2CR(3)+9.0           *(B2PR(3)-B2CR(3))/121.0
      A3(3)=A3CR(3)+9.0           *(A3PR(3)-A3CR(3))/121.0
      B3(3)=B3CR(3)+9.0           *(B3PR(3)-B3CR(3))/121.0
C FOURTH POINT
      M=3
      WRITE(6,66)M,B1(M),B2(M),B3(M),F1(M),F2(M),F3(M)
      CALL FCT(M)
      A1PR(4)=4.0*H     *(2.0*A1P(3)-A1P(2)-2.0*A1P(1))/3.0
```

```
      B1PR(4)=4.0*H     *(2.0*B1P(3)-B1P(2)-2.0*B1P(1))/3.0
      A2PR(4)=4.0*H     *(2.0*A2P(3)-A2P(2)-2.0*A2P(1))/3.0
      B2PR(4)=4.0*H     *(2.0*B2P(3)-B2P(2)-2.0*B2P(1))/3.0
      A3PR(4)=4.0*H     *(2.0*A3P(3)-A3P(2)-2.0*A3P(1))/3.0
      B3PR(4)=4.0*H     *(2.0*B3P(3)-B3P(2)-2.0*B3P(1))/3.0
 66   FORMAT(I5,6F16.6)
C MODIFIER
      A1MF(4)=A1PR(4)-112.0       *(A1PR(3)-A1CR(3))/121.0
      B1MF(4)=B1PR(4)-112.0       *(B1PR(3)-B1CR(3))/121.0
      A2MF(4)=A2PR(4)-112.0       *(A2PR(3)-A2CR(3))/121.0
      B2MF(4)=B2PR(4)-112.0       *(B2PR(3)-B2CR(3))/121.0
      A3MF(4)=A3PR(4)-112.0       *(A3PR(3)-A3CR(3))/121.0
      B3MF(4)=B3PR(4)-112.0       *(B3PR(3)-B3CR(3))/121.0
      A1(4)=A1MF(4)
      B1(4)=B1MF(4)
      A2(4)=A2MF(4)
      B2(4)=B2MF(4)
      A3(4)=A3MF(4)
      B3(4)=B3MF(4)
      M=4
      CALL FCT(M)
      A1CR(4)=0.125*(9.0*A1(3)-A1(1)+3.0*H*(A1P(4)+2.0*A1P(3)-A1P(2)))
      B1CR(4)=0.125*(9.0*B1(3)-B1(1)+3.0*H*(B1P(4)+2.0*B1P(3)-B1P(2)))
      A2CR(4)=0.125*(9.0*A2(3)-A2(1)+3.0*H*(A2P(4)+2.0*A2P(3)-A2P(2)))
      A3CR(4)=0.125*(9.0*A3(3)-A3(1)+3.0*H*(A3P(4)+2.0*A3P(3)-A3P(2)))
      B3CR(4)=0.125*(9.0*B3(3)-B3(1)+3.0*H*(B3P(4)+2.0*B3P(3)-B3P(2)))
      B2CR(4)=0.125*(9.0*B2(3)-B2(1)+3.0*H*(B2P(4)+2.0*B2P(3)-B2P(2)))
C FINAL VALUES
      A1(4)=A1CR(4)-9.0       *(A1PR(4)-A1CR(4))/121.0
      B1(4)=B1CR(4)-9.0       *(B1PR(4)-B1CR(4))/121.0
      A2(4)=A2CR(4)-9.0       *(A2PR(4)-A2CR(4))/121.0
      A3(4)=A3CR(4)-9.0       *(A3PR(4)-A3CR(4))/121.0
```

```
      B3(4)=B3CR(4)-9.0       *(B3PR(4)-B3CR(4))/121.0
      B2(4)=B2CR(4)-9.0       *(B2PR(4)-B2CR(4))/121.0
      DO 139 I=4,2045
      M=I
      CALL FCT(M)
      A1PR(M+1)=A1(M-3)+4.0*H     *(2.0*A1P(M)-A1P(M-1)+2.0*A1P(M-2))/3.0
      B1PR(M+1)=B1(M-3)+4.0*H     *(2.0*B1P(M)-B1P(M-1)+2.0*B1P(M-2))/3.0
      A2PR(M+1)=A2(M-3)+4.0*H     *(2.0*A2P(M)-A2P(M-1)+2.0*A2P(M-2))/3.0
      B2PR(M+1)=B2(M-3)+4.0*H     *(2.0*B2P(M)-B2P(M-1)+2.0*B2P(M-2))/3.0
      A3PR(M+1)=A3(M-3)+4.0*H     *(2.0*A3P(M)-A3P(M-1)+2.0*A3P(M-2))/3.0
      B3PR(M+1)=B3(M-3)+4.0*H     *(2.0*B3P(M)-B3P(M-1)+2.0*B3P(M-2))/3.0
C MODIFIER
      A1MF(M+1)=A1PR(M+1)-112.0       *(A1PR(M)-A1CR(M))/121.0
      B1MF(M+1)=B1PR(M+1)-112.0       *(B1PR(M)-B1CR(M))/121.0
      A2MF(M+1)=A2PR(M+1)-112.0       *(A2PR(M)-A2CR(M))/121.0
      B2MF(M+1)=B2PR(M+1)-112.0       *(B2PR(M)-B2CR(M))/121.0
      A3MF(M+1)=A3PR(M+1)-112.0       *(A3PR(M)-A3CR(M))/121.0
      B3MF(M+1)=B3PR(M+1)-112.0       *(B3PR(M)-B3CR(M))/121.0
      A1(M+1)=A1MF(M+1)
      B1(M+1)=B1MF(M+1)
      A2(M+1)=A2MF(M+1)
      B2(M+1)=B2MF(M+1)
      A3(M+1)=A3MF(M+1)
      B3(M+1)=B3MF(M+1)
      N=M+1
      CALL FCT(N)
      A1CR(M+1)=0.125*(9.0*A1(M)-A1(M-2)+3.0*H*(A1P(M+1)+2.0*A1P(M)-A1P
     1 (M-1)))
      B1CR(M+1)=0.125*(9.0*B1(M)-B1(M-2)+3.0*H*(B1P(M+1)+2.0*B1P(M)-B1P
     1 (M-1)))
      A2CR(M+1)=0.125*(9.0*A2(M)-A2(M-2)+3.0*H*(A2P(M+1)+2.0*A2P(M)-A2P
     1 (M-1)))
```

```
      B2CR(M+1)=0.125*(9.0*B2(M)-B2(M-2)+3.0*H*(B2P(M+1)+2.0*B2P(M)-B2P
     1 (M-1)))
      A3CR(M+1)=0.125*(9.0*A3(M)-A3(M-2)+3.0*H*(A3P(M+1)+2.0*A3P(M)-A3P
     1 (M-1)))
      B3CR(M+1)=0.125*(9.0*B3(M)-B3(M-2)+3.0*H*(B3P(M+1)+2.0*B3P(M)-B3P
     1 (M-1)))
C FINAL VALUES
      A1(M+1)=A1CR(M+1)-9.0       *(A1PR(M+1)-A1CP(M+1))/121.0
      B1(M+1)=B1CR(M+1)-9.0       *(B1PR(M+1)-B1CR(M+1))/121.0
      A2(M+1)=A2CR(M+1)-9.0       *(A2PR(M+1)-A2CP(M+1))/121.0
      B2(M+1)=B2CR(M+1)-9.0       *(B2PR(M+1)-B2CR(M+1))/121.0
      A3(M+1)=A3CR(M+1)-9.0       *(A3PR(M+1)-A3CR(M+1))/121.0
      B3(M+1)=B3CR(M+1)-9.0       *(B3PR(M+1)-B3CR(M+1))/121.0
 139  CONTINUE
      DO 1101 I=1,2046
 1101  A1(I)=B1(I)-B3(I)
      DO 201 I=1,2046
 201  TZ(I)=I
C     PLOTTING THE RESPONSE FOR DIFFERENT MODES
      B1(2047)=1.0
      B1(2048)=-1.0
      CALL SCALE (TZ,2046,20.0,TZMIN,TX,1)
      CALL SCALE (B1,2048,4.0,B1MIN,BX,1)
      CALL AXIS(XX,YY,2HTZ,-2,20.0,0.0,TZMIN,TX)
      CALL AXIS (XX,YY,2HB1,2,4.0,90.0,B1MIN,BX)
      CALL PLOT(XX,YY,-3)
      CALL LINE(TZ,B1,2046,1)
      XX=22.0
      YY=0.0
      DO 202 I=1,2046
 202  TZ(I)=I
      B2(2047)=1.0
```

```
      B2(2048)=-1.0
      CALL SCALE (TZ,2046,20.0,TZMIN,TX,1)
      CALL SCALE (B2,2048,4.0,B2MIN,BX,1)
      CALL AXIS(XX,YY,2HTZ,-2,20.0,0.0,TZMIN,TX)
      CALL AXIS (XX,YY,2HB2,2,4.0,90.0,B2MIN,BX)
      CALL PLOT(XX,YY,-3)
      CALL LINE(TZ,B2,2046,1)
      XX=22.0
      YY=0.0
      DO 203 I=1,2046
  203 TZ(I)=I
      B3(2047)=1.0
      B3(2048)=-1.0
      CALL SCALE (TZ,2046,20.0,TZMIN,TX,1)
      CALL SCALE (B3,2048,4.0,B3MIN,BX,1)
      CALL AXIS(XX,YY,2HTZ,-2,20.0,0.0,TZMIN,TX)
      CALL AXIS (XX,YY,2HB3,2,4.0,90.0,B3MIN,BX)
      CALL PLOT(XX,YY,-3)
      CALL LINE(TZ,B3,2046,1)
      DO 205 I=1,2046
  205 TZ(I)=I
C     PLOTTING OF THE RESPONSE AT THE CENTER OF THE STRING DUE TO ALL
1     THE 3 MODES COMBINED TOGETHER
      A1(2047)=1.0
      A1(2048)=-1.0
      CALL SCALE (TZ,2046,20.0,TZMIN,TX,1)
      CALL SCALE (A1,2048,4.0,A1MIN,AX,1)
      CALL AXIS(XX,YY,2HTZ,-2,20.0,0.0,TZMIN,TX)
      CALL AXIS (XX,YY,2HA1,2,4.0,90.0,A1MIN,AX)
      CALL PLOT(XX,YY,-3)
      CALL LINE(TZ,A1,2046,1)
      CALL PLOT(0.0,0.0,-4)
```

```
STOP
END
```

```
C      SUBROUTINE USED TO CALCULATE  THE FIRST AND SECOND DERIVATIVES
1      OF THE RESPONSE DUE TO DIFFERENT MODES
       SUBROUTINE FCT(M)
       COMMON    A1(2048),A2(2048),A3(2048),B3(2048),B1(2048),B2(2048),
      1 A1P(2048),A2P(2048),A3P(2048),B1P(2048),B2P(2048),B3P(2048),
      1 F1(2048),F2(2048),F3(2048)
       COMMON BETA1,BETA2,BETA3,W1,W2,W3,AR,TL,TO,E
       A1P(M)=-2.0*0.628318*A1(M)-(1.0+((AR*E)/(4.0*TO))*(3.14159/TL)**2
      1 *(B1(M)**2+4.0*B2(M)**2+9.0*B3(M)**2))*( 6.28318**2)*B1(M)+F1(M)
       B1P(M)=A1(M)
       A2P(M)=-2.0*0.628318*A2(M)-(1.0+((AR*E)/(4.0*TO))*(3.14159/TL)**2
      1 *(B1(M)**2+4.0*B2(M)**2+9.0*B3(M)**2))*(12.56636**2)*B2(M)+F2(M)
       B2P(M)=A2(M)
       A3P(M)=-2.0*0.628318*A3(M)-(1.0+((AR*E)/(4.0*TO))*(3.14159/TL)**2
      1 *(B1(M)**2+4.0*B2(M)**2+9.0*B3(M)**2))*(18.84954**2)*B3(M)+F3(M)
       B3P(M)=A3(M)
       RETURN
       END
```

```
C       PROGRAM FOR NONLINEAR PANEL RESPONSE DUE TO TURBULENT PRESSURE
1       FLUCTUATIONS FOR SUBSONIC BOUNDARY LAYER
        DIMENSION C(2,2),Q(2,2),W(2048), F(2,3000), HH(2,2),HHH(2,2),
       1 AX(4100,1,1),INV(2048),Z1(3),Z2(3),S(2,2),TZ(1505),
       1 XI(3), MV(3),DDX(2,4100),DX(3),FF(3000),
       1 A1PR(3000),A2PR(3000),B1PR(3000),B2PR(3000),
       1 A1MF(3000),A2MF(3000),B1MF(3000),B2MF(3000),
       1 A1CR(3000),A2CR(3000),B1CR(3000),B2CR(3000)
        COMMON A1(3000),A2(3000),B1(3000),B2(3000),
       1 A1P(3000),A2P(3000),B1P(3000),B2P(3000),
       1 F1(3000),F2(3000),BET1,BET2,
       1 C10,C11,C12,C21,C22,C33,C44,C20,C66,C55
        COMPLEXS,      DYY,    HH,HHH,YYY,DD,DDX,AX,XI,DX
C       COEFFICIENTS IN THE GOVERNING EQUATIONS
        BET1=0.5
        BET2=1.7
        KOUNT=1
 3532   SIGP=7500.0
        KOUT=1
 399    DO 401 I=1,2
        DO 401 J=1,2
        C(I,J)=0.0
 401    Q(I,J)=0.0
        DO 239 I=1,2
        DO 239 KA=1,2049
  239   DDX(I,KA)=CMPLX(0.0,0.0)
        WU= 1000.0*3.14159
        WU= 2000.0*3.14159
        WL=   0.0
        H4=56.0*128.0*8.9*12.0*0.91/((10.0**7)*144.0*SIGP)
        H=H4**0.25
        TH1=3.14159*C.5
```

```
      TH2=3.14159*0.5
      UINF=800.0
      XSI=0.157/12.0
      SA=10.0
      SB=20.0
      S1=5.0
      GNU=0.3
      RO=0.1*H/386.4
      N=2049
      XX=0.0
      YY=3.0
      UC=0.65*UINF*12.0
      CM=800.0/995.0
      ALP=0.5
      PI4=(3.14159)**4
      ALPS=ALP**2
      GNUS=GNU**2
      ROC=0.00089
      SV=995.0
      XN=N
      DW=(WU-WL)/(XN-1.0)
      KA=1
      E =10.0**7
      RIG=E*(H**3)/(12.0*(1-GNU**2))
      SQ=8.9*32.0
      DEMC= ROC*SV**2*SA*SB**2/(RIG*144.0)
      DEM=2.0*SQ*SA*SB**2/(RIG*144.0)
      C10=((ALP+1.0/ALP)**2)*PI4
      C20=((ALP+4.0/ALP)**2)*PI4
      C11=0.75*PI4*((1.0-GNUS)*(ALPS+1.0/ALPS)+2.0*(2.0*GNU+ALPS+1.0/
     1  ALPS))
      C12=0.75*PI4*((1.0-GNUS)*(4.0*(ALPS+1.0/ALPS)+81.0*ALPS
```

```
     1 /(1.0+4.0*ALPS)**2+ALPS/(9.0+4.0*ALPS)**2)+2.0*(5.0*GNU+ALPS+
     1 4.0/ALPS))
      C21=C12
      C22=0.75*PI4*((1.0-GNUS)*(ALPS+16.0/ALPS)+2.0*(8.0*GNU+ALPS+16.0
     1 /ALPS))
      C33=DEMC*(-SA/(PI4*S1))
      C44=-DEM*0.666/CM
      C66=DEM*0.6666/CM
      C55=SQRT(RIG)/(4.*CM*SB*UINF*SQRT(RO)*12.0)*DEM
      SD2= SQRT(RIG/RO)/(SA*SB)
      CONS1= (SIGP**2)*XSI*SD2/((3.14159**2)*3.136*UINF)
      DELT=SD2/(1000.0)
      DELT=SD2/(2000.0)
      WXX=SQRT(    DELT*4096.0)
      WRITE(6,466) RO,SQ,    DEMC,DEM,SD2,RIG ,DELT,WXX
  466 FORMAT(1X,8F13.6)
      WRITE(6,196) C10,C11,C12,C21,C20,C22,C33,C44,C55,C66
  196 FORMAT(10F12.5)
      SIG=H
C     INPUT SPECTRAL DENSITY FUNCTIONS OF THE GENERALIZED FORCES
   14 XK=KA
      W(KA)=(XK-1.0)*DW+WL
      CONS2=3.7*EXP(-2.0*W(KA) *XSI/UINF)
      CONS3=0.8*EXP(-.47*W(KA)*XSI/UINF)
      CONS4=3.4*EXP(-8.0*W(KA)*XSI/UINF)
      CONST=CONS1*(CONS2+CONS3-CONS4)
      M1=1
      M2=1
      N1=1
      N2=1
      CQ=0.1*W(KA)*10.0/UC
      ES=EXP(-0.1*W(KA)*10.0/UC)
```

```
      EX=EXP(0.1*W(KA)*10.0/UC)
      AG1=N1*3.14159+W(KA)*10.0/UC
      AG2=N1*3.14159-W(KA)*10.0/UC
      AC=CQ**2+AG1**2
      BC=CQ**2+AG2**2
      SAG1=SIN(AG1)
      CAG1=COS(AG1)
      SAG2=SIN(AG2)
      CAG2=COS(AG2)
C CONSTANTS ON PAGE 91
      CC=ES*(-CQ*SAG1-AG1*CAG1)
      DC=ES*(-CQ*SAG2-AG2*CAG2)
      EC=ES*(-CQ*CAG2+AG2*SAG2)
      FC=ES*(-CQ*CAG1+AG1*SAG1)
C CONSTANTS ON PAGE 93
      AA1=M1*3.14159+W(KA)*10.0/UC
      BB1=M1*3.14159-W(KA)*10.0/UC
      SA=SIN(AA1)
      SB=SIN(BB1)
      CA=COS(AA1)
      CB=COS(BB1)
      CC1=-CQ*SA-AA1*CA+AA1
      DD1=-CQ*SB-BB1 *CB+BB1
      CC2=CQ*SA-AA1*CA+AA1
      DD2=CQ*SB-BB1*CB+BB1
      EE1=-CQ*CA+AA1*SA+CQ
      FF1=-CQ*CB+BB1*SB+CQ
      GG1= CQ*CA+AA1*SA-CQ
      GG2= CQ*CB+BB1*SB-CQ
      AC1=CQ**2+AA1**2
      BC1=CQ**2+BB1**2
      ACC1=(14.30*W(KA)/UC)**2+(N2*3.14159)**2
```

```
      BCC1=(14.30*W(KA)/UC)**2+(M2*3.14159)**2
      C(1,1)=0.5*CQ/AC+0.5*CQ/BC+(0.25*AG1/AC+0.25*AG2/BC)*ES*
     1  (CC1/AC1+DD1/BC1)+(0.25*CC/AC+0.25*DC/BC)*EX*(CC2/AC1+DD2/BC1)
     1 +CQ*(0.25/BC-0.25/AC)*ES*(EE1/AC1+FF1/BC1)
     1 +(0.25*FC/AC-0.25*EC/BC)*EX*(GG1/AC1-GG2/BC1)
     1 +(14.30*W(KA)/UC+((3.14159)**2*(M2*N2)/BCC1)*(1.0+(-1.0)**(M2+N2)
     1 +EXP(-14.30*W(KA)/UC) *((-1.0)**(M2+1)+(-1.0)**(N2+1))))/ACC1
      C(1,1)=C(1,1)*CONST
      Q(1,1)= (0.25*AG1/AC+0.25*AG2/BC)*ES*(EE1/AC1+FF1/BC1)
     1 +(0.25*CC/AC+0.25*DC/BC)*EX*(GG1/AC1+GG2/BC1)
     1 +CQ*(0.25/BC-0.25/AC)*ES*(CC1/AC1+DD1/BC1)
     1 +(0.25*FC/AC-0.25*EC/BC)*EX*(CC2/AC1+DD2/BC1)
      Q(1,1)=Q(1,1)*CONST
      M1=1
      M2=1
      N1=2
      N2=1
      AG1=N1*3.14159+W(KA)*10.0/UC
      AG2=N1*3.14159-W(KA)*10.0/UC
      AC=CQ**2+AG1**2
      BC=CQ**2+AG2**2
      SAG1=SIN(AG1)
      CAG1=COS(AG1)
      SAG2=SIN(AG2)
      CAG2=COS(AG2)
C CONSTANTS ON PAGE 91
      CC=ES*(-CQ*SAG1-AG1*CAG1)
      DC=ES*(-CQ*SAG2-AG2*CAG2)
      EC=ES*(-CQ*CAG2+AG2*SAG2)
      FC=ES*(-CQ*CAG1+AG1*SAG1)
      C(1,2)=                          (0.25*AG1/AC+0.25*AG2/BC)*ES*
     1  (CC1/AC1+DD1/BC1)+(0.25*CC/AC+0.25*DC/BC)*EX*(CC2/AC1+DD2/BC1)
```

```
     1  +CQ*(0.25/BC-0.25/AC)*ES*(EE1/AC1+FF1/BC1)
     1  +(0.25*FC/AC-0.25*EC/BC)*EX*(GG1/AC1-GG2/BC1)
     1  +(14.30*W(KA)/UC+((3.14159)**2*(M2*N2)/BCC1)*(1.0+(-1.0)**(M2+N2)
     1  +EXP(-14.30*W(KA)/UC) *((-1.0)**(M2+1)+(-1.0)**(N2+1))))/ACC1
      C(1,2)=C(1,2)*CONST
      Q(1,2)=CQ/(AC*(M1*3.14159+N1*3.14159))-CQ/(BC*(M1*3.14159+N1*
     1 3.14159))
     1        +(0.25*AG1/AC+0.25*AG2/BC)*ES*(EE1/AC1+FF1/BC1)
     1  +(0.25*CC/AC+0.25*DC/BC)*EX*(GG1/AC1+GG2/BC1)
     1  +CQ*(0.25/BC-0.25/AC)*ES*(CC1/AC1+DD1/BC1)
     1  +(0.25*FC/AC-0.25*EC/BC)*EX*(CC2/AC1+DD2/BC1)
      Q(1,2)=Q(1,2)*CONST
      C(2,1)=C(1,2)
      Q(2,1)=-Q(1,2)
      M1=2
      M2=1
      N1=2
      N2=1
      AA1=M1*3.14159+W(KA)*10.0/UC
      BB1=M1*3.14159-W(KA)*10.0/UC
      SA=SIN(AA1)
      SB=SIN(BB1)
      CA=COS(AA1)
      CB=COS(BB1)
      CC1=-CQ*SA-AA1*CA+AA1
      DD1=-CQ*SB-BB1 *CB+BB1
      CC2=CQ*SA-AA1*CA+AA1
      DD2=CQ*SB-BB1*CB+BB1
      EE1=-CQ*CA+AA1*SA+CQ
      FF1=-CQ*CB+BB1*SB+CQ
      GG1= CQ*CA+AA1*SA-CQ
      GG2= CQ*CB+BB1*SB-CQ
```

```
      AC1=CQ**2+AA1**2
      BC1=CQ**2+BB1**2
      C(2,2)=0.5*CQ/AC+0.5*CQ/BC+(0.25*AG1/AC+0.25*AG2/BC)*ES*
     1  (CC1/AC1+DD1/BC1)+(0.25*CC/AC+0.25*DC/BC)*EX*(CC2/AC1+DD2/BC1)
     1 +CQ*(0.25/BC-0.25/AC)*ES*(EE1/AC1+FF1/BC1)
     1 +(0.25*FC/AC-0.25*EC/BC)*EX*(GG1/AC1-GG2/BC1)
     1 +(14.30*W(KA)/UC+((3.14159)**2*(M2*N2)/BCC1)*(1.0+(-1.0)**(M2+N2)
     1 +EXP(-14.30*W(KA)/UC) *((-1.0)**(M2+1)+(-1.0)**(N2+1))))/ACC1
      C(2,2)=C(2,2)*CONST
      Q(2,2)= (0.25*AG1/AC+0.25*AG2/BC)*ES*(EE1/AC1+FF1/BC1)
     1 +(0.25*CC/AC+0.25*DC/BC)*EX*(GG1/AC1+GG2/BC1)
     1 +CQ*(0.25/BC-0.25/AC)*ES*(CC1/AC1+DD1/BC1)
     1 +(0.25*FC/AC-0.25*EC/BC)*EX*(CC2/AC1+DD2/BC1)
      Q(2,2)=Q(2,2)*CONST
      DO 25 I=1,2
      DO 25 J=1,2
 25   S(I,J)=CMPLX(C(I,J),-Q(I,J))
C     CALCULATIONS OF THE GENERALIZED FORCES STARTS
      JJJ=2
      DO 29 I=1,JJJ
      DO 29 J=1,JJJ
      HH(I,J)=CMPLX(0.0,0.0)
 29   HHH(I,J)=CMPLX(0.0,0.0)
      HH(1,1)=  CSQRT(S(1,1))
      HHH(1,1)=HH(1,1)
      DO 110 J=2,JJJ
      HH(1,J) =     (S(1,J)/HH(1,1))
 110  HHH(J,1)= CONJG(HH(1,J))
      DO1120 I=2,JJJ
      DD=CMPLX(0.0,0.0)
      M=I-1
      DO113 LP=1,M
```

```
113   DD=DD+     (HH(LP,I)*CONJG(HH(LP,I)))
      YYY= S(I,I)-DD
      HH(I,I)= CSQRT(YYY)
      HHH(I,I)=HH(I,I)
      IF (I.EQ.JJJ) GO TO 1121
      NN=I+1
      MM=I-1
      DO1120 J=NN,JJJ
      DD=CMPLX(0.0,0.0)
      DO222 LP=1,MM
222   DD=DD+     (HH(LP,I)*CONJG(HH(LP,J)))
      HH(I,J)=       ((S(I,J)-DD)/HH(I,I))
      HHH(J,I)=CONJG(HH(I,J))
1120  CONTINUE
1121  CONTINUE
      DO 109 K=1,JJJ
      CALL GAUSS(17,0.707,0.0,V3)
      CALL GAUSS(23,0.707,0.0,V2)
      Z2(K)=V2
109   Z1(K)=V3
      DO 252 K=1,JJJ
252   XI(K)=CMPLX(Z1(K),Z2(K))
      DO 300 I=1,JJJ
      DD=CMPLX(0.0,0.0)
      DO 309 J=1,I
309   DD   =DD+HHH(I,J)*XI(J)
      DX(I)=DD
300   DDX(I,KA)=DX(I)
      IF(KA.EQ.2049) GO TO 40
      KA=KA+1
      GO TO 14
40    DO 600 I=1,JJJ
```

```
      DO 600 N=1,2047
      K=2049+N
      J=2049-N
 600  DDX(I,K)=CONJG(DDX(I,J))
      DO 800 J=1,JJJ
      DO 700 I=1,4096
 700  AX(I,1,1) =DDX(J,I)
      MV(1)=12
      MV(2)=0
      MV(3)=0
      CALL HARM(AX,MV,INV,P,1,IFEER)
      DO225 I=1,3000
      FF(I)=REAL(AX(I,1,1))/WXX
      F(J,I)=FF(I)
 225  CONTINUE
 800  CONTINUE
      DO 801 I=1,3000
      F1(I)=F(1,I)
 801  F2(I)=F(2,I)
C     SOLUTION OF THE GOVERNING DIFFERENTIAL EQUATIONS BY MODIFIED
1     PREDICTOR CORRECTOR METHOD STARTS
C INITIAL CONDITIONS
      M=1
      H=DELT
      A1(1)=0.0
      B1(1)=0.0
      A2(1)=0.0
      B2(1)=0.0
C STARTING VALUES
      CALL FCT(M)
C PREDIDTOR
      A1PR(2)= 4.0*H     *(2.0*A1P(I))/3.0
```

```
      B1PR(2)= 4.0*H     *(2.0*B1P(1))/3.0
      A2PR(2)= 4.0*H     *(2.0*A2P(1))/3.0
      B2PR(2)= 4.0*H     *(2.0*B2P(1))/3.0
C NO MODIFIER
      A1(2)=A1PR(2)
      B1(2)=B1PR(2)
      A2(2)=A2PR(2)
      B2(2)=B2PR(2)
      M=2
      CALL FCT(M)
C  CORRECTOR
      A1CR(2)=0.125*(9.0*A1(1)+ 3.0*H*(A1P(2)+2.0*A1P(1)))
      B1CR(2)=0.125*(9.0*B1(1)+ 3.0*H*(B1P(2)+2.0*B1P(1)))
      A2CR(2)=0.125*(9.0*A2(1)+ 3.0*H*(A2P(2)+2.0*A2P(1)))
      B2CR(2)=0.125*(9.0*B2(1)+ 3.0*H*(B2P(2)+2.0*B2P(1)))
C  FINAL VALUES
      A1(2)=A1CR(2)+9.0       *(A1PR(2)-A1CR(2))/121.0
      B1(2)=B1CR(2)+9.0       *(B1PR(2)-B1CR(2))/121.0
      A2(2)=A2CR(2)+9.0       *(A2PR(2)-A2CR(2))/121.0
      B2(2)=B2CR(2)+9.0       *(B2PR(2)-B2CR(2))/121.0
C THIRD POINT
      M=2
      WRITE(6,66)M,B1(M),B2(M),      F1(M),F2(M)
      CALL FCT(M)
      A1PR(3)=4.0     *H*(2.0*A1P(2)-A1P(1))/3.0
      B1PR(3)=4.0     *H*(2.0*B1P(2)-B1P(1))/3.0
      A2PR(3)=4.0     *H*(2.0*A2P(2)-A2P(1))/3.0
      B2PR(3)=4.0     *H*(2.0*B2P(2)-B2P(1))/3.0
C MODIFIER
      A1MF(3)=A1PR(3)-112.0       *(A1PR(2)-A1CR(2))/121.0
      B1MF(3)=B1PR(3)-112.0       *(B1PR(2)-B1CR(2))/121.0
      A2MF(3)=A2PR(3)-112.0       *(A2PR(2)-A2CR(2))/121.0
```

```
      B2MF(3)=B2PR(3)-112.0       *(B2PR(2)-B2CR(2))/121.0
      A1(3)=A1MF(3)
      B1(3)=B1MF(3)
      A2(3)=A2MF(3)
      B2(3)=B2MF(3)
      M=3
      CALL FCT(M)
      A1CR(3)=0.125*(9.0*A1(2)+3.0*H*(A1P(3)+2.0*A1P(2)-A1P(1)))
      B1CR(3)=0.125*(9.0*B1(2)+3.0*H*(B1P(3)+2.0*B1P(2)-B1P(1)))
      A2CR(3)=0.125*(9.0*A2(2)+3.0*H*(A2P(3)+2.0*A2P(2)-A2P(1)))
      B2CR(3)=0.125*(9.0*B2(2)+3.0*H*(B2P(3)+2.0*B2P(2)-B2P(1)))
C FINAL VALUES
      A1(3)=A1CR(3)+9.0       *(A1PR(3)-A1CR(3))/121.0
      B1(3)=B1CR(3)+9.0       *(B1PR(3)-B1CR(3))/121.0
      A2(3)=A2CR(3)+9.0       *(A2PR(3)-A2CR(3))/121.0
      B2(3)=B2CR(3)+9.0       *(B2PR(3)-B2CR(3))/121.0
C FOURTH POINT
      M=3
      CALL FCT(M)
      A1PR(4)=4.0*H     *(2.0*A1P(3)-A1P(2)-2.0*A1P(1))/3.0
      B1PR(4)=4.0*H     *(2.0*B1P(3)-B1P(2)-2.0*B1P(1))/3.0
      A2PR(4)=4.0*H     *(2.0*A2P(3)-A2P(2)-2.0*A2P(1))/3.0
      B2PR(4)=4.0*H     *(2.0*B2P(3)-B2P(2)-2.0*B2P(1))/3.0
 66   FORMAT(I5,4F16.6)
C MODIFIER
      A1MF(4)=A1PR(4)-112.0       *(A1PR(3)-A1CR(3))/121.0
      B1MF(4)=B1PR(4)-112.0       *(B1PR(3)-B1CR(3))/121.0
      A2MF(4)=A2PR(4)-112.0       *(A2PR(3)-A2CR(3))/121.0
      B2MF(4)=B2PR(4)-112.0       *(B2PR(3)-B2CR(3))/121.0
      A1(4)=A1MF(4)
      B1(4)=B1MF(4)
      A2(4)=A2MF(4)
```

```
      B2(4)=B2MF(4)
      M=4
      CALL FCT(M)
      A1CR(4)=0.125*(9.0*A1(3)-A1(1)+3.0*H*(A1P(4)+2.0*A1P(3)-A1P(2)))
      B1CR(4)=0.125*(9.0*B1(3)-B1(1)+3.0*H*(B1P(4)+2.0*B1P(3)-B1P(2)))
      A2CR(4)=0.125*(9.0*A2(3)-A2(1)+3.0*H*(A2P(4)+2.0*A2P(3)-A2P(2)))
      B2CR(4)=0.125*(9.0*B2(3)-B2(1)+3.0*H*(B2P(4)+2.0*B2P(3)-B2P(2)))
C FINAL VALUES
      A1(4)=A1CR(4)-9.0       *(A1PR(4)-A1CR(4))/121.0
      B1(4)=B1CR(4)-9.0       *(B1PR(4)-B1CR(4))/121.0
      A2(4)=A2CR(4)-9.0       *(A2PR(4)-A2CR(4))/121.0
      B2(4)=B2CR(4)-9.0       *(B2PR(4)-B2CR(4))/121.0
      DO 139 I=4,2999
      IF(I.GT.2500) WRITE(6,56) F1(M),F2(M),B1(M)
 56   FORMAT(3F16.6)
      M=I
      CALL FCT(M)
      A1PR(M+1)=A1(M-3)+4.0*H    *(2.0*A1P(M)-A1P(M-1)+2.0*A1P(M-2))/3.0
      B1PR(M+1)=B1(M-3)+4.0*H    *(2.0*B1P(M)-B1P(M-1)+2.0*B1P(M-2))/3.0
      A2PR(M+1)=A2(M-3)+4.0*H    *(2.0*A2P(M)-A2P(M-1)+2.0*A2P(M-2))/3.0
      B2PR(M+1)=B2(M-3)+4.0*H    *(2.0*B2P(M)-B2P(M-1)+2.0*B2P(M-2))/3.0
C MODIFIER
      A1MF(M+1)=A1PR(M+1)-112.0      *(A1PR(M)-A1CR(M))/121.0
      B1MF(M+1)=B1PR(M+1)-112.0      *(B1PR(M)-B1CR(M))/121.0
      A2MF(M+1)=A2PR(M+1)-112.0      *(A2PR(M)-A2CR(M))/121.0
      B2MF(M+1)=B2PR(M+1)-112.0      *(B2PR(M)-B2CR(M))/121.0
      A1(M+1)=A1MF(M+1)
      B1(M+1)=B1MF(M+1)
      A2(M+1)=A2MF(M+1)
      B2(M+1)=B2MF(M+1)
      N=M+1
      CALL FCT(N)
```

```
      A1CR(M+1)=0.125*(9.0*A1(M)-A1(M-2)+3.0*H*(A1P(M+1)+2.0*A1P(M)-A1P
     1 (M-1)))
      B1CR(M+1)=0.125*(9.0*B1(M)-B1(M-2)+3.0*H*(B1P(M+1)+2.0*B1P(M)-B1P
     1 (M-1)))
      A2CR(M+1)=0.125*(9.0*A2(M)-A2(M-2)+3.0*H*(A2P(M+1)+2.0*A2P(M)-A2P
     1 (M-1)))
      B2CR(M+1)=0.125*(9.0*B2(M)-B2(M-2)+3.0*H*(B2P(M+1)+2.0*B2P(M)-B2P
     1 (M-1)))
      A1(M+1)=A1CR(M+1)-9.0       *(A1PR(M+1)-A1CR(M+1))/121.0
      B1(M+1)=B1CR(M+1)-9.0       *(B1PR(M+1)-B1CR(M+1))/121.0
      A2(M+1)=A2CR(M+1)-9.0       *(A2PR(M+1)-A2CR(M+1))/121.0
      B2(M+1)=B2CR(M+1)-9.0       *(B2PR(M+1)-B2CR(M+1))/121.0
      IF(B1(M).GT.1000.) GO TO 732
  139 CONTINUE
  332 II=2047
      USUM=0.0
      DO 1 I=1500,3000
    1 USUM=USUM+B1(I)**2
      XII=3000.0-1500.0
      RMS=SQRT(USUM/XII)
      WRITE(6,96) SIG,RMS
   96 FORMAT(2F16.8)
  555 FORMAT(I6)
  732 WRITE(6,555) M
C     PLOTTING OF THE SIMULATED GENERALIZED FORCES AND THE RESPONSE
1     AT THE CENTER OF THE PLATE
      XX=0.0
      YY=3.0
      DO 2271 I=1,500
      II=I+2499
      TZ(I)=I
      F1(I)=F1(II)
```

```
      F2(I)=F2(II)
 2271 B1(I)=B1(II)
      B1(501)=2.0
      B1(502)=-2.0
      CALL SCALE  (TZ,500,20.0,TZMIN,TX,1)
      CALL SCALE  (B1,502,4.0,B1MIN,BX,1)
      CALL AXIS(XX,YY,2HTZ,-2,20.0,0.0,TZMIN,TX)
      CALL AXIS (XX,YY,2HB1,2,4.0,90.0,B1MIN,BX)
      CALL PLOT(XX,YY,-3)
      CALL LINE(TZ,B1,500,1)
      XX=22.0
      YY=0.0
      DO 3271 I=1,500
 3271 TZ(I)=I
      F1(501)=800.0
      F1(502)=-800.0
      CALL SCALE (TZ,500,20.00,TZMIN,TX,1)
      CALL SCALE (F1,502,4.00,F1MIN,FX,1)
      CALL AXIS(XX,YY,2HTZ,-2,20.0,0.0,TZMIN,TX)
      CALL AXIS (XX,YY,2HF1,2,4.0,90.0,F1MIN,FX)
      CALL PLOT(XX,YY,-3)
      CALL LINE(TZ,F1,500,1)
      XX=22.0
      YY=0.0
      DO 4271 I=1,500
 4271 TZ(I)=I
      F2(501)=800.0
      F2(502)=-800.0
      CALL SCALE (TZ,500,20.00,TZMIN,TX,1)
      CALL SCALE (F2,502,4.00,F2MIN,FX,1)
      CALL AXIS(XX,YY,2HTZ,-2,20.0,0.0,TZMIN,TX)
      CALL AXIS (XX,YY,2HF2,2,4.0,90.0,F2MIN,FX)
```

```
      CALL PLOT(XX,YY,-3)
      CALL LINE(TZ,F2,500,1)
      CALL PLOT(0.0,0.0,-4)
      STOP
      END
```

```
C      SUBROUTINE USED TO FIND THE FIRST AND SECOND DERIVATIVES
1      FOR SOLVING THE GOVERNING DIFF. EQUATIONS
       SUBROUTINE FCT(M)
       COMMON A1(3000),A2(3000),B1(3000),B2(3000),
      1 A1P(3000),A2P(3000),B1P(3000),B2P(3000),
      1 F1(3000),F2(3000),BET1,BET2,
      1 C10,C11,C12,C21,C22,C33,C44,C20,C66,C55
       A1P(M)= -BET1*A1(M)-(C10+C11*B1(M)**2+C12*B2(M)**2)*B1(M)+4.0*(
      1 F1(M)+C33*4.0*B1(M))
       B1P(M)=A1(M)
       A2P(M)=-BET2*A2(M)-(C20+C21*B1(M)**2+C22*B2(M)**2)*B2(M)+4.0*(
      1 F2(M))
       B2P(M)=A2(M)
       RETURN
       END
```

VITA

Ajit Kumar Sinha was born on [redacted], in [redacted]. In 1960 he graduated from local government high school and entered the St. Xavier's College, Ranchi, India, from where he obtained his Intermediate Science degree. In 1962, he was admitted to Bihar Institute of Technology, Sindri, India, where he received his B.S. degree in Mechanical Engineering in 1966. After having worked as a lecturer at the same institute for two and one-half years, Mr. Sinha joined the University of Mississippi Graduate School in September of 1969 from where he transferred to Virginia Polytechnic Institute in September 1970 to work towards the completion of Ph.D. requirements in the Engineering Mechanics Department. Upon completion, Mr. Sinha plans to work for the United Engineers and Constructors, a subsidiary of Raytheon Corp., in Philadelphia.